UNIVERSITY OF WEST BOHEMIA
FACULTY OF MECHANICAL ENGINEERING

Study program: N2301   Mechanical Engineering
Study field: Manufacturing Processes – Technology of Metal Cutting

DIPLOMA THESIS

Cutting tool durability when stainless steel is machined

Author: **Bc. Nazirjon Ismailov**

Supervisor: **doc. Ing. Miroslav ZETEK, PhD.**

Academic year 2018/2019

ZÁPADOČESKÁ UNIVERZITA V PLZNI
Fakulta strojní
Akademický rok: **2018/2019**

ZADÁNÍ DIPLOMOVÉ PRÁCE
(PROJEKTU, UMĚLECKÉHO DÍLA, UMĚLECKÉHO VÝKONU)

Jméno a příjmení: **Bc. Nazirjon ISMAILOV**

Osobní číslo: **S16N0001P**

Studijní program: **N2301 Strojní inženýrství**

Studijní obor: **Strojírenská technologie - technologie obrábění**

Název tématu: **Cutting tool durability when stainless steel is machined**

Zadávající katedra: **Katedra technologie obrábění**

Zásady pro vypracování:

1. Introduction

2. Description of the current state

3. Design and performance of experiments

4. Results evaluation

5. Conclusion

Rozsah grafických prací: **dle potřeby**

Rozsah kvalifikační práce: **50 - 70 stran**

Forma zpracování diplomové práce: **tištěná**

Seznam odborné literatury:

- DAVIM, J. PAULO: Moderm machining technology : a practical guide : Oxford, Woodhead Publishing, 2011, ISBN 978-0-85709-099-7

- ŠTUPLA, M.: CNC : programování obráběcích strojů. Praha : Grada Publishing, 2015, ISBN 978-80-247-5269-3

- ČEP R., PETRŮ J., Experimentální metody v obrábění, Ostrava : VŠB-TU Ostrava, 2011, 146 s. ISBN 978-80-248-2533-5

- Astakhof, Viktor P., Tribology and interface engineering series, Elsevier, 2006, ISBN 0-444-52881-4

- Shaw, Milton Clayton, Metal cutting principles, Oxford University Press, 2005, ISBN 0-19-514206-3

Vedoucí diplomové práce: **Doc. Ing. Miroslav Zetek, Ph.D.**
Katedra technologie obrábění

Konzultant diplomové práce: **Ing. Tomáš Bakša**
Regionální technologický institut

Datum zadání diplomové práce: **16. října 2018**

Termín odevzdání diplomové práce: **24. května 2019**

L.S.

Doc. Ing. Milan Edl, Ph.D.
děkan

Doc. Ing. Jan Řehoř, Ph.D.
vedoucí katedry

V Plzni dne 18. října 2018

Prohlášení o autorství

Předkládám tímto k posouzení a obhajobě bakalářskou/diplomovou práci, zpracovanou na závěr studia na Fakultě strojní Západočeské univerzity v Plzni.
Prohlašuji, že jsem tuto diplomovou práci vypracoval samostatně, s použitím odborné literatury a pramenů, uvedených v seznamu, který je součástí této bakalářské/diplomové práce.

V Plzni dne: …………………….   . . . .
                                                                    podpis autora

Foreword

SUMMARY OF DIPLOMA SHEET

AUTHOR	**Surname** Ismailov		**Name** Nazirjon
FIELD OF STUDY	N2301 "Manufacturing Processes – Technology of Metal Cutting"		
SUPERVISOR	**Surname (Inclusive of Degrees)** doc. Ing. Zetek, PhD.		**Name** Miroslav
INSTITUTION	ZČU - FST - KTO		
TYPE OF WORK	**DIPLOMA**	~~**BACHELOR**~~	**Delete when not applicable**
TITLE OF THE WORK	Cutting tool durability when stainless steel is machined		

FACULTY	Mechanical Engineering	DEPARTMENT	Machining technology	SUBMITTED IN	2019

NUMBER OF PAGES (A4 and eq. A4)

TOTALLY	75	TEXT PART	70	GRAPHICAL PART	5

BRIEF DESCRIPTION **TOPIC, GOAL, RESULTS AND CONTRIBUTIONS**	This thesis deals with machining of austenitic stainless steels with indexable carbide inserts. The main task is to determine build-up edge (BUE) formation and other type of wear on the cutting edge and to compare two different milling cutters performance where one milling cutter is made using DMLS (Direct Metal Laser Sintering) technique – 3D printing of metal. The results of this work will be used for further researches in the future.
KEY WORDS	austenitic stainless steel, BUE formation, tool life, durability, face milling, 3D printing, milling cutter, additive manufacturing

ANOTAČNÍ LIST DIPLOMOVÉ PRÁCE

AUTOR	**Příjmení** Ismailov		**Jméno** Nazirjon	
STUDIJNÍ OBOR	N2301 „Strojírenská technologie – technologie obrábění"			
VEDOUCÍ PRÁCE	**Příjmení (včetně titulů)** doc. Ing. Zetek, Ph.D		**Jméno** Miroslav	
PRACOVIŠTĚ	ZČU - FST - KTO			
DRUH PRÁCE	**DIPLOMOVÁ**	~~**BAKALÁŘSKÁ**~~	**Nehodící se škrtněte**	
NÁZEV PRÁCE	Trvanlivost nástroje při obrábění nerezové oceli			

FAKULTA	strojní		KATEDRA	KTO	ROK ODEVZD.	2019

POČET STRAN (A4 a ekvivalentů A4)

CELKEM	75	TEXTOVÁ ČÁST	70	GRAFICKÁ ČÁST	5

STRUČNÝ POPIS (MAX 10 ŘÁDEK) **ZAMĚŘENÍ, TÉMA, CÍL POZNATKY A PŘÍNOSY**	Tato diplomová práce se zabývá obráběním austenitických nerezových ocelí s karbidovými vyměnitelnými břitovými destičkami. Hlavním úkolem je stanovit tvorbu nárůstku na břitu, opotřebení břitu a porovnat dva rozdílné druhy fréz, kde je jedna fréza vyrobena metodou DMLS (Direct Metal Laser Sintering) – 3D tisk kovu. Výsledky této práce budou v budoucnu využity pro další výzkum.
KLÍČOVÁ SLOVA **ZPRAVIDLA JEDNOSLOVNÉ POJMY, KTERÉ VYSTIHUJÍ PODSTATU PRÁCE**	austenitická nerezová ocel, tvorba nárůstku, trvanlivost, rovinnné frézování, 3D tisk, fréza, aditivní technologie

Contents

List of figures

List of tables

List of graphs

Nomenclature

Notations

Symbol	Unit	Description
v_c	m/min	Cutting speed
f_z	mm	Feed rate
D_c	mm	Cutter diameter
a_p	mm	Axial depth of cut
a_e	mm	Radial depth of cut
VB_B	μm	Flank wear
VB_{max}	μm	Maximum flank wear
Δt	min.	Cutting time
γ	degrees (°)	Rake angle
α	degrees (°)	Flank angle

Abbreviations

SS	Stainless steel
BUE	Build-up edge
PVD	Physical Vapor Deposition
CVD	Chemical Vapor Deposition
HRA	Rockwell hardness scale A
WC	Tungsten carbide
MQL	Minimum Quantity Lubrication
AISI	Americal Iron and Steel Institute
ČSN	CzechTechnical Standard
PCBN	Polycrystalline Cubin Boron Nitride
DMLS	Direct Metal Laser Sintering

1.   Introduction

Nowadays stainless steels can be found in almost every manufacturing field. Their application range can reach from the food- to the automotive industry. Its incredible physical and chemical properties and inexpensive price comparing to other non-corrosive materials are the main reasons of wide usage. Despite that a piece of raw material can`t be directly used in most applications. It has to be changed to a desired final shape. There are many processes where one can change the size and shape of raw material and machining is one of the widely used processes.

Machining is a cutting process where a raw material is cut into a desired shape by a controlled material removal. There is a need for a cutting tool to cut a workpiece material. To cut a raw material, cutting tool must be hard enough. So, it means the main selection criteria to choose proper cutting tool is the cutting tool material. One of the widely used cutting tool material is cemented carbide and it`s general choice to machine stainless steel. As stainless steels are considered as difficult-to-machine materials, rapid tool wear and high cutting temperature are the main problems [1].

One of the main reason for rapid tool wear is built-up edge (BUE), in other words, accumulation of workpiece material on the tool edge. These adhered or welded particles on the tool edge changes the position of the cut. Additionally, the BUE can damage the machined surface when it`s pressed under the flank face. Tool wear can be observed when BUE breaks away from the cutting edge and tool material can be torn away with broken BUE. Therefore it is important to learn about this phenomenon, its formation conditions and how to avoid. Figure 1.1 [2] shows a schematic diagram of built-up edge formation.
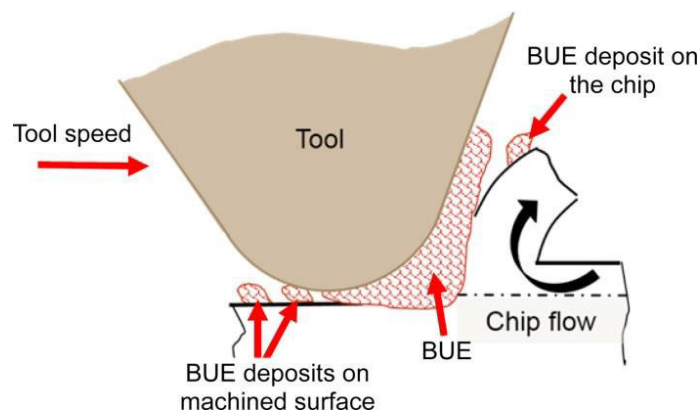
Figure 1.1 *Schematic diagram of BUE formation during machining processes [2]*

1.1   Purpose

The goal of this thesis work is to increase the knowledge regarding BUE during milling of stainless steel. As the representative of stainless steel, AISI 304 has been chosen since that type of stainless steel has a high tendency to form an unstable BUE. Thesis work is based on following hypothesis:

- BUE formation and its properties vary at different milling conditions and there is defined cutting speed and feed where BUE starts to form.

Based on hypothesis thesis searches for an answer to the following question:

- How much coolant usage effects BUE formation?
- How much BUE effect to cutting tool durability (tool life)?

1.2   Thesis outline

Thesis is divided into 5 main sections. Section 2 is a description of the current state and it consists of two main parts.

The first part provides the overall background of AISI 304 stainless steel, its machining and tool wear. The background is followed by describing BUE, its formation and effects. In the second part is a collection of previous work concerning milling and BUE formation of AISI 304 steel. Design methods, performance of experiments and characterization are described in Section 3.

The results are evaluated and discussed in Section 4. Finally, in Section 5, there is overall conclusion consisting of main details and features of this study.

2. Description of the current state

2.1 Stainless steels and their classification

Stainless steels are iron-base alloys containing 10.5% or more chromium (Cr). Chromium is the main alloying element that improves corrosion-resistant quality by combining with oxygen and forming a thin, transparent chromium-oxide protective film on the metal surface. Other alloying elements may be added during melting, such as nickel, molybdenum, titanium, which serve to change or enhance certain properties or characteristics. According to metallurgical structure, stainless steels can be divided into five categories: austenitic, ferritic, martensitic, precipitation hardening and duplex.

Austenitic stainless steels contain chromium and nickel as the principal alloying elements. Some of the nickel can be replaced by manganese. According to AISI (American Iron and Steel Institute), they are identified as AISI 200 series or 300 series types, respectively. As heat treatment serves to soften austenitic stainless steels, they can be hardened only by cold working. They are not magnetic in the annealed condition. To improve machining characteristics sulphur and calcium can be added where increase in the nitrogen content can enhance strength characteristics.

Ferritic stainless steels are steels with low carbon-to-chromium ratio and they are identified by 400 series types.

Category with having higher carbon-to-chromium ratio than the ferritic group is called martensitic stainless steels [3].

2.2 Machining and milling

Machining is one of the technologies of manufacturing, as described in Figure 2.1 [4]. The term manufacturing is used to describe the industrial activity that changes the form, size, shape and surface quality of workpiece to create a finished product. Machining is the unwanted raw material removal to obtain a finished product by using cutting techniques [4]. An idealized cutting model is demonstrated in Figure 2.2 [5]. In general, there are factors that have an influence to the cutting process. In order to identify factors, it`s possible to divide machining process agents into two types of variables, independent and dependent, respectively. The major independent variables: tool material and coatings; tool shape;
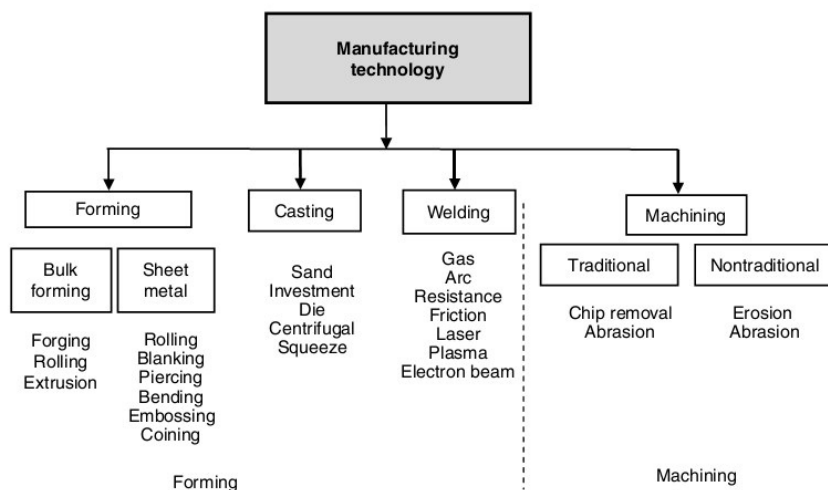
Figure 2.1 Classification of manufacturing processes [4]

workpiece material and condition; cutting parameters; cutting fluids; machine tool characteristics; work holding.

Those variables that are influenced by changes in the independent variables are dependent and include: tool wear/failure; cutting force; types of chip produced; surface finish and its integrity.

(a)   *(b)*
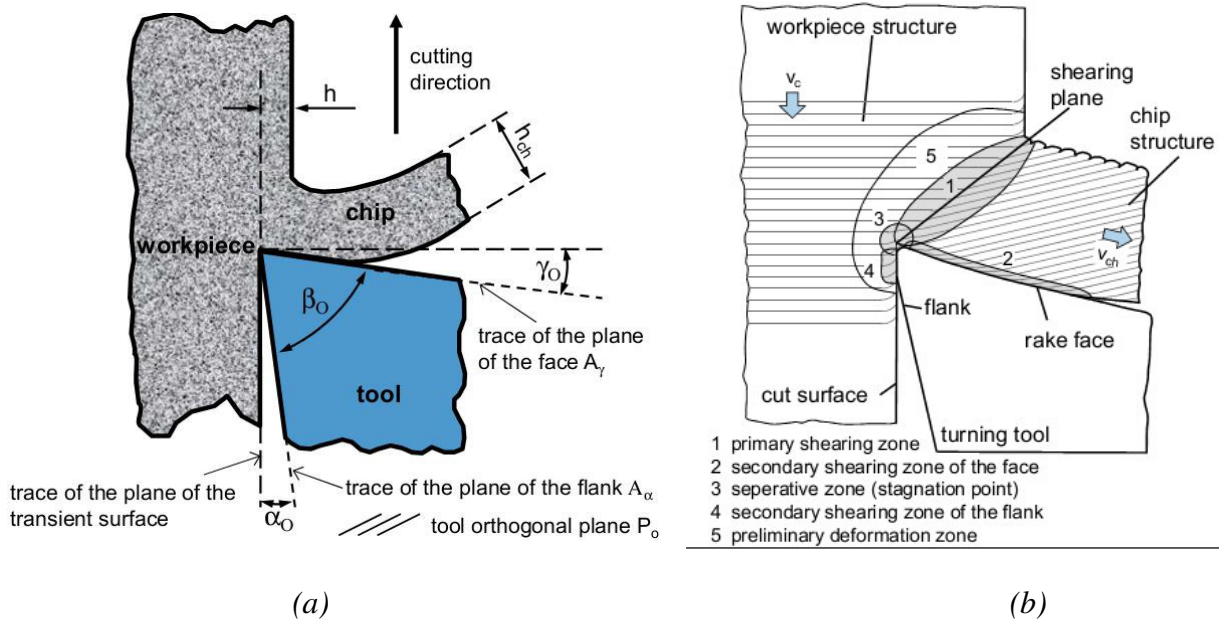
Figure 2.2 *Idealized cutting model: (a) chip formation (b) shear zones in cutting process [5]*

A chip is formed ahead of the tool by plastic deformation and shearing action on material along the shear plane in the primary shearing zone and there is a close dependence of the nature of chip formation to workpiece material properties. For example, shorter chips are produced during a brittle material machining, such as cast iron where a ductile material, such as austenitic steels produce longer chips. In general, continuous and long chips are not preferred as they are not easily controllable [6].

One of the most flexible machining processes is milling, in which a milling cutter removes material by moving along various axes with respect to the workpiece. When the rotation axis of a cutter is parallel to the workpiece surface, it can be called as peripheral milling, when it is perpendicular to the surface, it is face milling. These two classes are considered as a major [6]. In general, the cutting edges or teeth cut into and exit from the material repeatedly, meaning that the tool is always partly engaged during cutting. This leads to temperature variations at the cutting edge which in turn the cutting edge is subjected to thermal shocks. It can result in cracking or tool failure [7]. That is why milling is considered as a complicated machining process.

The cutting process is apparently influenced by changing the cutting parameters of milling. They can be defined as cutting speed (v_c) in [m/min], feed per tooth (f_z) in [mm/tooth], axial depth of cut (a_p) in [mm], radial depth of cut (a_e) in [mm], specified diameter of cutter (Dc) in [mm]. Some of them are demonstrated in Figure 2.3.
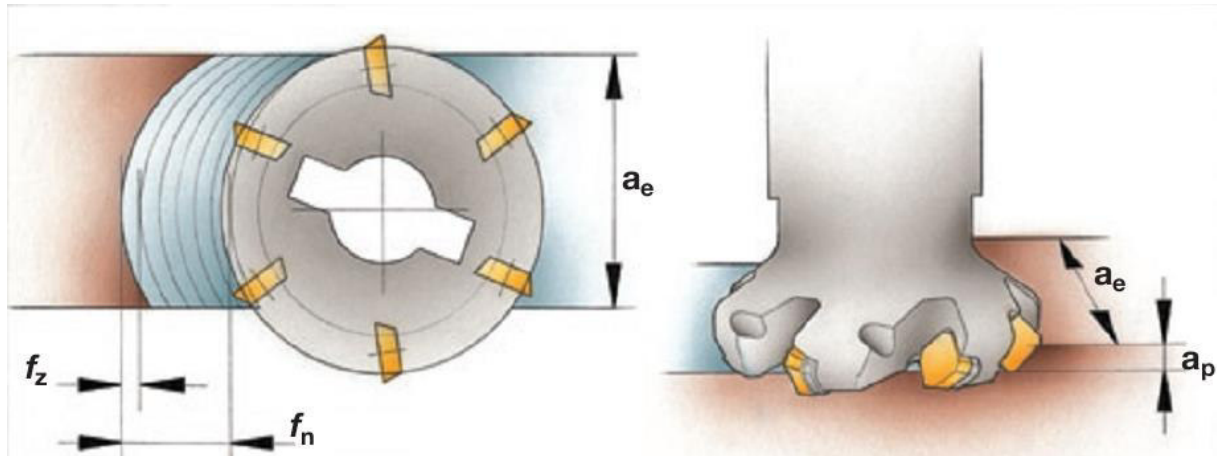
Figure 2.3 *Face milling parameters [8]*

2.3   Austenitic stainless steel machinability

The term "machinability" can`t be defined using a single parameter, meaning it is related to physical and chemical properties of the material as well as the manufacturing process used to produce a part. Usually, to rate the machinability parameters such as cutting speed, tool life or surface finish is considered. A brief definition of machinability is shown in Figure 2.4.
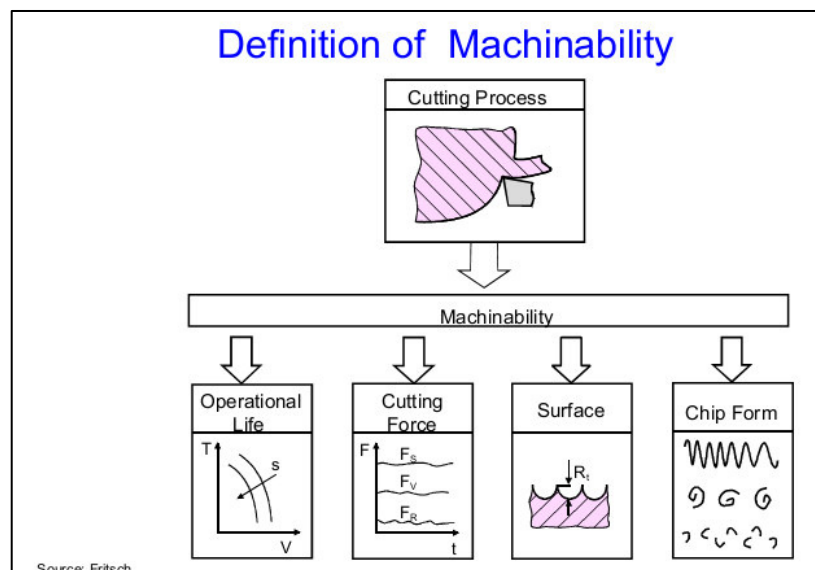
Figure 2.4 *Definition of machinability [9]*

AISI 304 is an austenitic stainless steel and relative machinability of austenitic stainless steels is described in Figure 2.5. According to it, austenitic type has about 60% of relative machinability comparing to other types of stainless steels. It is mainly because of higher friction coefficients, toughness, poor chip breaking and very rapid work hardening properties [3]. Low thermal conductivity generates a lot of heat in cutting area. A large area of ductile strain is the cause for long, tough and continuous chip formation which is difficult to break. Austenitic steels are usually machined in either quenched or solution-annealed state [10].

10

Transformation from austenite to martensite during deformation leads to rapid work-hardening rate. Machinability is improved by adding alloying elements, such as sulfur, calcium or copper [17].
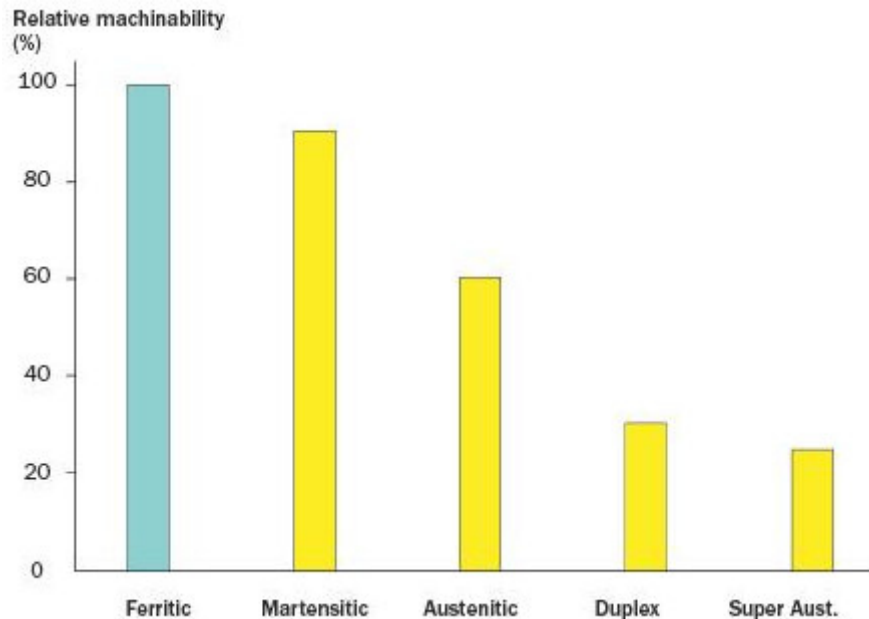
Figure 2.5 Relative machinability of stainless steels [8]

According to one of the leading tool manufacturer "Seco", mechanical cutting forces in machining austenitic stainless steels are not higher than typical traditional steels and the most of the energy consumption to machine austenitic stainless steel is the result of its thermal properties [11]. Austenitic stainless steel is a deformation-resistant steel. This property causes more heat generation during machining since metal cutting is a deformation process. Usually, most of the generated heat is absorbed and carried away by chips. But as austenitic stainless steel has a low thermal conductivity, produced chips can absorb a heat in a limited proportion. As a result, other portion of heat is distributed into the cutting tool, leading to a short tool life.

As stated above, austenitic stainless steel has a limit on heat absorption. More heat can be absorbed by chips when larger chips with higher volume are produced. In this case, the heat absorbed by each cubic millimetre of chip material increases. Larger chips can be achieved by applying the largest possible cutting depth and feed rate [11]. By applying it, the number of cutting passes can be also decreased. Decreasing the number of passes is the another important issue because of work-hardening property of austenitic stainless steel. But there are some factors which limit to apply the largest cutting depth and feed rate and some of these factors are strength of cutting tool, surface finish requirements, power available from the machine tool and etc.

During machining of ductile austenitic steels, burr formations become a serious problem. For components that are expected to be produced burr-free, up to 20% of production costs may result from burr removal [10].

2.4   Tooling for austenitic stainless steel machining

One of the important factors during planning a successful cutting operation is a tool material and grade selection. The selection is based on the workpiece material to be machined, the component type and shape, machining conditions and the level of surface quality required for each operation.

During machining operation, the cutting tool is subjected to high contact stresses, high and rapid varying temperatures. There is a high friction along tool-chip interface and along the machined surface. As a result, the cutting tool must own the characteristics such as hot hardness where the shape and sharpness of the tool under high temperatures is ensured. In addition, tool must have enough toughness and impact strength, so that impact forces on the tool do not chip or fracture the tool. High impact forces is mostly observed repeatedly in interrupted cutting operations such as milling. Other properties such as thermal shock resistance, wear resistance, chemical stability should also be taken into account to avoid tool-chip diffusion [6].

Essential rule during austenitic stainless steel machining is to keep a cutting tool sharp. As noted above, austenitic stainless steel has a high deformation-resistance property. Deformation caused by tool generates more heat. Therefore, using sharp tool increases the chance to cut the material than deforming it. In order to get sharp and accurate face angles, careful grinding and honing of the tool faces is important. As a result, tool life and workpiece accuracy is optimised. Tool breakages and power requirement is reduced. Correct tool geometry helps to minimise build-up edge formation on the tool. As austenitic stainless steels are prone to produce long spiral chips, it`s highly recommended to use tools with chip breakers. Chip breakers can prevent from chip jamming or become entangled around the tool.

In order to achieve successful machining, not only workpiece – cutting tool – machine tool relationship should be considered, but cutting condition and cutting environment should be also taken into consideration. Coolant usage is one of the such cutting condition and it`s a practical way to prevent more heat generation. A high quality coolant with 8-9 percent oil content in an oil/water emulsion with high pressure makes a remarkable improvement on surface finish and tool life [11]. It`s important to have a high-pressure stream of coolant directly to the cutting zone. There is a continual research on tool development to make a coolant supply more efficient. Internal coolant ducts directly in the tools, high pressure application has many benefits in terms of tool life and surface quality. In addition to usual coolant, MQL (Minimum Quantity Lubrication) usage can help to minimize re-welding of the material and significantly improve the surface quality of machined austenitic steels. As a medium, synthetic ester oils are used [10].

One of such tools with high pressure coolant in stainless steel machining is turning tool by Walter Tools which is described in Figure 2.6, namely Precision Cooling (-P) turning tool [11]. Tool holder is equipped with direct coolant ducts that makes possible to stream coolant directly to cutting zone at high pressure.
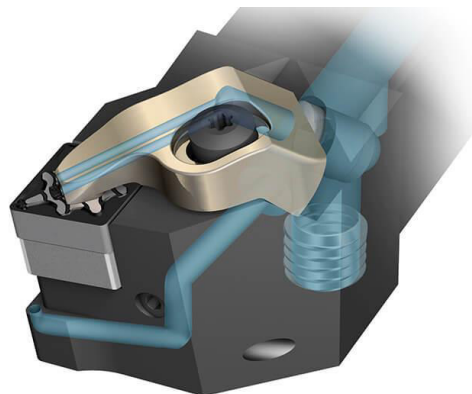
Figure 2.6 *Precision cooling (-P) turning tool by Walter Tools [11]*
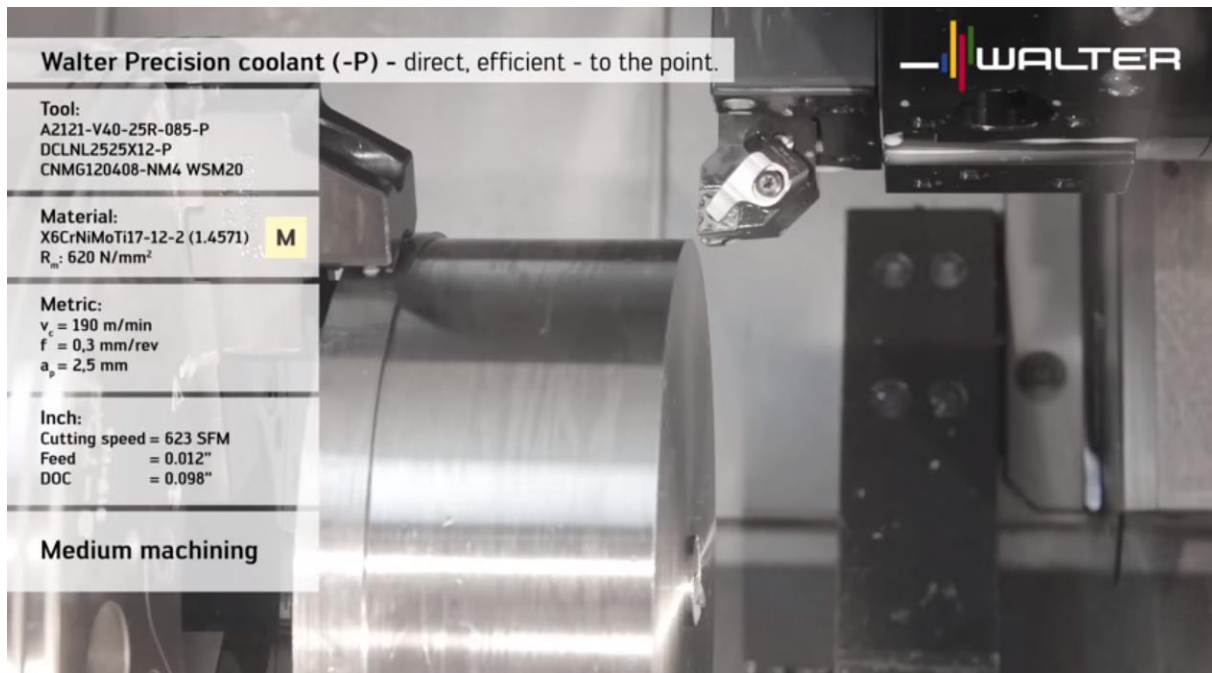
Figure 2.7 Chosen parameters for medium turning by Walter Tools [13]

In order to test the inovated tool and to define high pressure coolant impact on machining, the trial was done by Walter Tools. As a workpiece material, austenitic stainless steel was chosen. Cutting parameters for turning, tool data and workpice material data is shown in Figure 2.7. Two types of coolant supply are used with different turning tool holders, namely, external and precision (or direct). Additionally, two types of pressure are applied with precision cooling turning tool: 20 bar and 80 bar. Carbide insert grade and geometry used was the same for all 3 cases. After certain time of turning, an indexable insert condition (e.g., tool wear) was checked and compared. According to Figure 2.8, better results are achieved in terms of tool wear with Precision cooling (-P) turning tool by Walter Tools with internal cooling. Even the lowest tool wear is achieved with increased pressure of coolant. Moreover, it`s possible to define slight build-up edge formation even with direct coolant application at 20 bar of coolant pressure. By increasing the pressure to 80 bar, build-up edge on the cutting edge disappeared. The worst case of build-up edge and the highest amount of tool wear is observed on conventional tool holder with external coolant comparing to two other cases.

Chip formation during austenitic stainless steel finish turning was also observed by using the same tool holders, but different carbide insert grade and geometry. The pressure values are kept the same. Tool data with cutting parameters and workpiece data is shown in Figure 2.9. Different formed chips can be seen in Figure 2.10. Relatively shorter chips are achieved with Precision cooling (-P) turning tool at coolant pressure of 80 bar.

From this experiment it can be concluded that the direct coolant with high pressure application has a significant impact on stainless steel machining in terms of tool life and chip formation. Substantial improvements can be observed with pressure increasing.
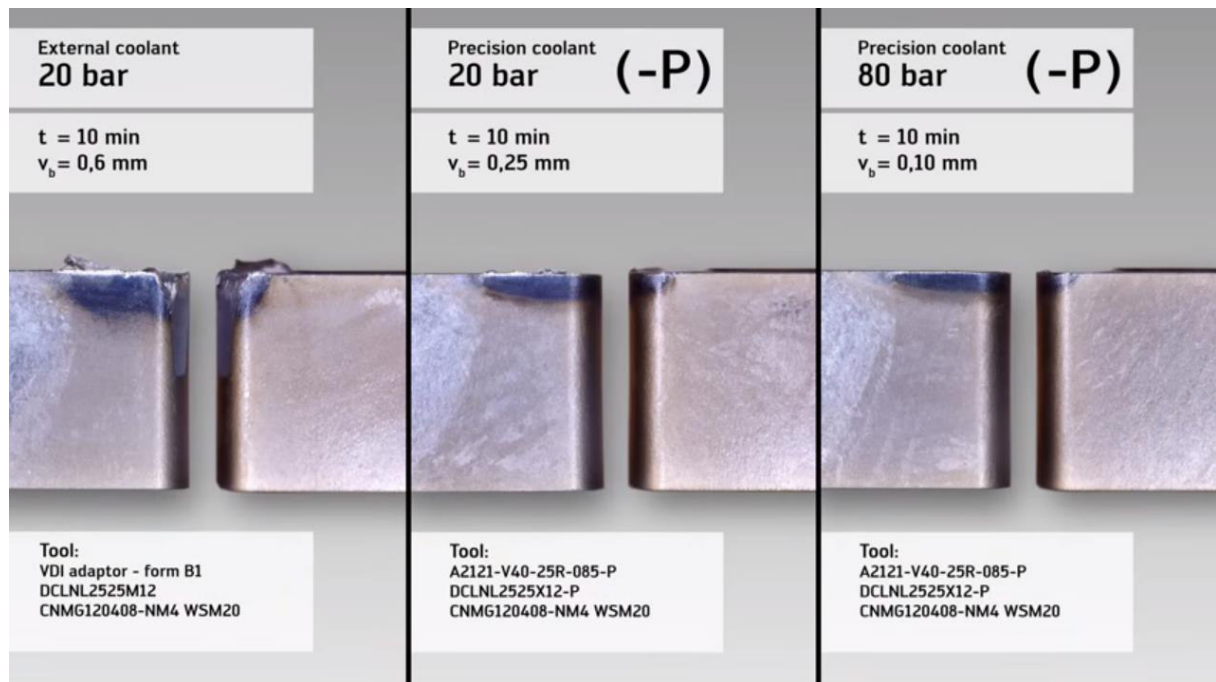
(a)   *(b)*   *(c)*

Figure 2.8 *Tool wear comparison on medium turning:(a) Tool wear of insert on conventional tool holder with external coolant 20 bar; (b) Tool wear of insert on Precision cooling (-P) turning tool holder with direct coolant 20 bar; (c) Tool wear of insert on Precision cooling (-P) turning tool holder with direct coolant 80 bar [13]*
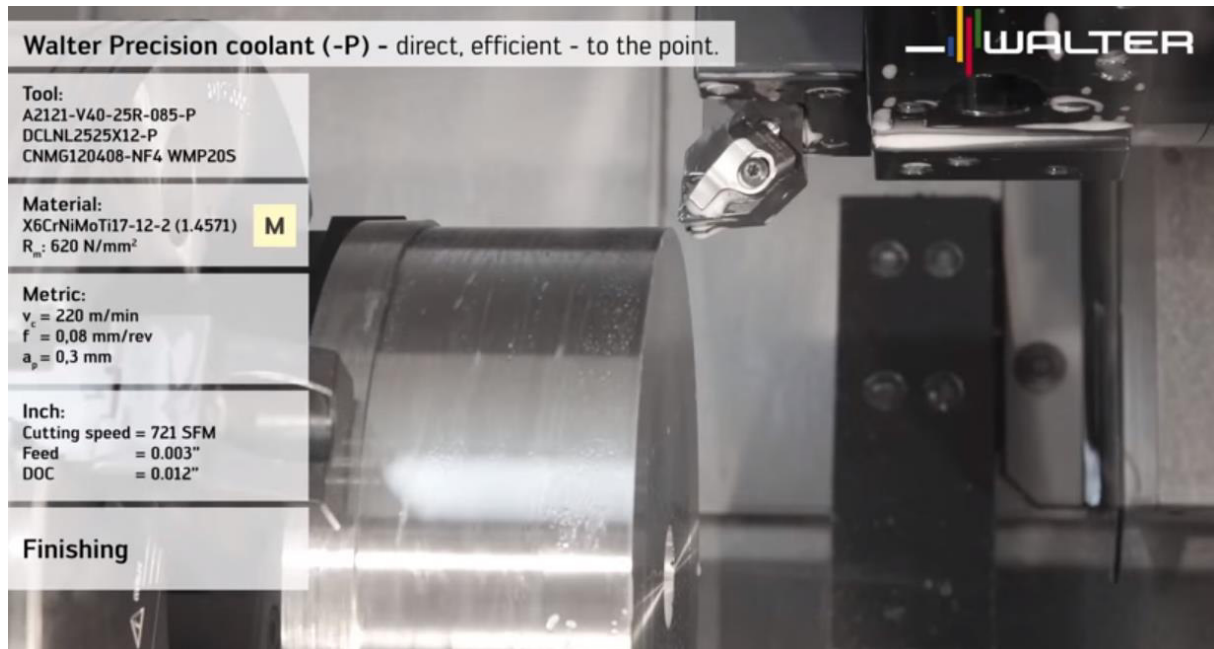
Figure 2.9 *Chosen parameters for finish turning by Walter Tools [13]*

Another method to increase tool life, workpiece quality and productivity is applying surface coatings to the tools and nowadays coated tools constitute the majority of the cutting tools. During a coating process, a very thin layer (in micrometers) is adhered to the cutting

(a)   *(b)*   *(c)*
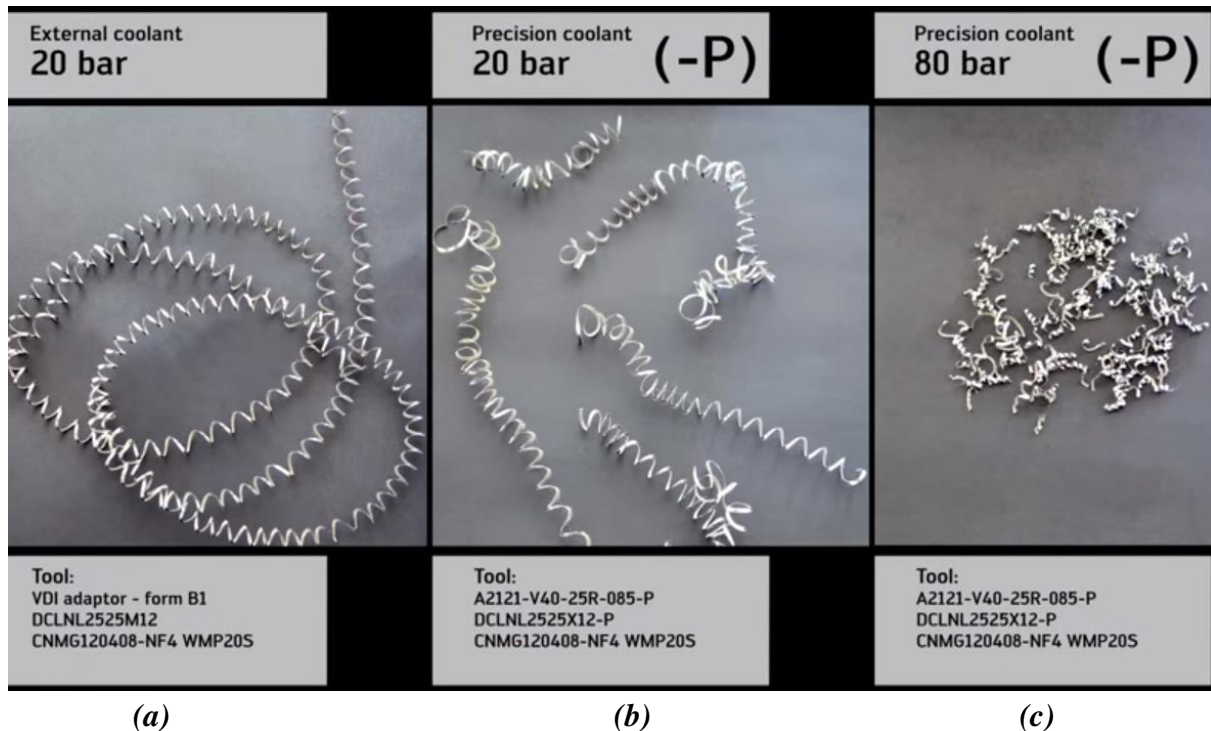
Figure 2.10 Chip formation comparison finish turning by Walter Tools: (a) Chip formed when conventional tool holder with external coolant 20 bar is used; (b) Chip formed when Precision Cooling (-P) turning tool holder with direct coolant 20 bar is used (c) Chip formed when Precision Cooling (-P) turning tool holder with direct coolant 80 bar is used [13]

tool surface. Coatings are applied by using Physical Vapor Deposition (PVD) and Chemical Vapor Deposition (CVD) processes.

PVD is a vacuum coating process in which an employed material is physically removed from a source (where it can be solid or liquid) by evaporation in the form of atoms or molecules. After that, it is transported in the form of vapor, and condensed as a film on the surfaces of placed parts under vacuum. Chemical compounds are deposited by either using a similar source material, or by introducing reactive gases such as nitrogen, oxygen, containing the desired reactants, thus reacting with metal from the PVD source [14]. The temperature that PVD coatings are applied to cutting tools is in the range of 450-550 °C.

Unlike to PVD process, chemical vapor deposition (CVD) is a heat-activated process based on the reaction of gaseous chemical compounds with appropriately heated and prepared substrates [14]. Typical deposition temperatures range from 800 to 1200 °C. This high range of temperature allows a strong bond of coating with the substrate. Comparing to PVD process, thick layers are produced in CVD process. Layer thickness and its uniformity is influenced by deposition temperature and deposition rate.

As noted above, austenitic stainless steels have a tendency to adhere to the cutting tool since they have a high ductility. This property leads to use tools with sharp cutting edges. In general, coating must be thick enough to insulate the tool substrate from the heat, but the thick coating does not adhere well to a sharp geometry. Since thin coatings are produced by PVD process at lower temperatures, sharp cutting edges is retained after coating process which makes PVD process essential for stainless steels machining. In addition, PVD coatings have a relatively smooth surface that generates less frictional heat and PVD coating resists build-up edge formation.
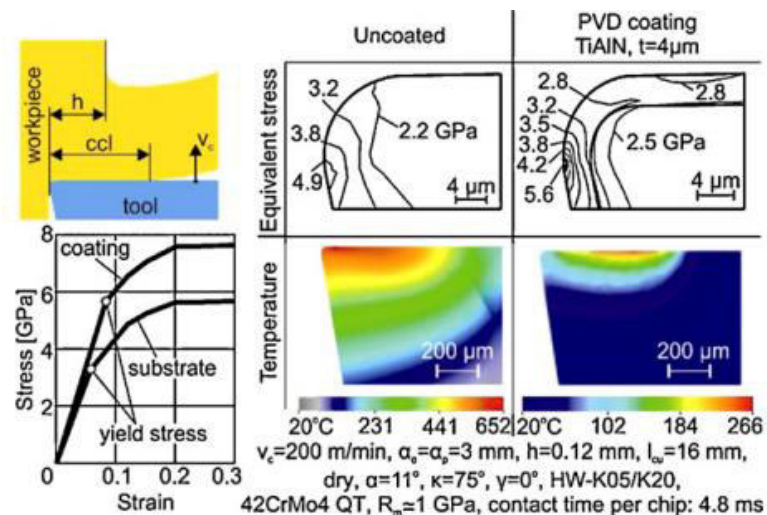
Figure 2.11 Mechanical and thermal loads comparison of coated and uncoated tool[14]

Advantages of coated tools in terms of mechanical and thermal loads can be explained in Figure 2.11. During milling of hardened steel, the maximum equivalent stress in the TiAlN PVD coating on cemented carbide insert reaches 5.6 GPa on the cutting edge rounding close to the flank, remaining below the film yield stress (5.9 GPa) [14]. In addition, the substrate of coated tool is less stressed (max. equivalent stress ≈ 3 GPa) comparing to the uncoated tool where stress of 4.9 GPa exceeds its yield strength of ≈ 3.2 GPa. Subsequently, this leads to wear growth acceleration in uncoated tool. Heat or maximum temperature that is transferred to the tool is relatively higher in uncoated tool (652 °C) comparing to coated tool (266 °C) during tool-chip contact time of 4.8 ms [14].

Titanium nitride (TiN), titanium carbonitride (TiCN), titanium aluminium nitride coating are the most widely used PVD coatings for stainless steel machining. With the addition of chromium (Cr) to (Ti, Al)N coating, nano-crystalline AlTiCrN coating is formed and it has competitive mechanical strength, thermal stability, chemical inertness and oxidation re-sistance up to 1100 °C [15]. Nowadays, tool manufacturers make an investigation to define such coatings that are thin but at the same time are good barriers against heat during stainless steel machining. Technical parameters of some widely used coatings are described in Table 2.1. According to it, Al_2O_3 coating has a competitive resistance to adhesion and it is a good thermal barrier to heat and these properties are mostly required during austenitic stainless steel machining.

Traditionally, cutting parameters that are recommended by tool manufacturers are based on toughness and hardness properties of material. But for machining austenitic stainless steels and other high-performance alloys thermal factors also should be taken into account since austenitic stainless steel has a low thermal conductivity. Tool manufacturers currently co-operate with academic instutions to perform tool testing procedures by taking into account certain materials` thermal characteristics [11].

The cutting tool materials that are described below are used mostly for austenitic steel machining in industry with a high rate of production which is equipped with modern CNC machines. Widely used tool material for austenitic stainless steel machining is uncoated or coated conventional WC-Co cemented carbide or WC-Co with composite carbide concentra-tion. Cermets are used especially for semi-finishing and finishing operations and nowadays high speed steels have a limited use in austenitic steel machining. Usually PCBN tools are not used to austenitic steel machining as it can stick to the cutting edge.

16

	TiN	TiCN	TiC	TiAlN	CrN	Al_2O_3
Production process	PVD/CVD	PVD/CVD	CVD	PVD	PVD	CVD/PVD
Coating thickness/μm	1 to 5	1 to 5	1 to 5	1 to 5	1 to 10	1 to 5
Microhardness/HV 0,05 [1]	2300	3000	3100	3000	1900	2100 HV 0.1
Oxidation temperature/°C [2]	> 450	> 350	> 350	> 700	> 600	– [3]
Thermal barrier effect [4]	+++	++	+	++++	+	+++++
Resistance to abrasion	++	+++	+++	+++	++	++
Resistance to wear due to adhesion (against steel)	++	++	+	++	++	+++
Resistance to wear due to diffusion (to steel)	++	+	+	+++	++	+++
Protection of basis material against corrosion [5]	+	+	+	+	++	+

[1] For the microhardness, mean values are indicated. They are obtained from reported measured values resulting from different compositions, coating thicknesses and internal stresses.

[2] The oxidation temperature is the temperature at which oxidation of the coating material begins, considerably affecting the characteristics of the coating.

[3] Al_2O_3 is already an oxide.

[4] Being poor conductors of heat, the coatings act as a thermal barrier to the heat produced during metal-cutting so that most of the heat can be removed through the chip.

[5] As the aforementioned hard coatings themselves do not corrode, they protect the basis material from corrosion. (Leaks in hard coatings may lead to the development of local galvanic elements and to pitting corrosion).

Table 2.1 Technical parameters of different coatings acc. to VDI 3824/1 [10]

Actually, PCBN tools are intended to machine workpiece materials harder than 48 HRc. When machining materials with lower hardness, the higher Fe content in the materials can lead to increase a chemical wear [10].

Cemented carbide tools

Cemented carbide is a powder metallurgical material consisting of hard phase of tungsten carbide (WC) in a cobalt (Co) binder matrix. The microstructure of cemented carbide which is shown in Fig. 2.12 can be divided into three phases: alpha-phase with hard particles of tungsten carbide; beta-phase consisting of cobalt and gamma-phase, usually consisting of titanium carbide (TiC), tantalum carbide (TaC), niobium carbide (NbC) and these carbide elements added to improve hot hardness [8].
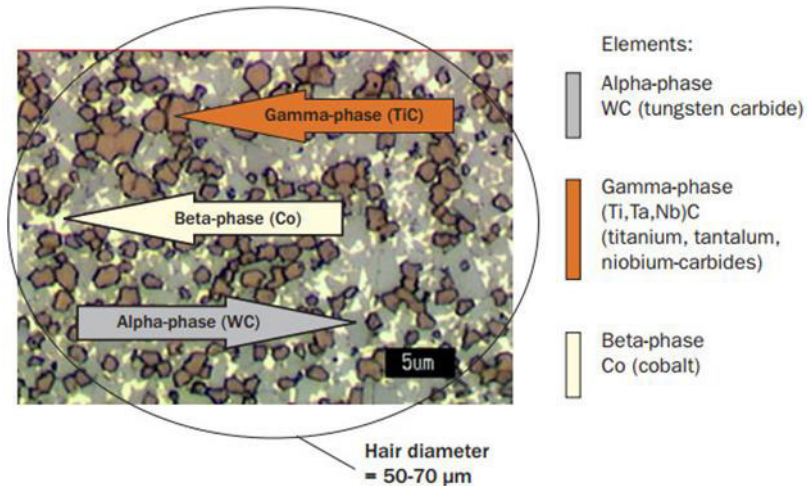
Figure 2.12 *Cemented carbide microstructure [8]*
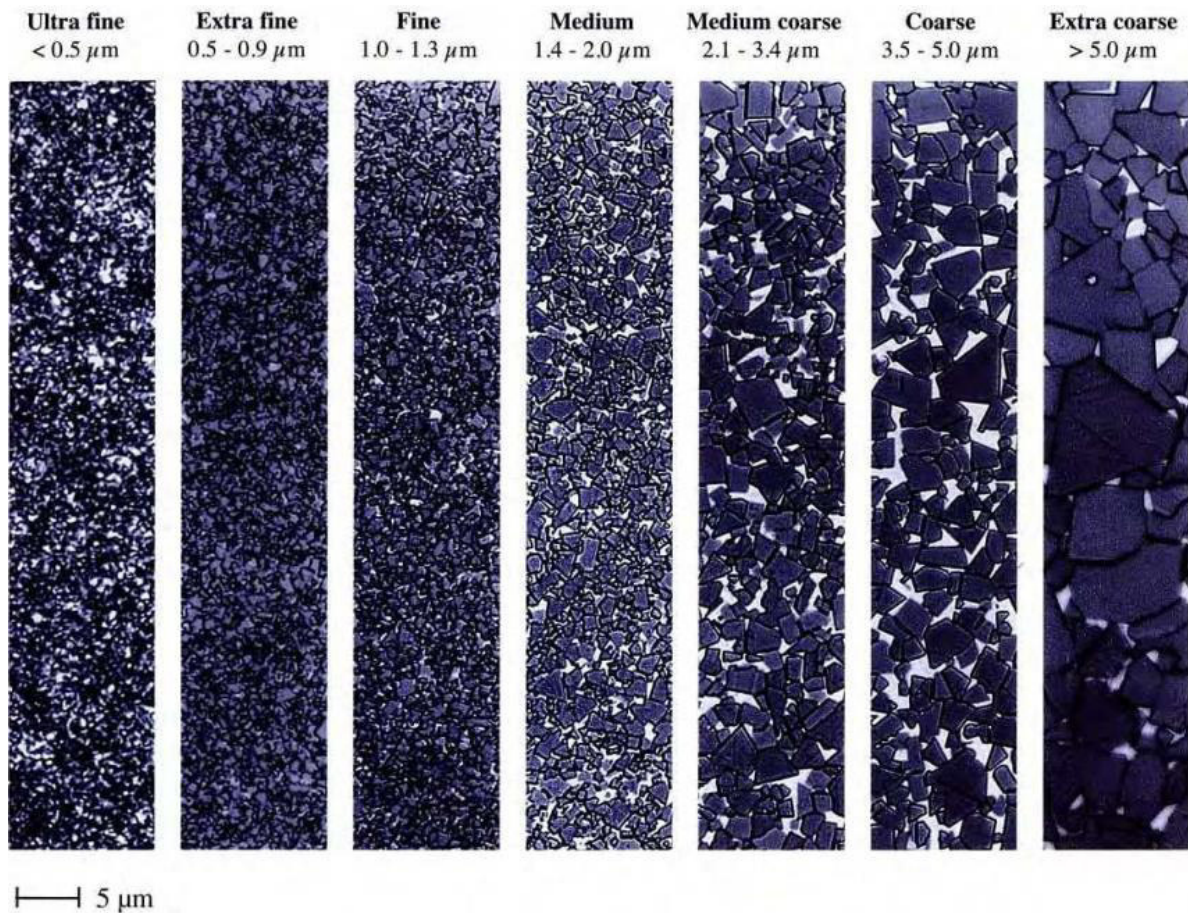
Figure 2.13 *Grain size classification, Sandvik Hard Materials [8]*

The first cemented carbide tools were used around 1930 [6]. From that time, trials and experiments were made to improve strength and toughness of carbide tools since they are abrasive and chemically reactive with other materials. Machining efficiency and improvement in performance was achieved by using coated tools in 1970s and nowadays they are used in 40 to 80% of all machining operations [6].
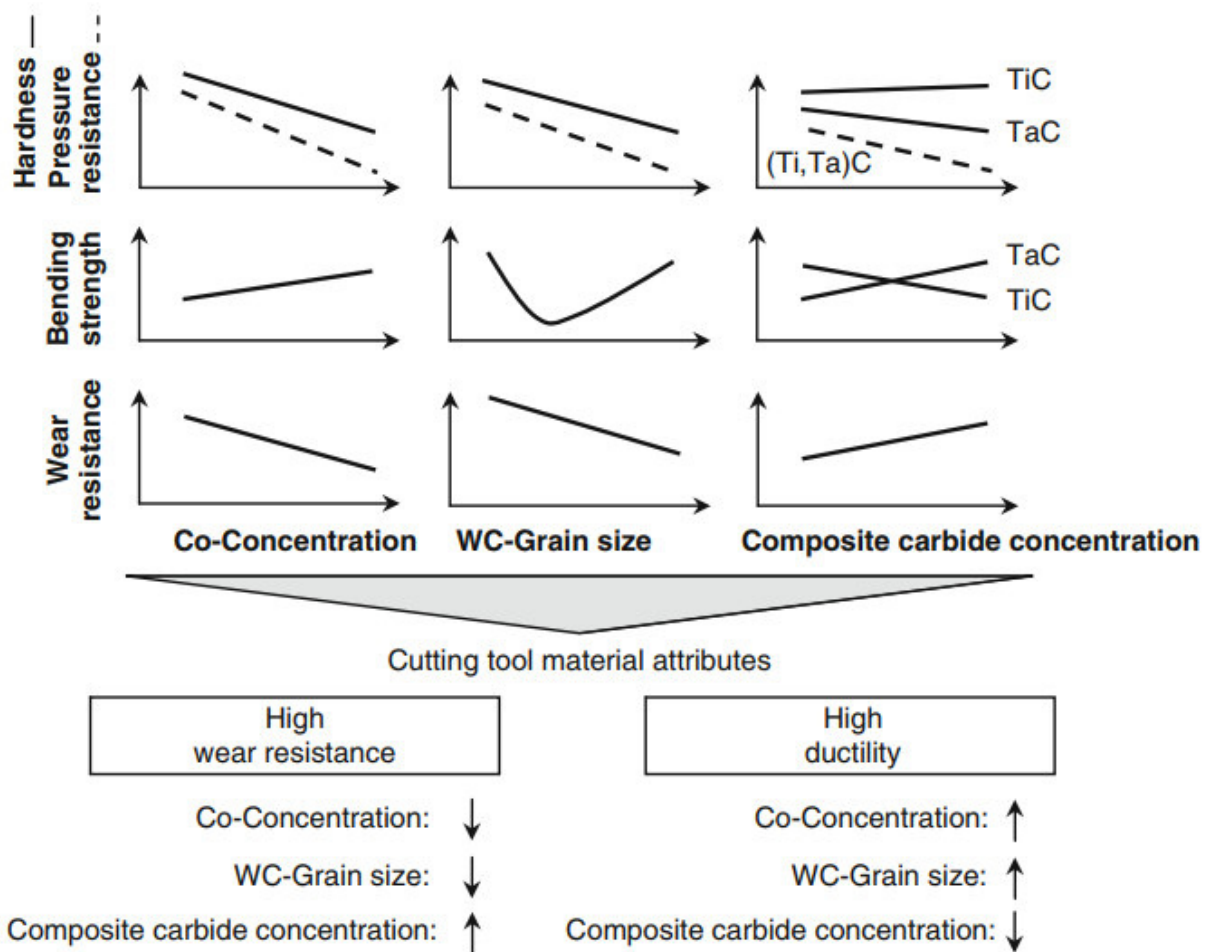
Figure 2.14 *Influencing factors for wear resistance and toughness of cemented carbides [10]*

The characteristics of the cemented carbide is determined by the grain size of WC and the amount of binder phase. Grain size classification according to Sandvik Hard Materials can be seen in Figure 2.13. Additionally, nano-grain (<0.2 µm) carbide is being developed for very small tools and to machine exotic materials [16].

Typical Co content in cemented carbide ranges from 4 to 15% of total weight [8]. With the increasing content of cobalt (Co) and grain size, fracture toughness can be increased, but it causes lowering the hardness and wear resistance at the same time [8]. Influence of WC grain size, binder phase (Co) and composite carbide concentration to toughness and wear resistance is shown in Figure 2.14.

Abrasive wear resistance can be increased with increasing TiC content in cemented carbides. Fracture toughness can be achieved also with coarse grain WC but since it has less wear resistance than finer grades, it is used primarily in roughing operation [16].

Fine grade cemented carbides are still used in the areas where cutting edge sharpness and toughness is on demand such as steel milling, finishing, grooving and parting-off operations. But extra-fine and ultra-fine grades are much better comparing to conventional fine-grain cemented carbides in hardness, toughness, edge strength. With reduction of WC crystallite size below 1 µm with equal binder content, increase in hardness and bending strength is achieved [10].

19
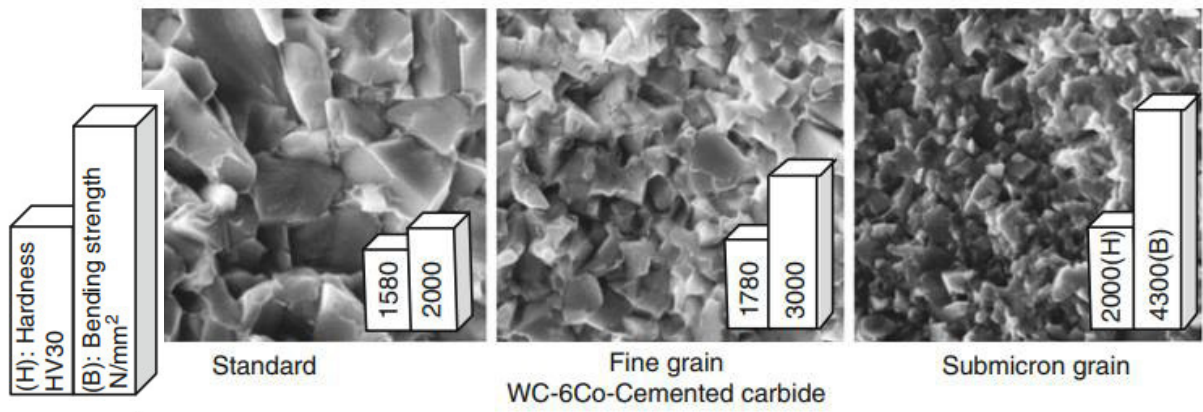
Figure 2.15 *Comparison of microstructure and properties of different grain sized WC-Co cemented carbide*
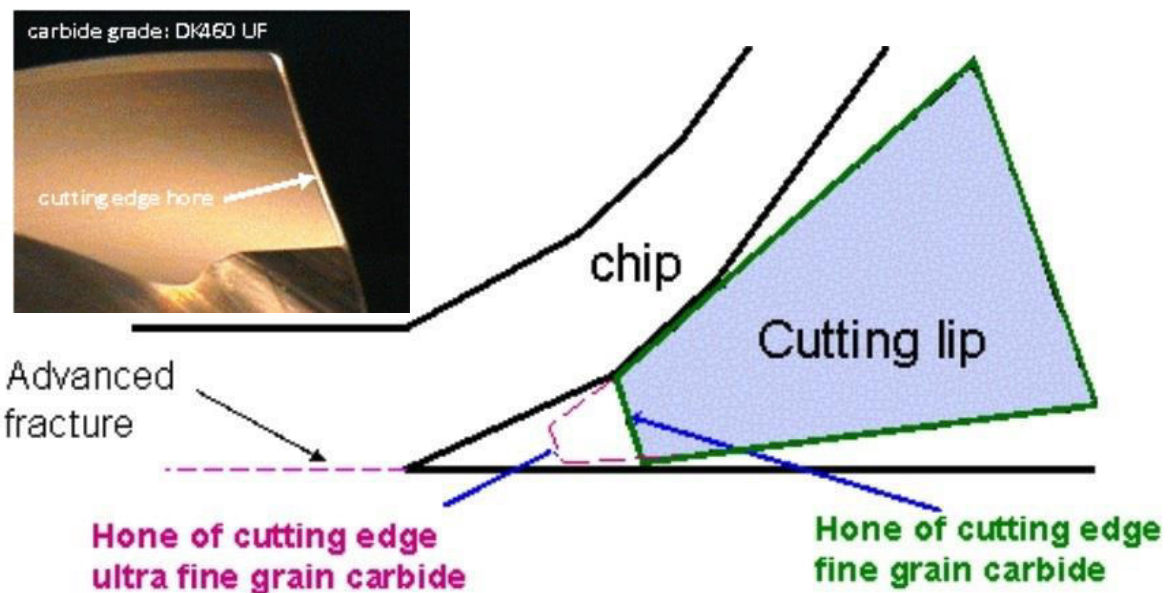
Figure 2.16 *Grain size influence on edge honing. Drill with carbide grade DK460 by Gühring KG [19]*

This special combination of properties can be seen in Figure 2.15. In addition, ultra-fine grain cemented carbides have a small inclination to adhesion and to wear by diffusion [10].

Moreover, sharper edges be achieved with ultra-fine grain carbide grades since that type of grain makes smaller hone width possible during cutting edge honing process. Cutting edge honing is cutting edge preparation process and it is used to reduce fracturing on the cutting edge. As it can be seen in Figure 2.16, sharpness of cutting edge is decreased with increase in honing width. So, smaller hone width retains sharper cutting edges.

In case of WC-Co cemented carbide, both, uncoated and coated tools are used for austenitic stainless steel machining. When uncoated carbide tools are used, relatively low cutting speeds are applied (v_c < 100 m/min) [10]. For instance, in austenitic stainless steel turning, crater wear formation on the rake face is observed with the increasing of cutting speed and it is shown in Figure 2.17.
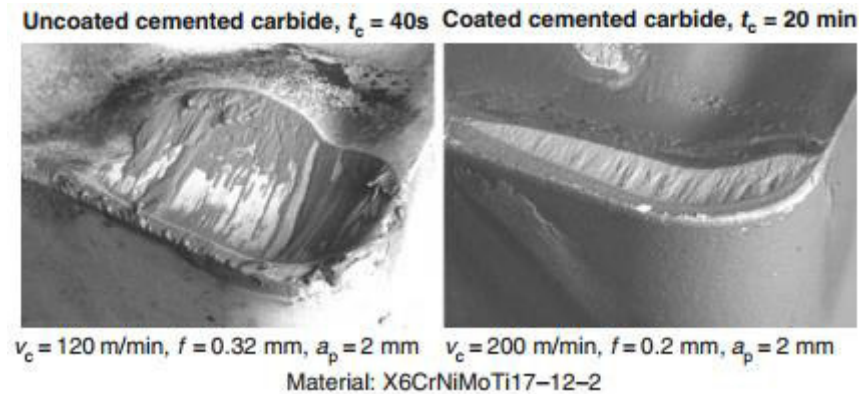
Figure 2.17 *Formation of crater wear on uncoated and coated cemented carbide in austenitic stainless steel turning [10]*

Uncoated WC-Co cemented carbide itself is prone to diffusion with steel materials at high temperatures. Diffusion phenomena between uncoated WC-Co cemented carbide and steel is presented in Figure 2.18. Diffusion leads to material bonding. And material bonding in turn activates build-up edge formation in the contact zone. After specific time of contact, crater wear occurs on the rake face as a result of the abrasive effect of the chip on the substrate.
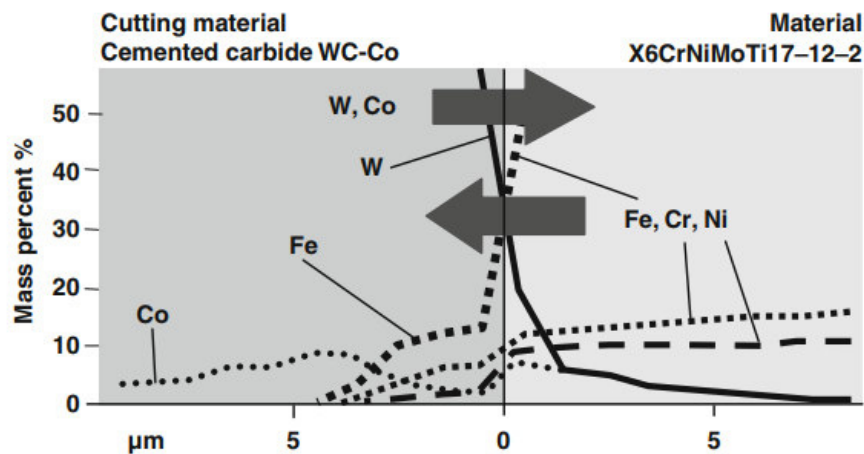
Figure 2.18 *Diffusion phenomena presentation in cemented carbide tools and steel [10]*

The most effective way to reduce crater wear is to use coated cemented carbide [10]. Coating prevents direct contact between the substrate and workpiece material. As it is shown in Figure 2.17, crater wear with smaller area is still present with coated tool also. Because diffusion process still occurs with TiN or TiCN coating layers. The reason can be explained with materials` crystal structure. Austenitic stainless steel has a face-centered cubic crystal lattice. Tungsten carbide (WC) on cemented carbides has a hexagonal crystal lattice where crystal structure of binding metal (Co) is face-centered cubic at temperature above 690 K (≈ 419 °C) and it is favorable for adhesive processes. The titanium-based coatings have face-centered cubic structures, resulting in a strong tendency to adhesion during austenitic stainless steels.

21
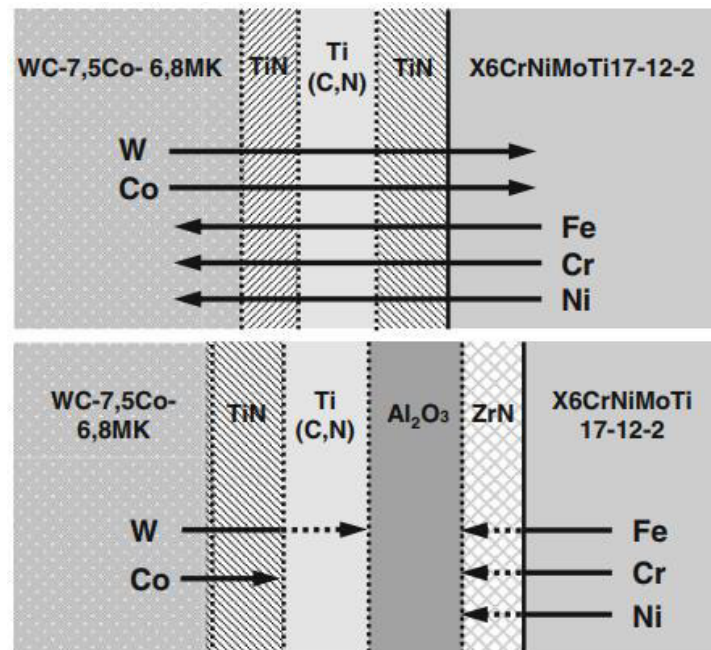
Figure 2.19 *Verification of the diffusion phenomena between coated cemented carbide and steel depending on coating on the basis of annealing tests [10]*

Consequently, the strong adhesive tendency leads to de-coating of coated tools and material loss in the tool-chip contact zone. But, according to annealing tests shown in Figure 2.19, no more diffusion takes place in the case of coated cemented carbide with aluminium oxide (Al_2O_3) as an intermediate layer. Al_2O_3 layer acts as a diffusion barrier [10]. No elements from workpiece material or from tool substrate diffused through intermediate layer Al_2O_3. Elements from workpiece material such as iron (Fe), nickel (Ni), chrome (Cr) are found in ZrN surface layer, while tungsten (W) and cobalt (Co) are found in the TiN boundary layer. The reason is explained as with electrically isolated oxide layers like Al_2O_3, migration of electrons is not possible. In contrast, in semi-conductive or conductive nitride or carbon nitride layers, electrons can be transferred through the layer, leading finally iron transfer through the layer to alloy with substrate [10].

Usually, cutting tool material and coating define heat resistance, wear resistance and a balance of hardness and toughness. On the other hand, tool geometry is more crucial. The amount of material that are being removed in a certain time, heat generation and its direction, chip formation and surface finish that are being achieved depends on the tool geometry. As stated in previous pages, a sharp edge geometry is preferred for austenitic stainless steel machining, but in terms of strength, generally, a rounded edge has more benefits than sharp edge.

Tool geometry recommendation from cutting tool making companies can be found from wide range of handbooks. Based on workpiece material and operation type (e.g., roughing, finishing) appropriate tool geometries can be chosen. One of such kind of example for carbide inserts from Sandvik Coromant is shown in Figure 2.20. Letter "M" is used to define stainless steel material group according to ISO standard designation, where letter "P" represents unalloyed, alloyed steels and steel castings. Letter "K" is used to represent cast iron. For steels machining, tools with high rake angles are used comparing to tools for cast iron machining.

Figure 2.20 *Carbide insert geometries according to type of operation [8].*

As these materials have different characteristics, there is a difference on cutting edge geometries. In general, tools that are used for steel machining have higher positive rake angles than tools for cast iron machining.

Since relationship between hardness and toughness is disproportional, cemented carbide tool development attempts to find a balance between hardness and toughness. In other words, a tool shouldn`t be so hard that it fractures but it should be hard enough to resist deformation. Main disadvantage of cemented carbide tools are their brittleness where it leads to vibration and tool chatter during machining. Another limit or restriction is bending strength reduction with increasing coating thickness and coating temperature. This reduction has a negative influence in interrupted cutting operations where cutting tool is subjected to dynamic stresses. One of the interrupted cutting operation is milling, therefore, cemented carbide grades with thinner coatings should be used in milling and thicker coatings can be used in turning. On the other hand, with reduced coating thickness, reduction of wear resistance should be expected. As stated in previous chapters, thicker coatings are produced during traditional high temperature CVD processes. It is believed that substrate properties such as toughness and composition is affected by high temperature during classic CVD process. Over the years new CVD methods are discovered. One of such CVD methods is PA-CVD (Plasma activated CVD) where coating temperature ranges from 450 to 650°C. Using this method, no changes in substrate should be expected as temperature is relatively low [10].

Cermets

The name "cermet" is the combination of the words "ceramic" and "metal". As the name suggests, a typical cermet consists of 30% of titanium carbide and 70% of aluminum oxide where other cermets contain various oxides, carbides and nitrides [6]. According to other literatures, cermets are cemented carbides based on titanium carbide (TiC) and titanium nitride (TiN) with nickel (Ni), cobalt (Co) binder phase and denoted as TiC/TiN-Co,Ni cemented carbides [10]. As stated in previous chapters, the relationship between hardness and toughness is disproportional and cermet is designed mainly to improve both of them. Metallic phase is added to improve toughness where improvement of hardness is achieved by adding ceramic

phase. As described in Figure 2.21, the structure of cermet includes only rounded composite carbide nitrides forming core/shell structure. Dark cores in the centre of the hard material particles represent TiN and it is surrounded by titanium-rich composite carbon nitride (Ti, Ta, W)(C,N). Outer lighter shell represents (Ti, Ta, W, Mo)(C,N) composite carbide. This lighter shell can be found as a light core at the same time which is surrounded by titanium- and nitrogen-rich shell (Ti, Ta, W, Mo,)(C,N). The abbreviation "HT" is used to represent cermet according to DIN ISO 513 and "P15" indicates material application group.
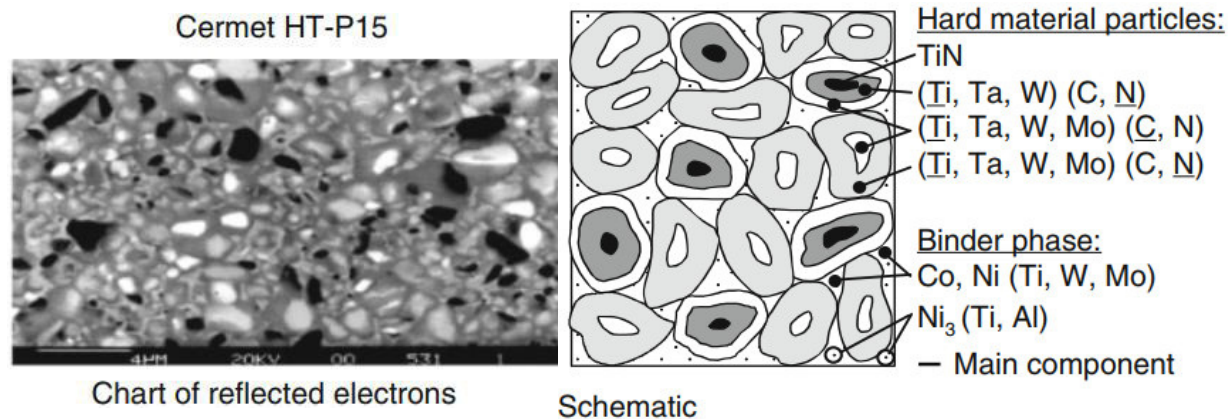
Figure 2.21 *Microstructure of cermet [10]*

Comparing to conventional WC-Co cemented carbides based on Table 2.2, cermets have a lower thermal conductivity which enables more heat dissipation with chip, resulting less heat transfer to cutting tool. In contrast, relatively higher thermal expansion coefficient leads to temperature increase inside the tool material. Consequently, high compressive and tensile stresses are formed in the cutting tool material. Later, these stresses can be a cause of comb cracks on the cutting edge, especially in interrupted cutting. In milling, tool constantly engages and exits the workpiece resulting thermal alternating stresses with rapid temperature change. As cermets are very hard and have a lower tendency to adhesion, build-up edge formation and diffusion, they are suitable to machine austenitic stainless steels.

In cermets, high temperature wear resistance is combined with high edge strength to abrasive wear. This property is special for better surface finish qualities with high cutting speeds. In recent years, tougher cermet grades development made it to expand its application field including roughing operations. In cutting technology industry, cermets are basically used in turning and in milling, but they are suitable also for grooving and thread turning [10]. During milling, it should be used dry, without coolant as they have an inclination to form comb cracks because of rapid temperature changes in interrupted cutting. To provide smooth operation, chip-breaker features are important for cermet inserts [6].

Properties	HW-K10 WC-Co cem. carbide	HW-M10 WC-(Ti,Ta,Nb)C-Co cem. carbide		HT-P10 TiC/TiN-Co,Ni cem. carbide - cermet	
Composition [mass %]	WC-6Co	WC	84.5	Carbon nitrides	85.7
		(Ti,Ta,Nb)C	9.5	Additive nitrides	0.8
		Co	6.0	Co/Ni	13.5
Density [g/cm^3] (ISO 3369)	14.9	13.1		7.0	
Hardness HV30 (ISO 3878)	1580	1700		1600	
Pressure resistance (cylinder test) [N/mm^2] (ISO 4506)	5400	5950		4700	
Bending strength [N/mm^2] (ISO 3327)	2000	1750		2300	
Young`s modulus [10^3·N/mm^2] (ISO 3312)	630	580		450	
Fracture toughness [N·m$^{1/2}$/mm^2]	9.6	9.0		7.9	
Poisson constant	0.22	0.22		0.22	
Heat conductivity [W·m^{-1}·K^{-1}]	80	83		11.0	
Coefficient of thermal expansion	5.5	6.0		9.4	

Table 2.2 *Comparison of properties of conventional cemented carbides and cermet [10]*

2.5   Main tool wear types during stainless steel milling

Tool wear rate is the most important factor to determine tool life and it is dependent on the tool wear mechanisms that occur in a specific process. The tool wear mechanism depends on the workpiece material, the machining operation, the cutting condition, the cooling/lubrication system and the properties of tool material [20]. By considering these factors, tool wear mechanism can be adhesive, abrasive, thermo-mechanical and chemical. According to conducted experiments and researches, the most common types of wear that occur during machining of stainless steel include flank wear, build-up edge (BUE) formation, notch wear and chipping due to comb cracks (thermal cracking).

Flank wear is caused by abrasive wear mechanism and it is caused by hard constituents in the workpiece material. It occurs on the flank side of the tool by wearing off the tool material as a result of shear stress from normal pressure, when the tool slides over the newly cut surface of workpiece material. It is a typical wear type and tool life can be predicted when it

Section A-A

KT

KB

KM

KF

Geometrical indicators of tool wear
VB_B – average flank wear land width
VB_{Bmax} – maximum flank wear land width
VB_N – width of notch wear
VB_C – width of flank wear at tool corner
KT – crater depth
KM – distance from the cutting edge to the deepest crater point
KB – distance from the cutting edge to the back crater contour
KF – width of the land between the crater and cutting edge
KE – radial displacement of the tool corner

(a)

KE

Rake face

Crater

r_ε

(b)

Zone C   Zone B   Zone N   Notch wear

VB_C VB_B VB_N

r_ε VB_{Bmax} $\frac{b}{4}$

b

View on the flank face

Figure 2.22 *Typical wear patterns according to ISO 3685[22]*

occurs. Development of flank wear is noted by appearing close to the cutting edge line at first, and then growing perpendicular down over the flank face, growing away from the cutting edge line. Flank wear measurement is standardized and it can be measured according to ISO 3685 as described in Figure 2.22. During the measurement, the distance between the main edge and lower contour of worn area is measured and two values of wear, VB_B and VB_{max} are defined. VB_B is the average distance with linear characteristic and VB_{max} is the maximum distance [21].

Built-up edge (BUE) is formed by adhesive wear mechanism as the workpiece material adheres to the cutting edge. The adhesion process or micro-welds between two friction agents (workpiece material and cutting tool material) can occur by chemical adhesion or by mechanical adhesion. In chemical adhesion, atomic interaction occurs. In other words, thermally induced diffusion or electron exchange between the workpiece material and cutting tool material take place. In mechanical adhesion, workpiece material becomes extremely plastically deformable with the cutting tool material under high temperatures [10]. The term adhesive wear is used when a piece of cutting tool material is separated as a result of micro-welds shearing-off. This type of wear is common during machining of sticky materials such as stainless steels, aluminium. Because of strong adhesion, build-up edge can form. BUE formation in austenitic stainless steels can be clarified with high plastic deformability of these materials [10]. The BUE formation mechanism is explained by pressure welding of the chip to the cutting edge where gradual and cyclic accumulation of workpiece material on the cutting edge happens under high pressure. In other words, the thin layers of workpiece material are adhered one at a time, eventually creating BUE. As described in Figure 2.23, built-up edge particles can lead to increased flank wear as these particles repeatedly slip between flank face of the tool and machining surface. Relationship between flank wear and built-up edge can be observed in Figure 2.24. Usually, flank wear rate is increased with cutting speed increase.

26
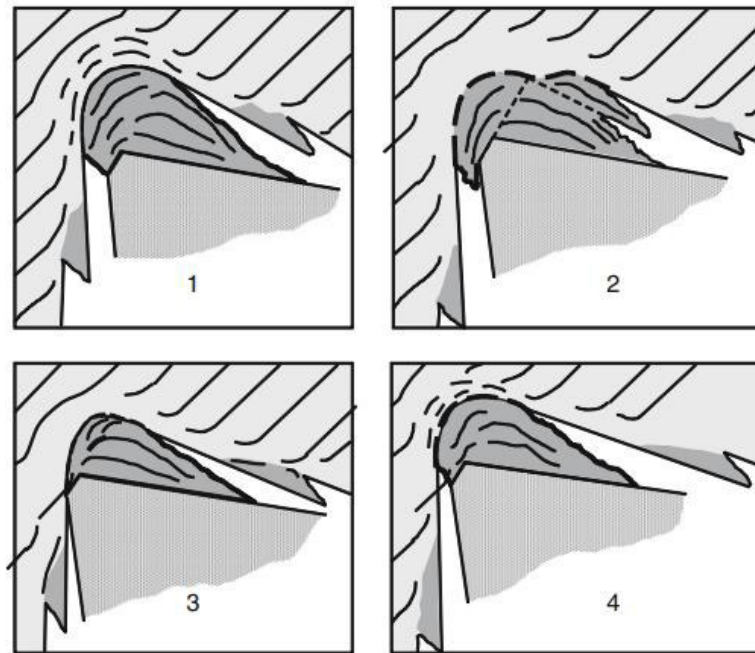
Figure 2.23 BUE periodic growth scheme [10]

But it reaches maximum and minimum values at different cutting speeds and flank wear is related to BUE. Flank wear reaches its maximum when BUE has the largest dimension (at v_c = 20m/min). Minimum wear is achieved when there was no BUE formation at higher speed (v_c = 30m/min). In other words, despite of increase in cutting speed, flank wear is decreased after reaching the maximum. This flank wear decrease can be related to BUE. As at higher speed, no longer BUE slip occurs between the machined surface and the flank face. It also has an influence on the accuracy and the tolerances of the machined part as the geometry of cutting edge is shifted with BUE formation. It can be deposited on the machined surface or scratch the surface in the case of shearing off and passing along the clearance face of the cutting tool.
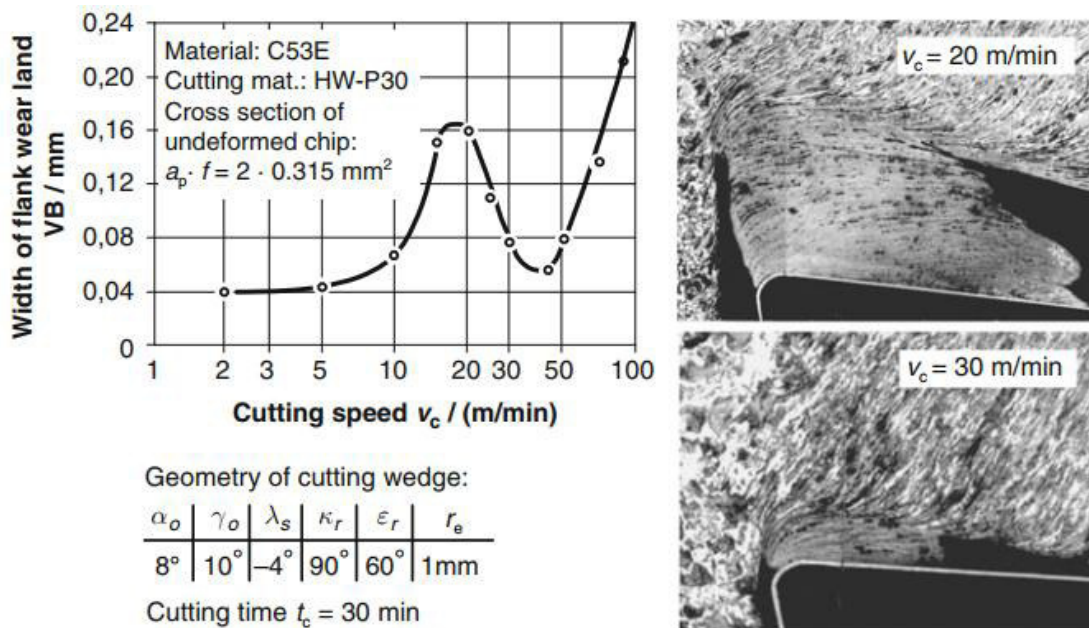
Figure 2.24 Relationship between flank wea and BUE [10]

According to experiments on stainless steel machining, BUE forms at low cutting speeds. By increasing the cutting speed, the deformation rate is increased at high temperatures. In other words, soft layers that are created at elevated temperatures accelerate the plastic flow of material [24]. As it was stated above, BUE formation occurs under high pressure, decreasing the pressure and cutting force is necessary to prevent its formation. Making more positive rake angle can decrease the pressure and the cutting force, but as a consequence cutting edge strength is decrease. Friction between tool and chip in contact area is another important factor for BUE formation. Less contact and welding can be achieved by applying lubricant/coolant or using a polished rake face. Lubricants containing sulphur or chlorine can form a non-metallic film between tool and material providing less contact [25]. Using lubricants at low cutting speeds is very important and coolant should be applied at higher cutting speeds due to increased temperature in the cutting zone.

(a)   *(b)*

(c)   *(d)*
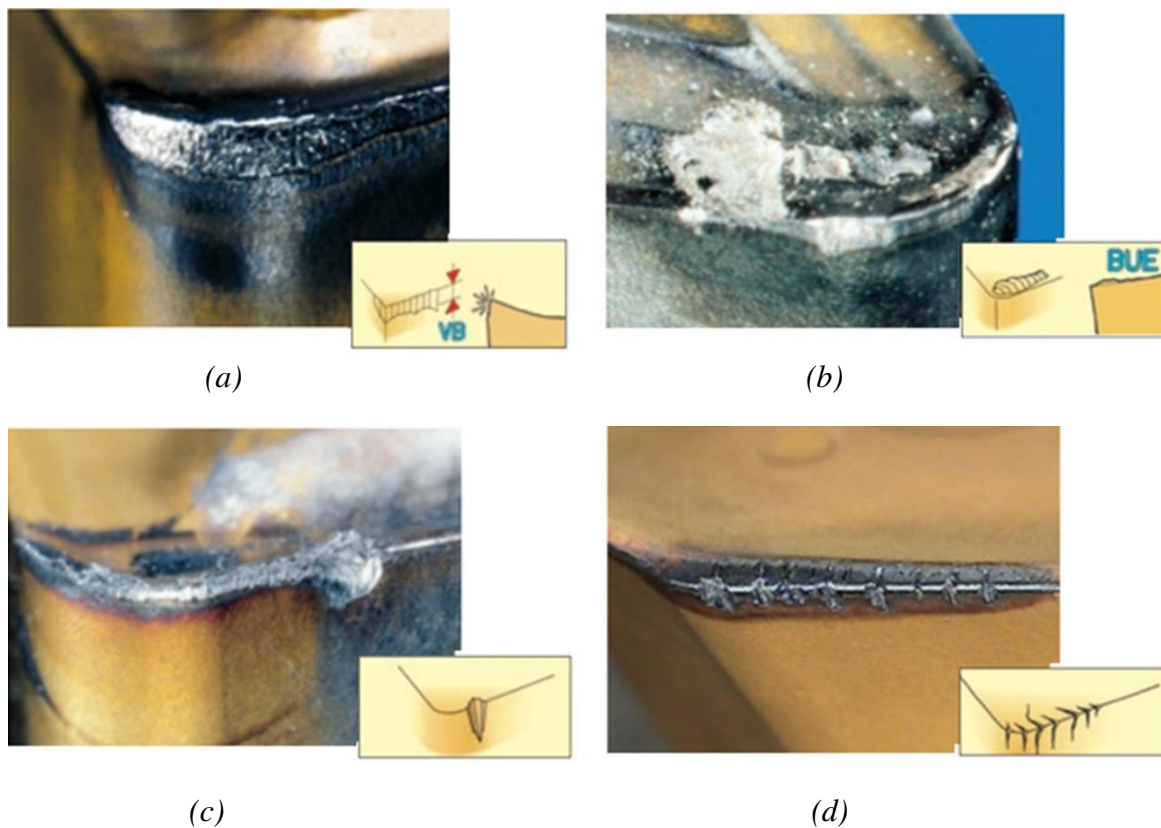
Figure 2.25 *The most common types of wear that occur during SS machining: (a) Flank wear; (b) Build-up edge; (c) Notch wear; (d) Thermal cracks [8]*

Notch wear is another common type of wear and it is caused by a deformation hardened surface during stainless steel machining. Notch wear is determined as a tear on both the rake face and flank of the inserts. A tear is the result of deformation hardening on the surface. Its position is defined at the depth of cut-line [18].

Chipping or fracture on the cutting edge can occur as a result of comb cracks existence. During intermittent machining, thermal fluctuations inside the tool cause stress that leads to form comb cracks which grow perpendicular towards the cutting edge line. Its formation can be described as tensile stresses that form on the surface of the tool due to temperature difference between the surface and core of the tool. Comb cracks start to form when these tensile stresses exceed the tool material strength [21].

2.6   Previous experiments and findings

Several authors conducted an investigation on milling of stainless steel, especially AISI 304 steel. Main topics of discussion were the effect of tool coating, the effect of coolant methods, the effect of tool geometry to tool wear and surface quality. Single-layer coated and multi-layer coated carbide inserts are the most tested type of cutting tools during experiments. Adhesive and abrasive wear including notch wear are found as the main type of tool failure mode. BUE formation that was observed during experiments can be considered as the one type of wear mechanism.

The effect of cutting fluids in end milling of AISI 304 austenitic stainless steels with multilayered TiN/TiCN/TiN PVD coated carbide insert was investigated by K.A. Abou-El-Hossein. According to experiment, BUE was found at low-cutting speed (150 m/min) in dry machining and it was one of the dominant tool failure modes. BUE formation was explained as a result of more heat since AISI 304 has a low thermal conductivity, lack of coolant, and prolonged contact time of tool and workpiece as it occurred at low-cutting speed. On the other hand, nose wear mechanism was found at high-cutting speeds in dry milling. In wet milling or milling with coolant, vertical grooving and notch wear were observed at low- and high-cutting speeds, respectively. Notch wear which is common wear mechanism for work-hardened materials, but it was not found during dry milling. In terms of tool life, it was concluded that the coolant usage is more efficient for low cutting speed and in general, coolant helps to improve tool life [27]. Cutting edge condition after tests is shown in Figure 2.26.

(a)   *(b)*

(c)   *(d)*
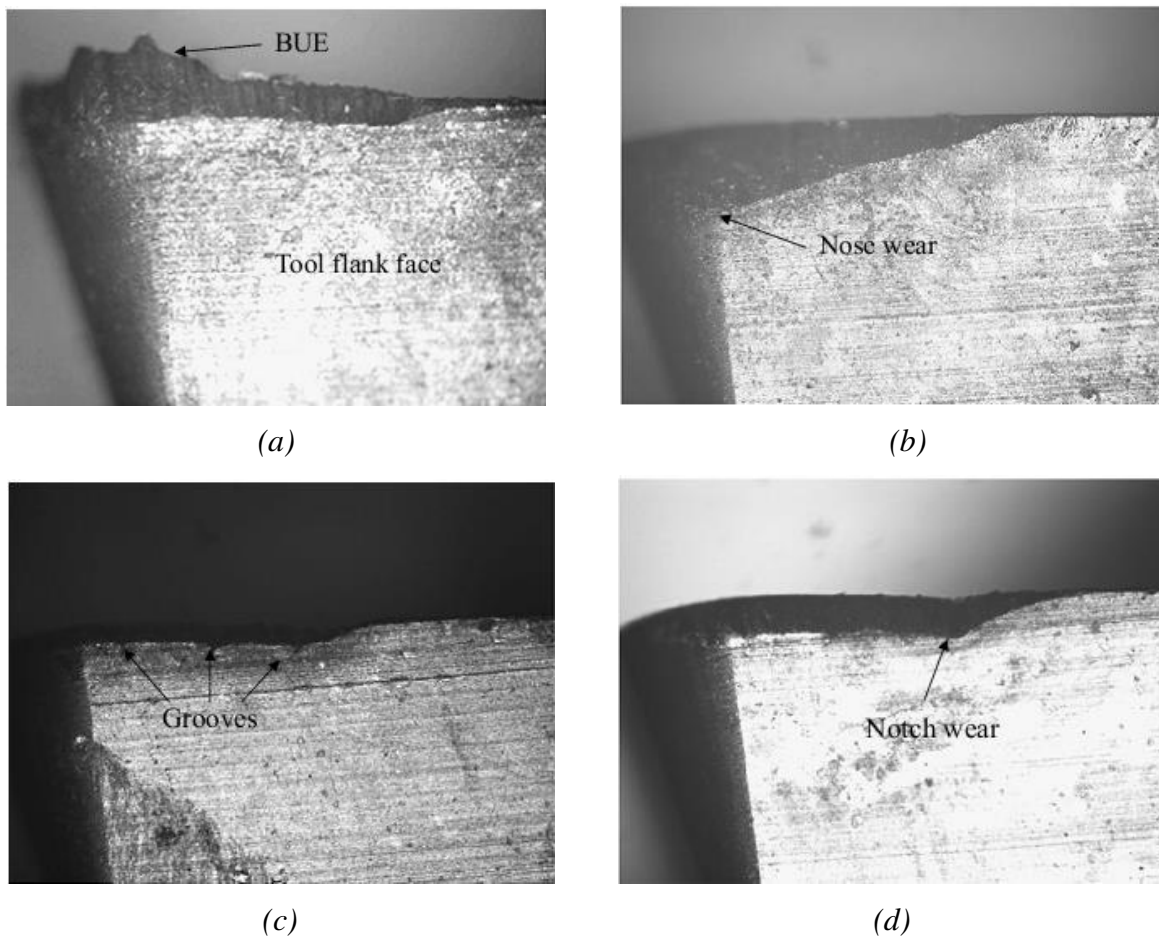
Figure 2.26 *Tool wear at different cutting speed and coolant modes: dry cutting: (a) v_c = 150 m/min; (b) v_c = 260 m/min; wet cutting: (c) v_c = 150 m/min; (d) v_c = 260 m/min. [27]*

K.A. Abou-El-Hossein conducted another experiment with Z. Yahya on stainless steel milling. Test was similar to previous one, but this time all trials are made with usage of coolant. Tool life and tool wear were studied by using different cutting speed and feed rate. During the trial, BUE formed mostly at medium cutting speed and higher feed, 190 m/min and 0.075 mm/rev, respectively and it was absent at higher or lower cutting speed and feed. Development of flank wear was more rapid at low feed than high feed with the same value of cutting speed. It was explained that the contact time between the cutting edge and the workpiece is more at lower feeds. In addition, increasing the cutting speed at lower feeds resulted in chipping and grooving of the cutting edge at the next stage of flank wear. And the reason for chipping was estimated as thermal shocks produced by non-uniform coolant effect. It was concluded that the main cause for tool failure is notch wear at the flank face which was occurred at high feed due to work hardening effect of stainless steel. Maximum tool life was achieved at low cutting speed and medium feed, 150 m/min, 0.075 mm/rev, respectively [28]. Cutting edge condition in case of BUE formation and chipping is described in Figure 2.27.
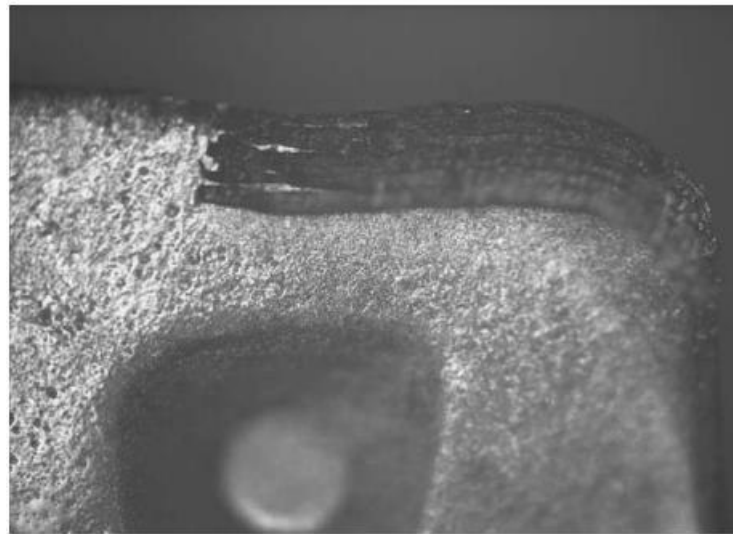
(a)
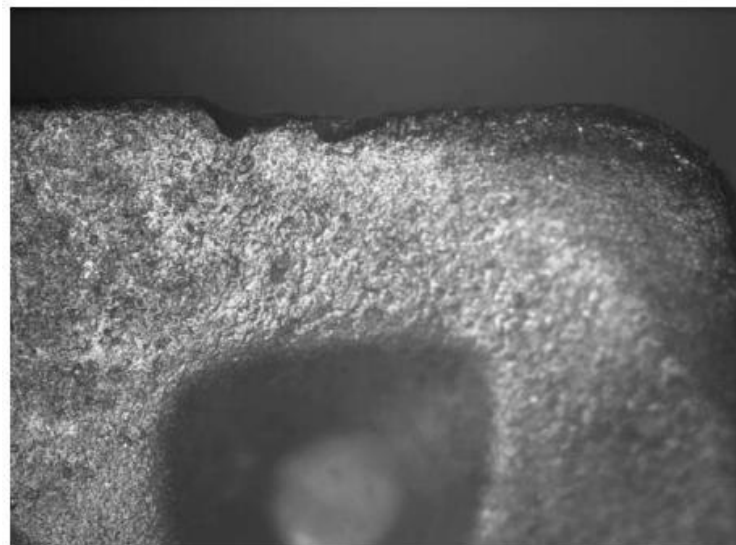
(b)

Figure 2.27 *Cutting edge condition in milling tests: (a) BUE formation at v_c = 190 m/min and f_n = 0.075 mm/rev. (b) Chipping at v_c = 190 m/min and f_n = 0.025 mm/rev. [28]*

The influence of multilayered coatings comparing to single-layered was studied by Nordin et al. Based on the experiments, limiting factor of tool life during stainless steel machining was chipping of the cutting edge as a result of comb cracks. Comb cracks density is affected by coatings. With multilayered coatings a lower comb crack density was achieved due to lower tool-chip interaction. Hence, tool with a multilayered coating achieves longer tool life [29].

Muthusamy et al. studied tool wear analysis in stainless steel milling with ethylene glycol – based TiO_2 nanoparticle coolant and water-soluble coolant. In general, better performance in terms of tool life was observed during end-milling with nanofluid by achieving tool life value more than 40% comparing to water-soluble coolant [30]. As main tool failure modes were found flank wear, chipping, cracking and fracture with water-soluble coolant. In addition to this, BUE was found at low cutting speed.

Nalbant and Yildiz made an investigation on AISI 304 stainless steel milling using cryogenic cooling, in which liquid nitrogen is used as a coolant and dry milling. According to authors, cryogenic machining helps to remove heat effectively from the cutting zone by having a temperature as low as -196 °C at 101.325 kPa. As a tool wear mechanism, only tool frittering around the nose radius of the insert is found. The reason is explained as excessive cryogenic cooling is followed by heat during chip removal in the discontinuous cutting can cause thermal shocks around the insert nose. Additionally, insert material can be brittle at lower temperatures. Based on the results, cryogenic cooling has no extraordinary effect comparing dry milling [31].

As coolant has a significant effect on stainless steel milling, Chocalingam and Hong Wee investigated surface roughness and tool wear using different cooling conditions. They compared the effect of synthetic oil, water-based emulsion and compressed air on machining process. According to overall experiment, better surface finish was obtained with water-based emulsion. The worst surface roughness was found with compressed air as cooling air doesn`t contain lubricant, as a result, the friction between tool and workpiece surface is higher. Surface finish can be improved by applying lower feed rate. Chipping was found as the initial wear mode and tool is subjected to more chipping and fractures in case of compressed air. It was concluded that lubricant has a significant role in reducing tool wear [32].
Chip form and surface roughness by MQL (Minimum Quantity Lubrication) method on milling is studied by Uysal et al. AISI 304 (austenitic stainless steel) and AISI 420 (martensitic stainless steel) was chosen as a testing material. Dry milling and MQL milling using uncoated and coated cutting tool were compared. It can be seen in Figure 2.28 that cutting fluid has a great impact on chip formation.

Figure 2.28 *Chip forms in AISI 304 milling: (a) dry milling with WC; (b) dry milling with TiN coated WC; (c) MQL millin with WC; (d) MQL milling with TiN coated WC [25]*

The better surface roughness and chip forms are obtained in MQL milling with TiN coated tool than dry milling. When comparing two materials AISI 420 martensitic stainless steel showed better surface roughness than AISI 304 austenitic stainless steel. In addition chips that formed during AISI 304 machining were more elongated or scrolled than chips of AISI 420 steel [33].

Trial for determination of cutting parameters during turning of AISI 304 austenitic stainless steel was conducted by Korkut et al. During the experiment the influence of cutting speed on tool wear and surface roughness was investigated. Three range of cutting speeds were chosen keeping the feed rate and depth of cut constant. According to their findings, lower cutting speeds increases the contact time on the rake face by slow movement of chips and that longer contact time on the rake face causes thermal softening of the tool by heat conduction from the chips to the tool. As a consequence, wear resistance of the tool reduces. Surface roughness values were decreased with the increasing the cutting speed and one of the reasons could be the presence of build-up edge (BUE) at the lower cutting speeds [34].

3   Design and performance of experiments

The experimental design and general procedure of testing is explained with all used materials and equipment.

3.1   Indexable insert

A total of 10 cemented carbide cutting inserts with the same geometry were used during the test. The insert shape was round with a designation RPHT1204MOEN-GL which is shown in Figure 3.1 and it is manufactured by OSG Corporation. The insert has a positive rake angle and relief angle ($\alpha = 11°$) with special designed chip breaker GL and grade XP2040. According to manufacturer, chip breaker type GL is a breaker with a large rake angle and a small flat land to reduce cutting force and it`s designed especially for stainless steel milling. Grade XP2040 is composed of a tough and high strength carbide with wear-resistant coating [35]. Cutting parameters that are used during the test were chosen based on recommendation by manufacturer on tool catalogue. Table 3.1 and 3.2 provide detailed information about grade and chip breaker technology, respectively.

In order to distinguish inserts, reference names were given to inserts and during the experiment report is made using these names. In addition, the front side of insert contained the numbers and signs from the manufacturer and during the test these symbols are used in order to make it possible to differentiate cutting edge sides of the round insert. Reference names that are used in the report are shown in Table 3.3. As stated above, only one type of insert is used during the whole experiment.
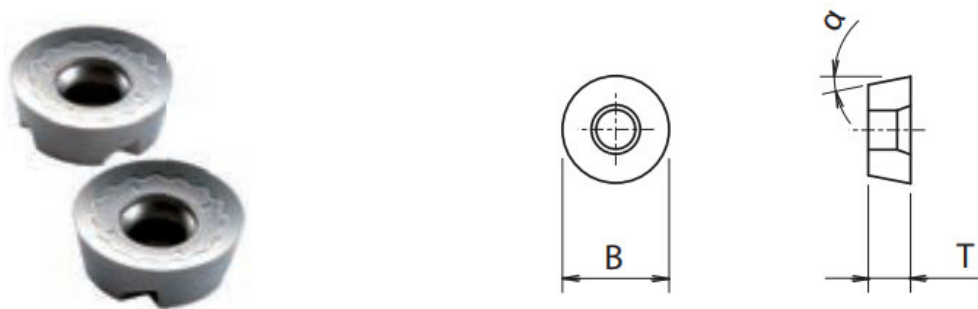
Figure 3.1 OSG PRC round inserts [35]

Workpiece material	ISO M
Grade	XP2040
Coolant/dry	Coolant
Coating type	PVD
Hardness (HRA)	89,6
Surface main component	TiAlN
Coating thickness	5 μm
Features	For machining stainless steel and steel. Grade for general-purpose milling. A tough, high-strength carbide grade with an anti-chipping and wear resistant coating

Table 3.1 Insert grade information [35]
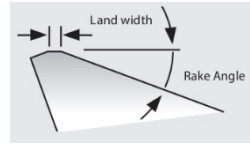
Chip breaker	Material	Cutting edge	Rake angle γ	Features
GL	ISO P ISO M		25°	For milling stainless steel. Chip breaker with a large rake angle and a small flat land to reduce cutting force

Table 3.2 *Chip breaker design [35]*

Insert	Reference name
Round insert 1	VBD-1
Round insert 2	VBD-2
Round insert 3	VBD-3
Round insert 4	VBD-4
Round insert 5	VBD-5
Round insert 6	VBD-6
Round insert 7	VBD-7
Round insert 8	VBD-8
Round insert 9	VBD-9
Round insert 10	VBD-10

Table 3.3 *Inserts and their reference names that were used in the report*

3.2   Milling cutter heads

Two types of milling cutters with different nominal diameters were used during the tests. The performance of conventional milling cutter head with indexable inserts having nominal diameter (D_c) 100 mm is compared with milling cutter head with nominal diameter 125 mm. Conventional milling cutter with D_c = 100 mm is produced by OSG, shown in Figure 3.2 while milling cutter with D_c = 125 mm is manufactured using DMLS (Direct Metal Laser Sintering) additive technology, shown in Figure 3.3. Comparing to conventional milling cutter heads, new type of cutter produced using DMLS technique has a weight only more than 1 kg where conventional milling cutters with the same diameter have about 3 kg of weight. In addition, new type of cutter is equipped with direct coolant system that makes direct coolant streaming to rake and clearance face possible. Milling cutter with D_c = 125 mm containing totally 6 indexable insert pockets is made from EOS MaragingSteel MS1 metal powder grade and its equivalent according to chemical composition is demonstrated in Table 3.4.

Material name	ČSN	Material no.	DIN	AISI
EOS Maraging steel MS1	19902	1.2709	X3NiCoMoTi 18-9-5	18 Mar 300

Table 3.4 *MS1 metal powder grade equivalent table*

The word "maraging" is a combination of words "martensite" and "aging" (type of treatment) as it is a low carbon steel with martensitic structure. This material shows excellent strength and toughness, high density and it is heat treatable using age hardening process where it can obtain hardness more than 50 HRC by age hardening at 490°C for 6 hours. In addition, it is easily machinable and has a good thermal conductivity. In general, these steels

are originally developed as high-strength for aerospace engineering, but conventionally used for injection moulding tools. Key properties of MS1 can be seen in Table 3.5. Values before and after age hardening conditions can be compared [36].

Figure 3.2 *Conventional milling cutter Dc=100 mm by OSG (PRC Bore) [27]*

Property	As built	After age hardening (6 hours at 490°C)
Ultimate Tensile Strength	1100 MPa ± 100 MPa	1950 MPa ± 100 MPa
Yield Strength (R_p 0.2%)	1000 MPa ± 100 MPa	1900 MPa ± 100 MPa
Elongation at break	8% ± 3%	2% ± 1%
Youngs Modulus	180 GPa ± 20 GPa	
Hardness	33-37 HRC	50-54 HRC
Ductility	45 J ± 10 J	11 J ± 4 J
Relative Density	approx. 100 %	

Table 3.5 *Mechanical properties of EOS MaragingSteel MS1 [36]*

As stated above conventional milling cutter head with D_c=100 mm is manufactured by OSG with official product name PRC Bore in OSG Phoenix Series Round Cutters which can be found in OSG tool catalogues. Milling cutter is equipped with coolant holes. Milling cutter view and its specification are given in Figure 3.2 and Table 3.6, respectively [35].
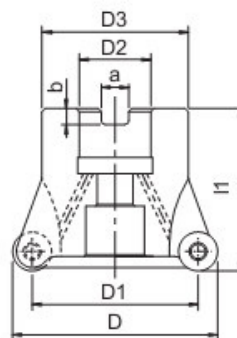
Designation	Z	D	D1	l1	D3	D2	a	b
PRC12R100M32-6	6	100	88	50	70	32	14.4	8

Table 3.6 *Milling cutter Dc=100 mm specification [35]*

35
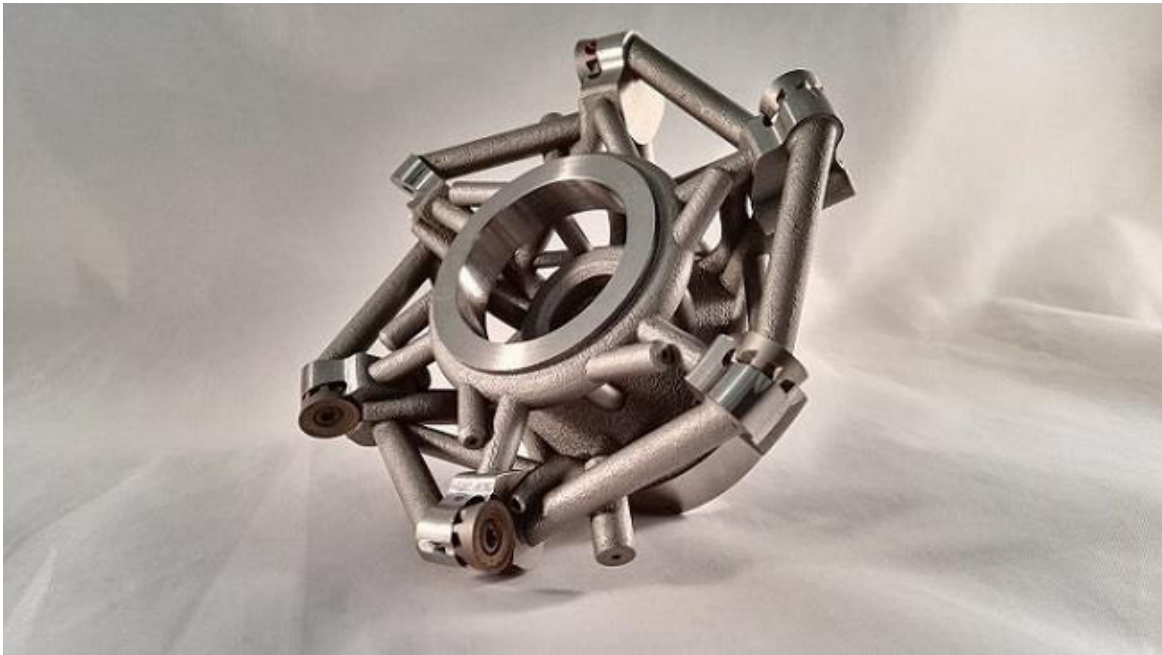
Figure 3.3 *Special light milling head produced by 3D metal printing [37]*

3.3   Workpiece material

As the workpiece material austenitic stainless steel with grade 304 (according to AISI) was chosen. Its equivalent grade is 17 240 according to ČSN. The form of material was rectangular cuboid having dimensions 150x90x100 mm. Cuts were made along 150x90 plane. A typical chemical composition of workpiece is given in Table 3.7.

C<	Si<	Mn<	P<	S<	Cr	Ni
0.07	1.0	2.0	0.045	0.03	17.0-20.0	9.0-11.5

Table 3.7 *AISI 304 typical chemical composition, in wt% [38]*

3.4   Experimental setup

The face milling tests were performed on DMU 40 eVo linear machining center in Regional Technological Institute at West Bohemian University in Pilsen. Basically, testing variations are divided into 5 stages. The tests were performed with and without coolant at 5 different cutting speeds starting with the lowest value and ending with the highest. Cutting parameters are chosen based on recommendation by manufacturer on tool catalogue. Only two values of feed rate was used where axial depth of cut was constant. Radial depth of cut was used in two variations: it was equal to the width of the workpiece and it followed by setting it to half width of the workpiece. According to previous experiments, it was believed that cutting speed has a high influence on BUE formation comparing to other cutting parameters. It was the reason to use cutting speed in high range. All cutting parameters that used during the tests are following:

- Cutting speed v_c [m/min]: 80 / 140 / 200 / 280 / 350
- Feed rate f_z [mm/tooth]: 0.2 / 0.3
- Axial depth of cut a_p [mm]: 1 / 2.4
- Radial depth of cut a_e [mm]: 45 / 90

The tests were conducted by taking into account certain criteria for tool life testing. Cutting length at one pass was 150 mm in case of a_e = 90 mm and it was 300 mm in case of a_e=45 mm which was the equal to the length of the workpiece. At certain time frequency and depending on cutting insert condition the flank wear progression was observed using an optical microscope Blickle Multicheck PC500 G2.

Figure 3.4 *DMU 40 eVo linear machining center [39]*

Figure 3.5 *Blickle Multicheck PC500 [40]*

The test with certain insert was stopped when the maximum (critical) flank wear value reached 0.3 mm and the machining time spent to reach that value was calculated. The term "maximum flank wear" is used in thesis when the amount of wear is equal or more than critical value. A single insert was mounted on the milling cutter during the test. Only one test was performed mounting all 6 inserts on the milling cutter. As a milling method basically was used down milling. The applied milling method is described in Figure 3.5.

Before starting the test, the insert mask was prepared by getting the flank view of the unused (new) insert sample. The mask was used to compare cutting edge condition and flank wear progression during the experiment and it is shown in Figure 3.3.

The first trial (TEST-1) was conducted using coolant. There was a change on the axial depth of cut. It was changed from 2.4 mm to 1 mm since the cutting tool was overloaded with the value of 2.4 mm. The changed value of axial depth of cut was kept constant until the end of the experiment. The radial depth of cut was changed to 45 mm during the test with milling cutter diameter D_c=100 mm.
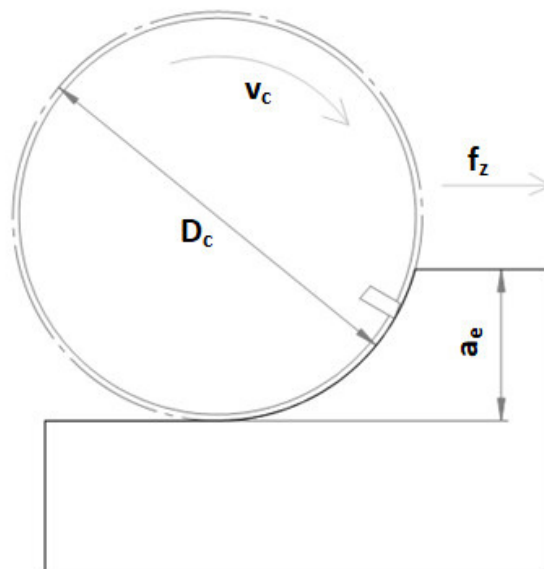
Figure 3.6 Applied milling method

The flank wear progression was checked. Insert was changed after reaching critical or maximum wear for each varied cutting speed. The cutting parameters that were used during the first test is A 3.8. Actually the first test was preparation and checking the correspondence, applicability of chosen cutting parameters.

Cutter diameter D_c [mm]	v_c [m/min]	f_z [mm/tooth]	a_p [mm]	a_e [mm]	Coolant
125	80	0.3	2.4	90	
125	140	0.3	1	90	YES
125	200	0.3	1	90	
100	200	0.3	1	45	

Table 3.8 Cutting condition that was used during TEST-1

The second trial (TEST-2) was performed again using coolant. Radial depth of cut was changed to 45 mm or in other words, half of the testing workpiece as the width of the workpiece was 90 mm. Usually in face milling, the cutter diameter should be 20 to 50% larger than

the width of the workpiece. In addition, the milling cutter should be positioned slightly off-centre as described in Figure 3.7 below. By moving off the cutter from the centre, a more constant and favorable direction of forces will be obtained. During central milling, combination of climb and up milling is observed. As a result, compressive stress forms during tool engagement and tensile stress is formed on the tool exit.

Avoid positioning cutters on-centre.
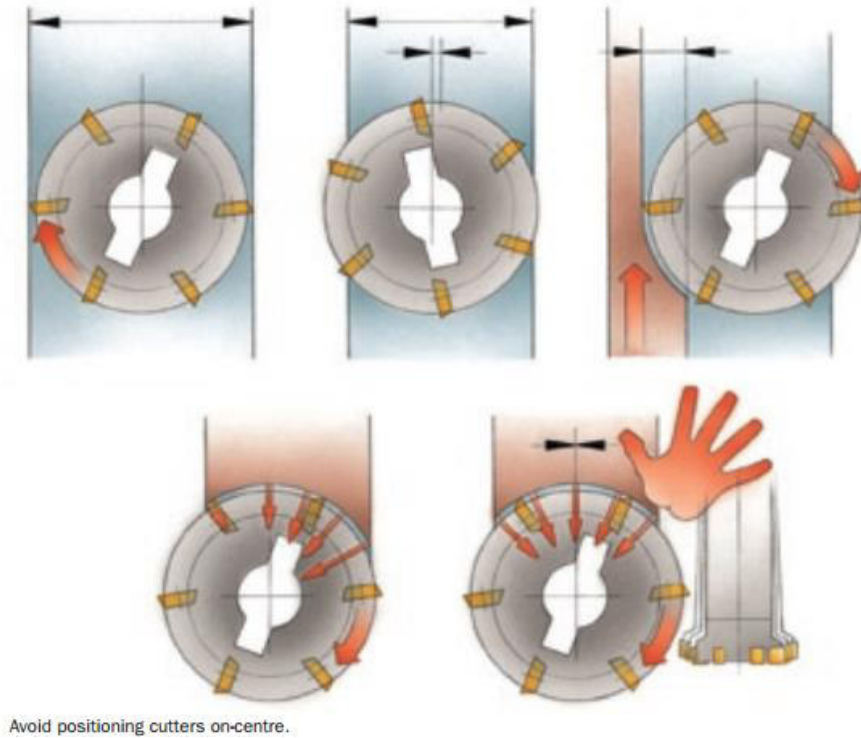
***Figure 3.7** Milling cutter position recommendation [8]*

As radial depth of cut was changed to 45 mm, tool wear was checked after cutting length 300 mm, but not after every 150 mm. Insert was changed after reaching critical wear for each varied cutting speed. The cutting parameters used during the second test is shown in Table 3.9.

Cutter diameter D_c [mm]	v_c [m/min]	f_z [mm/tooth]	a_p [mm]	a_e [mm]	Coolant
125	80	0.3	1	45	YES
	140	0.3			
	200	0.3			
	280	0.3			
	350	0.3			

***Table 3.9** Cutting parameters that were used during TEST-2*

The third trial (TEST-3) was conducted using thermal imaging camera FLIR to define cutting temperature consequently, heat that was generated and the test was performed only for milling cutter with D_c = 125 mm. As milling cutter D_c = 125 mm is produced using DMLS technique, it was essential to observe heat generation if it is different than conventional milling cutters. Thermal imaging camera measures the temperature using non-contact infra-red method. As stated above, width of the testing workpiece was 90 mm. According to test design, the radial depth of cut was 45 mm or half of the testing workpiece and cutting was divided into two stages. At the first stage of the test, coolant was used while keeping the cutting speed at minimum, v_{c1} = 80 m/min and it was kept constant during the whole test. At the se-

cond stage of the test, second half of the workpiece (45 mm) was machined using variable cutting speeds (v_{c2}) and dry milling was applied in order to record and measure the cutting temperature. Insert was changed for each varied cutting speed. The cutting parameters used during the third test is shown in Table 3.10.

v_{c1} [m/min]	v_{c2} [m/min]	f_z [mm/tooth]	a_p [mm]	a_{e1} [mm]	a_{e2} [mm]	Coolant at the 1st half (a_{e1})	Coolant at the 2nd half (a_{e2})
80	80	0.3					
140	140	0.3					
200	200	0.3	1	45	45	YES	NO
280	280	0.3					
350	350	0.3					

Table 3.10 Cutting parameters that were used during TEST-3

On the fourth trial (TEST-4), the milling cutter with $D_c = 100$ mm was tested applying the same cutting conditions as TEST-2 where the test was performed with milling cutter $D_c = 125$ mm. Exception was the feed and it was kept constant from the beginning till the end of the test with milling cutter $D_c = 100$ mm. Insert was changed after reaching critical wear for each varied cutting speed. The cutting parameters used during the third test can be seen in Table 3.11.

Cutter diameter D_c [mm]	v_c [m/min]	f_z [mm/tooth]	a_p [mm]	a_e [mm]	Coolant
	80	0.3			
	140	0.3			
100	200	0.3	1	45	YES
	280	0.3			
	350	0.3			

Table 3.11 Cutting condition that was used during TEST-4

The fifth trial (TEST-5) was performed on the milling cutter with $D_c = 125$ mm by fully mounted 6 inserts (Z = 6). Radial depth of cut was changed from 90 mm to 45 mm after the first pass. It the end, edge condition was checked only in one insert. The cutting parameters used during the third test can be seen in Table 3.12.

Cutter diameter D_c [mm]	v_c [m/min]	f_z [mm/tooth]	a_p [mm]	a_e [mm]	Coolant
125	80	0.2	1	90	YES
	80	0.2	1	45	

Table 3.12 Cutting condition that was used during TEST-5

3.5   Obtained values and results

Flank wear measurements and machining time calculation that were obtained during tests are given in following tables. Reference names of inserts are used to make difference among inserts. If the same insert reference name is repeated on the other test report with different value of cutting speed, it means that another cutting edge of the same insert is used. As stated above, TEST-1 was preparation and checking the correspondence, applicability of chosen cutting parameters. Cutting edge condition and tool wear progression that is corresponding to

used cutting parameters is shown on the following figures respectively. On the following pages average flank wear rate and maximum flank wear are denoted as VB_B and VB_{max}, respectively. In addition, VB_B and VB_{lin} are interchangeable in this thesis. Because of time and resource limits, trials couldn`t be repeated as with repeated trials` results would be more exact and comparable.

No. of passes	v_c [m/min]	f_z [mm]	a_p [mm]	a_e [mm]	VB_{lin1} [μm]	VB_{lin2} [μm]	ΔVB_{lin}	VB_{max} [μm]	Δt [min]
VBD-1 to D_c = 125mm									
1	80	0.3	2,4	90	0	124		-	2.36
2	machine stopped, tool was overloaded, damaged insert								
VBD-2 to D_c = 125mm									
1	80	0.3	1	90	0	98	98	-	2.36
2	80	0.3	1	90	98	115	17	-	2.36
4	80	0.3	1	90	115	122	7	-	4.71
11	80	0.3	1	90	122	303	181	638	16.49
Max. wear has been reached									**25.91**
VBD-3 to D_c = 125mm									
1	140	0.3	1	90	-	-	-	536	1.35
Max. wear has been reached									**1.35**
VBD-4 to D_c = 125mm									
1	200	0.3	1	90	0	151	151	297	0.94
Max. wear has been reached									**0.94**
VBD-4 to D_c = 100mm									
1	200	0.3	1	45	0	91	91	144	1.6
stopped									
TEST-1 is stopped									

Table 3.13 TEST-1 cutting parameters and obtained values

In the first trial, tool overloading was observed with a_p = 2.4 mm, then depth of cut is changed to 1 mm. As it can be seen from flank wear values in the 1st trial, average (or linear) flank wear was higher with higher depth of cut comparing to decreased depth of cut after first pass.
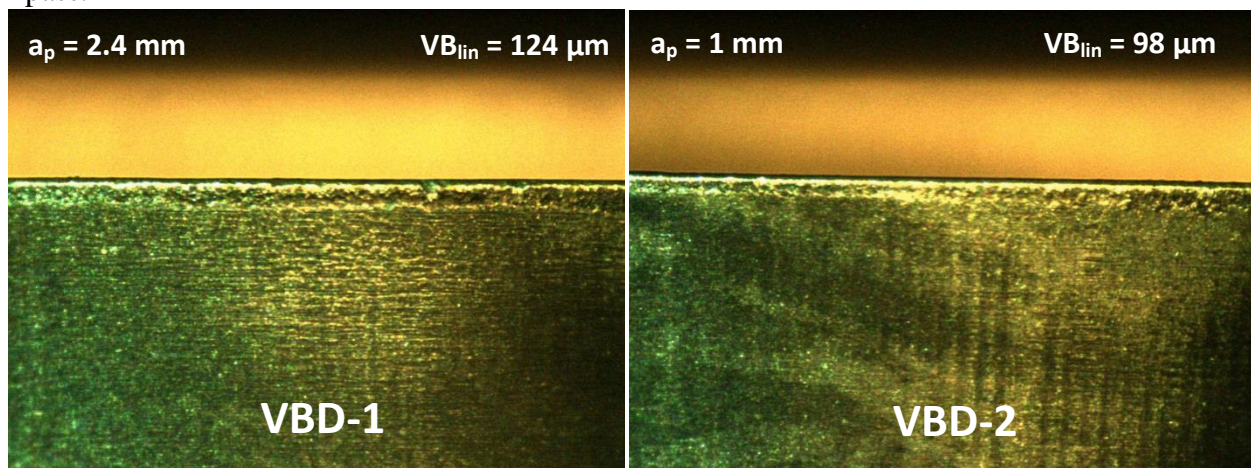

Figure 3.8 Differences in flank wear rate with different depth of cut while v_c = 80 m/min, f_z = 0.3 mm and a_e = 90 mm in TEST-1

In Figure 3.8 flank wear rates after first pass are compared. After changing depth of cut to 1 mm, total 11 passes or 1650 mm length is machined at cutting speed $v_c = 80$ m/min and feed rate $f_z = 0.3$ mm. After some passes cutting edge condition was checked and flank wear rate was constantly increasing as it can be seen. Built-up edge formation hadn`t been observed.
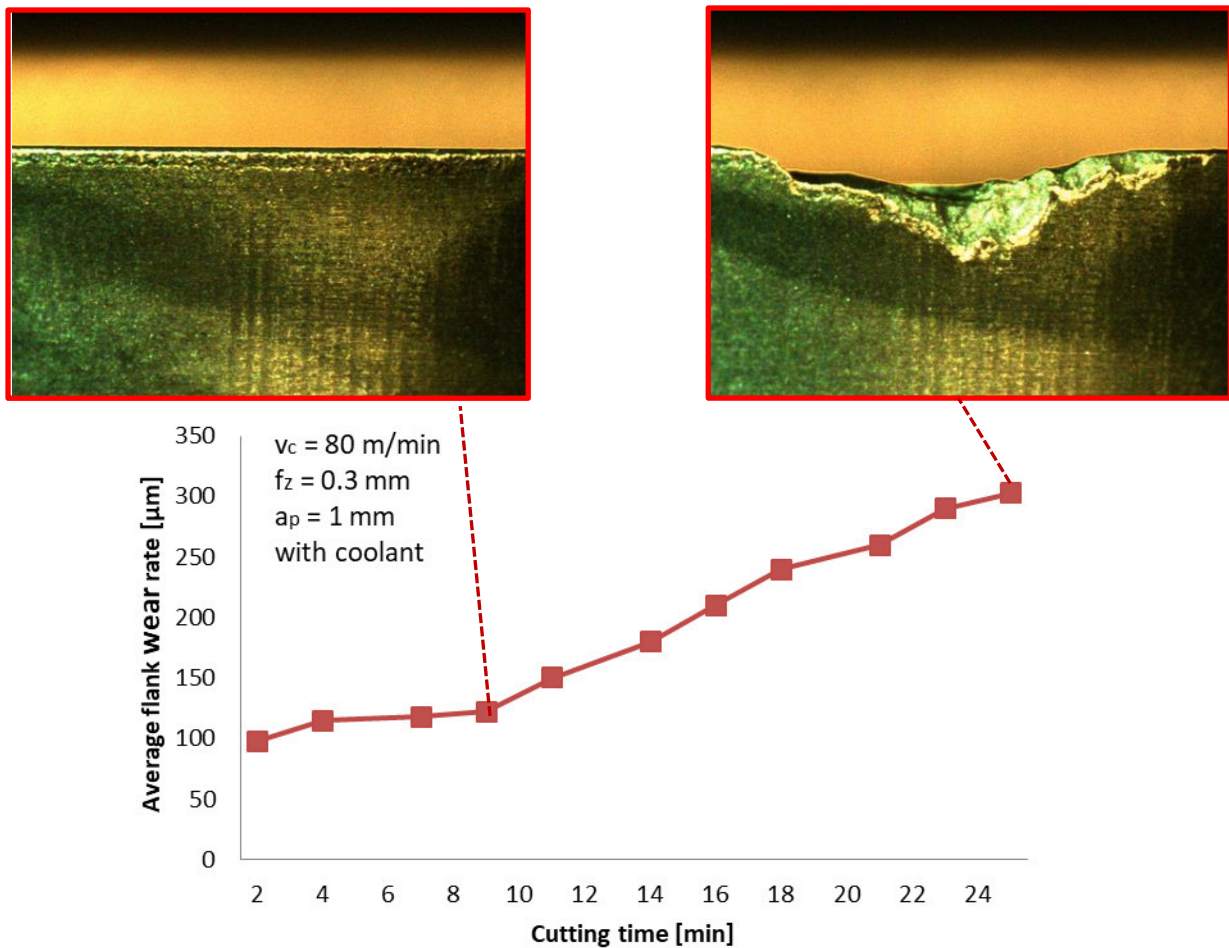
Graph 3.1 *Flank wear rate at $v_c = 80$ m/min ($D_c = 125$ mm) during TEST-1*

At the lowest cutting speed $v_c = 80$ m/min, chipping of the cutting edge partly in combination with notch wear is observed after 11th pass where average flank wear reached the amount more than 300 μm and 1st trial with $v_c = 80$ m/min was stopped reaching machining time about 26 minutes. As a machining time, cutting time (or time that tool spends to cut the material) is meant without considering approach time or tool departure.

At medium cutting speeds $v_c = 140$ m/min and $v_c = 200$ m/min, intensive cutting edge chipping with notch wear is observed just after the 1st pass as shown in Figure 3.9 below. After that, the reason for such heavy wear after 1st pass is examined. As one possible reason could be radial width of cut, a_e. As noted above, cutter positioning or cutter engagement is important in terms of forces and stresses acting on the cutting tool as shown below in Figure 3.10 and due to this reason center-off milling is recommended as shown on the right side of Figure 3.10. Comparing to a low speed, at medium speeds milling with full engagement didn`t seem to be productive as forces and stresses are increased with increasing cutting speed. After that, radial depth of cut is reduced to half of the workpiece width ($a_e = 45$ mm) and conventional milling cutter behaviour at cutting speed $v_c = 200$ m/min is observed. With decreasing in radial depth of cut, time to cut a workpiece is increased twice. When cutting
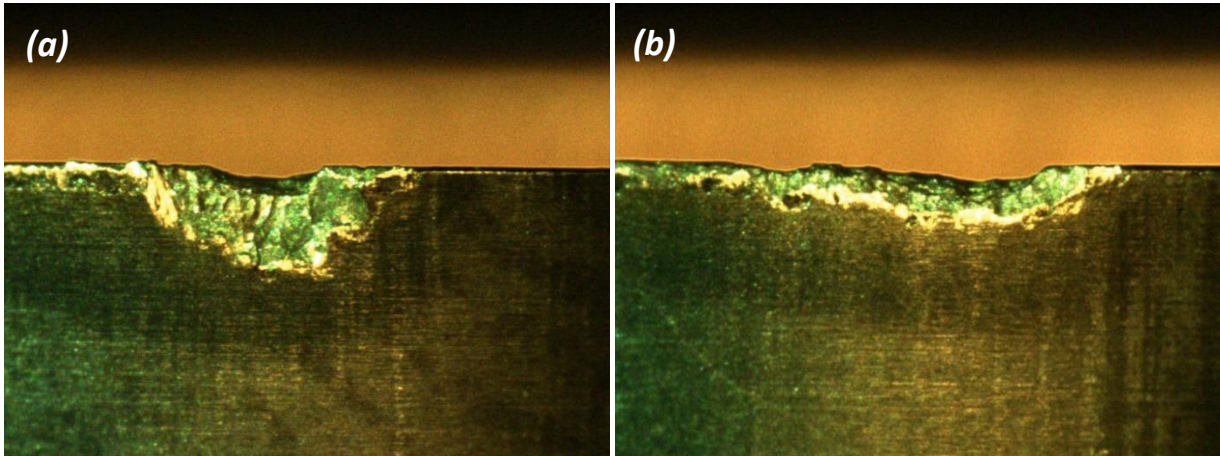
Figure 3.9 *Tool wear at different cutting speeds when D_c = 125 mm, a_e = 90 mm during TEST-1: (a) v_c = 140 m/min, VB_{max}=536 µm; (b) v_c = 200 m/min, VB_{max} = 297 µm.*
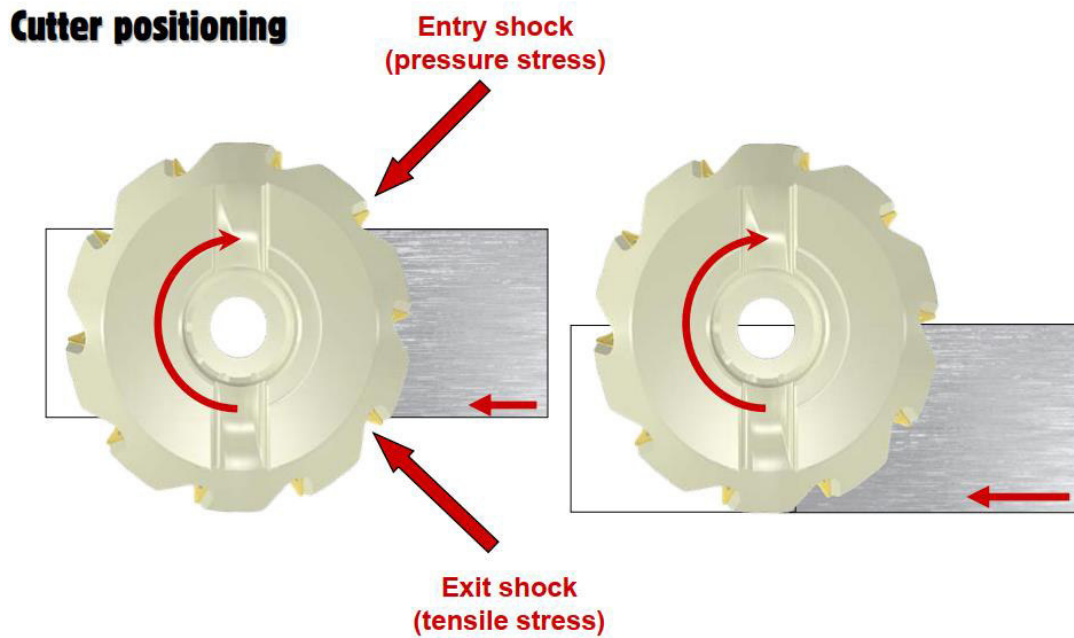
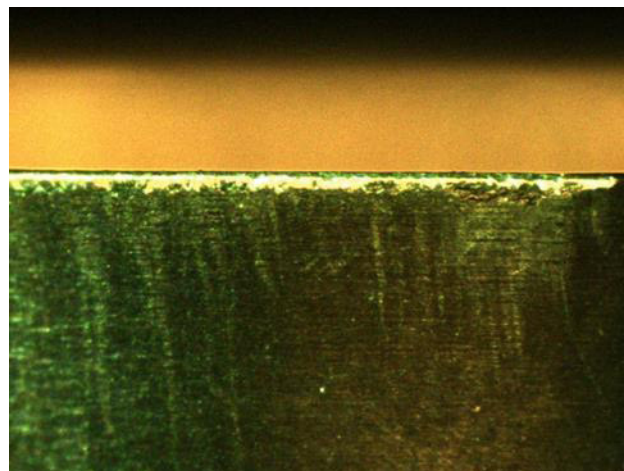

Figure 3.10 *Milling cutter positioning [11]*

Figure 3.11 *Tool wear after 1st pass in TEST-1: D_c = 100 mm, v_c = 200 m/min, a_e = 45 mm*

edge was checked after 1st pass, average or linear flank wear was equal to 91 µm and maximum flank wear was about 144 µm. Flank wear on cutting edge when conventional milling cutter D_c =100 mm is used can be seen in Figure 3.11. As stated above in previous pages, 1st trial was the kind of setting test in order to check practicability of chosen parameters and define suitable cutting conditions. Based on 1st trial, important presumptions are made as described above and these points are applied in the following trials. According to previous experiments, built-up edge formation is expected at low or medium cutting speeds, but during the 1st trial, type of wear observed was flank wear and chipping of cutting edge in combination with notch wear. Longer tool life was achieved at low speed.

In the 2nd trial (TEST-2), an insert wear and BUE formation is observed with cutting conditions described below in the Table 3.14. Milling cutter was not fully engaged, radial depth of cut was decreased to half width of workpiece (a_e = 45 mm). So, workpiece surface is milled with two radial passes. As a result, milling length is increased from 150 to 300 mm. Another change applied was feed rate change, from 0.3 mm to 0.2 mm. But after 6 passes (on the 7th pass) feed rate value is replaced back due to increased time spent on machining. In addition negligible influence of feed rate change on tool wear and BUE formation as it can be seen in Figure 3.12 and in the table. Coolant is used during entire trial. Cutting time reached and flank wear values also can be seen in the table. At low speed and at medium cutting speeds where number of passes was possible to use, flank wear behaviour was increasing as it was in previous case. After certain amount of passes, chipping of cutting edge in combination with notch wear is formed as in previous case.

No. of passes	v_c [m/min]	f_z [mm/z]	a_p [mm]	a_e [mm]	VB_{lin1} [µm]	VB_{lin2} [µm]	ΔVB_{lin}	VB_{max} [µm]	Δt [min]
VBD-5									
1	80	0.2	1	45	0	101	101	-	7.08
5	80	0.2	1	45	101	110	9	-	28.30
7	80	0.3	1	45	-	-	-	-	9.43
10	80	0.3	1	45	110	120	10	345	14.15
Max. wear has been reached									**58.96**
VBD-6									
1	140	0.3	1	45	0	103	103	-	2.69
3	140	0.3	1	45	103	134	31	390	5.38
Max. wear has been reached									**8.08**
VBD-7									
1	200	0.3	1	45	0	112	112	-	1.88
2	200	0.3	1	45	112	148	36	460	3.77
Max. wear has been reached									**5.65**
VBD-8									
1	280	0.3	1	45	0	158	158	300	1.35
Max. wear has been reached									**1.35**
VBD-9									
1	350	0.3	1	45	0	151	151	359	0.54
Max. wear has been reached									**0.54**

***Table 3.14** TEST-2 (D_c = 125 mm) cutting parameters and obtained values*

Figure 3.12 *Tool wear after certain passes in TEST-2 D_c = 125 mm, v_c = 80 m/min, f_z = 0.2 mm: (a) after 300 mm; (b) after 1500 mm*

Built-up edge formation was not observed at the lowest cutting speed. But adhered shiny small fragments are observed on the cutting edge after 1st pass of milling at medium cutting speeds as described in Fig. 3.13 and Fig. 3.14. These fragments were not found at higher cutting speeds.

Figure 3.13 *Tool wear after certain passes in TEST-2 D_c = 125 mm, v_c = 140 m/min, f_z = 0.3 mm: (a) after 300 mm; (b) after 900 mm*
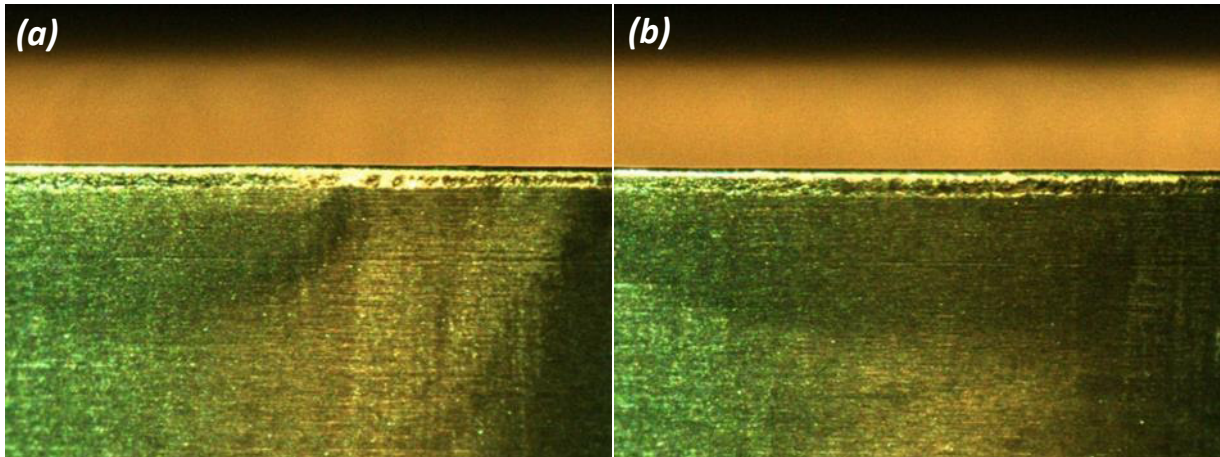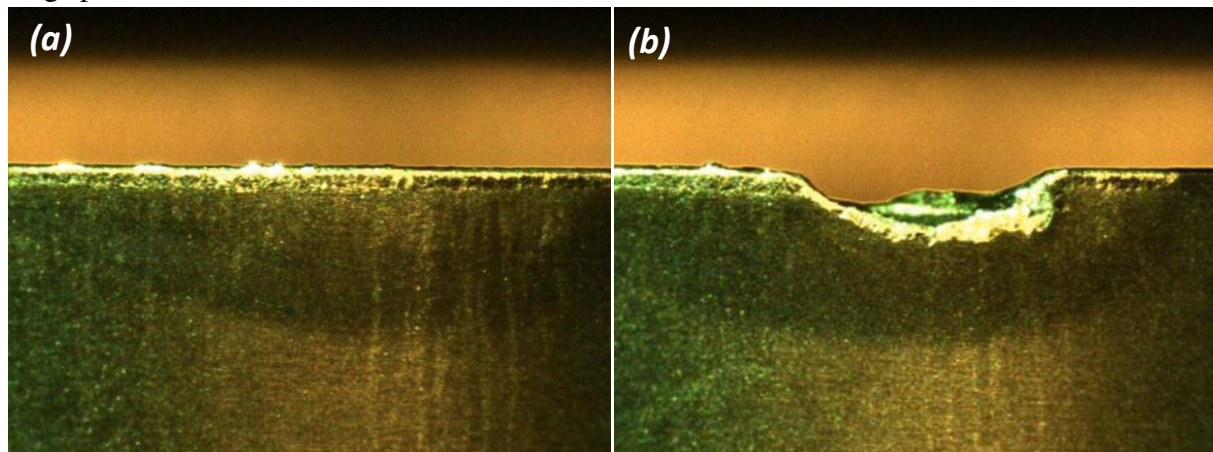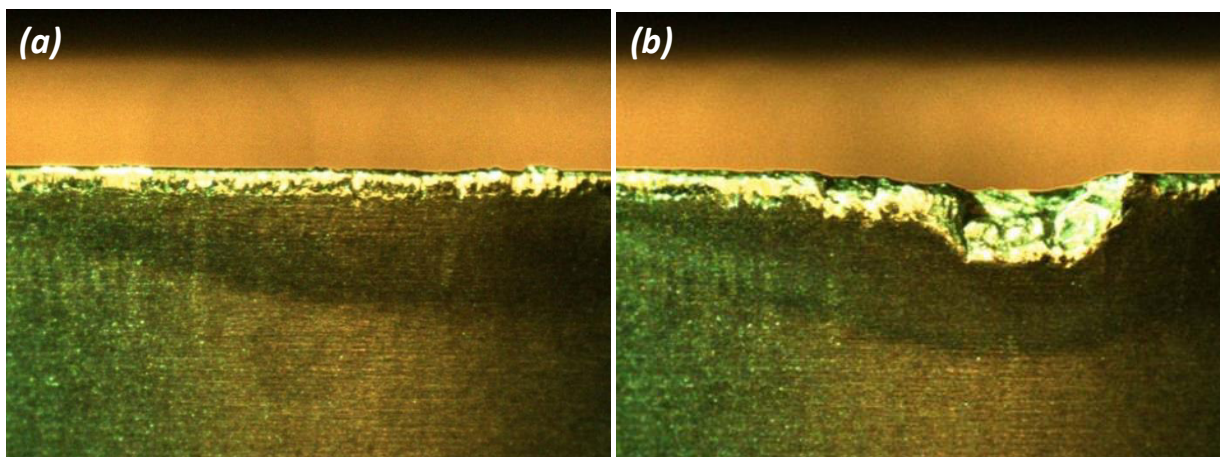

Figure 3.14 *Tool wear after certain passes in TEST-2 D_c = 125 mm, v_c = 200 m/min, f_z = 0.3 mm: (a) after 300 mm; (b) after 900 mm*

But instead, edge crumbling or edge frittering is observed with increasing cutting speed. In addition, number of passes is dramatically decreased with increased cutting speed value as flank wear rate is accelerated. For instance, at v_c = 280 m/min, critical wear is achieved after one pass. And at v_c = 350 m/min, half pass was enough to get critical wear rate on the flank as shown in the following figures. In all cases during the 2nd trial, with increment of number of passes, edge crumbling is followed by notch wear (Figure 3.15).
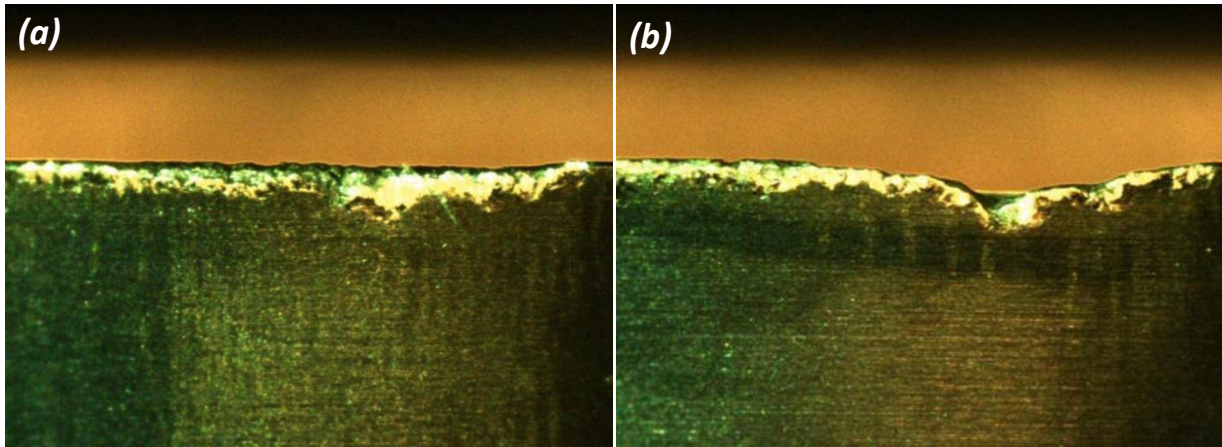
Figure 3.15 *Tool wear at higher cutting speeds in TEST-2 D_c = 125 mm, f_z = 0.3 mm:*
(a) v_c = 280 m/min, after 300 mm; (b) v_c = 350 m/min, after 150 mm

Cutting temperature and heat generation during tool and workpiece interaction is studied during the 3rd trial (TEST-3). As noted above, heat generation and temperature on milling cutter D_c = 125 mm is studied since milling head is made of powder metallurgy using DMLS technique. During 3rd trial, wet milling as well as dry milling is used in order to measure temperature by thermal imaging camera. Investigation can be divided into single phases or stages according to milled length intervals: heat generation and heat transfer at the beginning of the cut, after some distance had been cut which is further divided into segments, and in the end of the cut or in the end of observation, Each figure below includes demonstration of insert approach to workpiece (1), cutting (2), insert exit or after cutting (3).
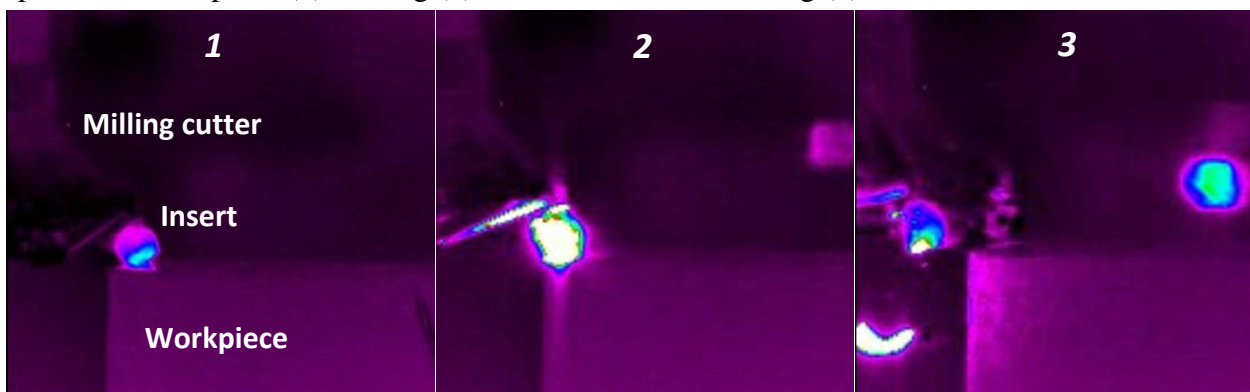
Figure 3.16 *Heat generation demonstration at the beginning phase of milling*

As it can be seen in Figure 3.16, heat is mainly generated during tool and workpiece interaction where chip forms. As tool exits, part of the heat is transferred to the insert as seen in insert exit (3). In on-going phase (Figure 3.17) or after some length of cut, insert at approach is more heated than it was at the beginning and as tool cuts further, chip gets thicker in milling, heat generation area during tool-chip interaction increases. As a result, some part of gen-

erated heat is transferred to milling head heat is transferred to milling head insert pocket and close area through insert as it can be seen in tool exit (3) in Figure 3.17.
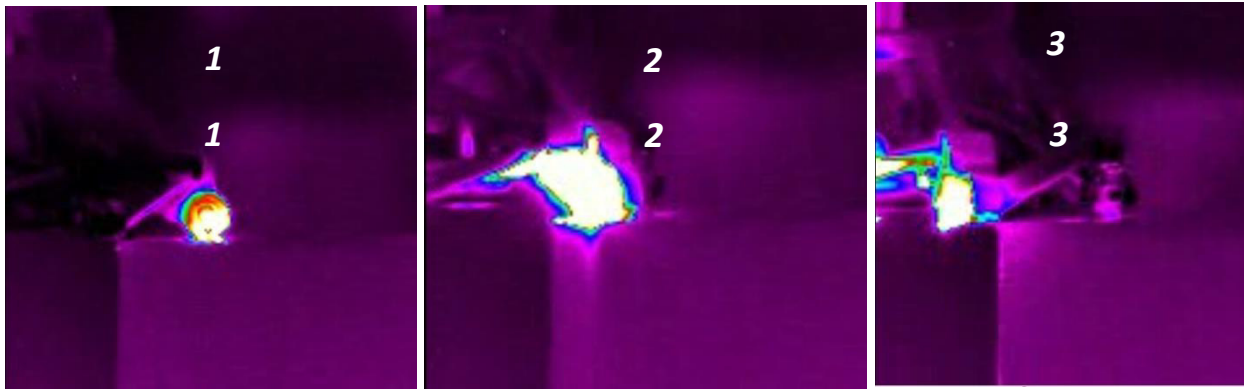
Figure 3.17 Heat generation demonstration in onging phase of milling
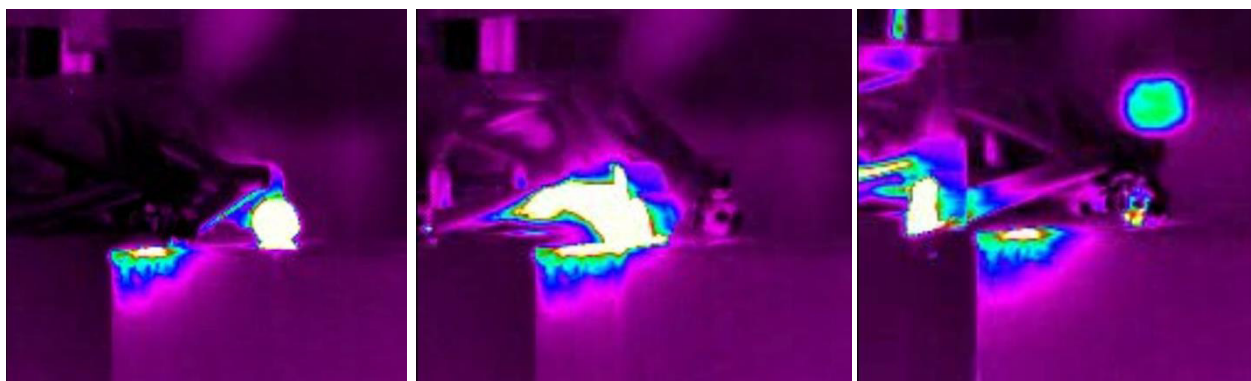
Figure 3.18 Heat generation demonstration in the first intermediate phase of milling

With milling further distances, generated heat during tool-chip interaction transfers to workpiece after certain amount time. As described in Figure 3.18, workpiece milled area is affected by heat as tool periodically engages and exits the workpiece as milling is intermittent type of operation. Meanwhile, transferred heat area increases on milling head as heat transfer to rib structure of milling head is observed in tool exit picture (3) of Figure 3.18.
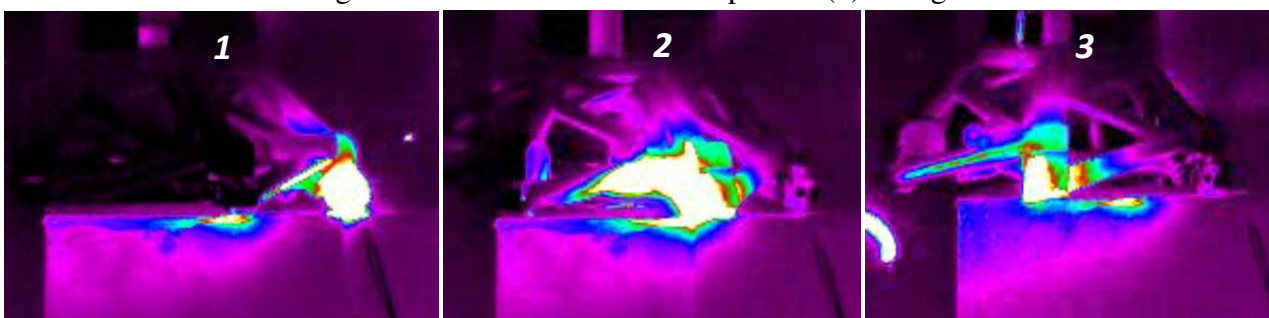
Figure 3.19 Heat generation demonstration in the second intermediate phase of milling

As milling cutter cuts forward, the generated heat on machined surface is transfered into other parts of workpiece because of thermal conductivity property of a material. Heat source diminished area cools down slowly. Other areas of workpiece is effected by heat as milling cutter is fed forward. At the same time, heat transfer on the milling cutter increased. More areas of milling cutter got heated. For cutting tools, heat dissipation is beneficial than heat gathering in terms of tool life and wear. More heat transfer with chip is essential. In the end phase of milling or observation, more heat on milling cutter is observed.
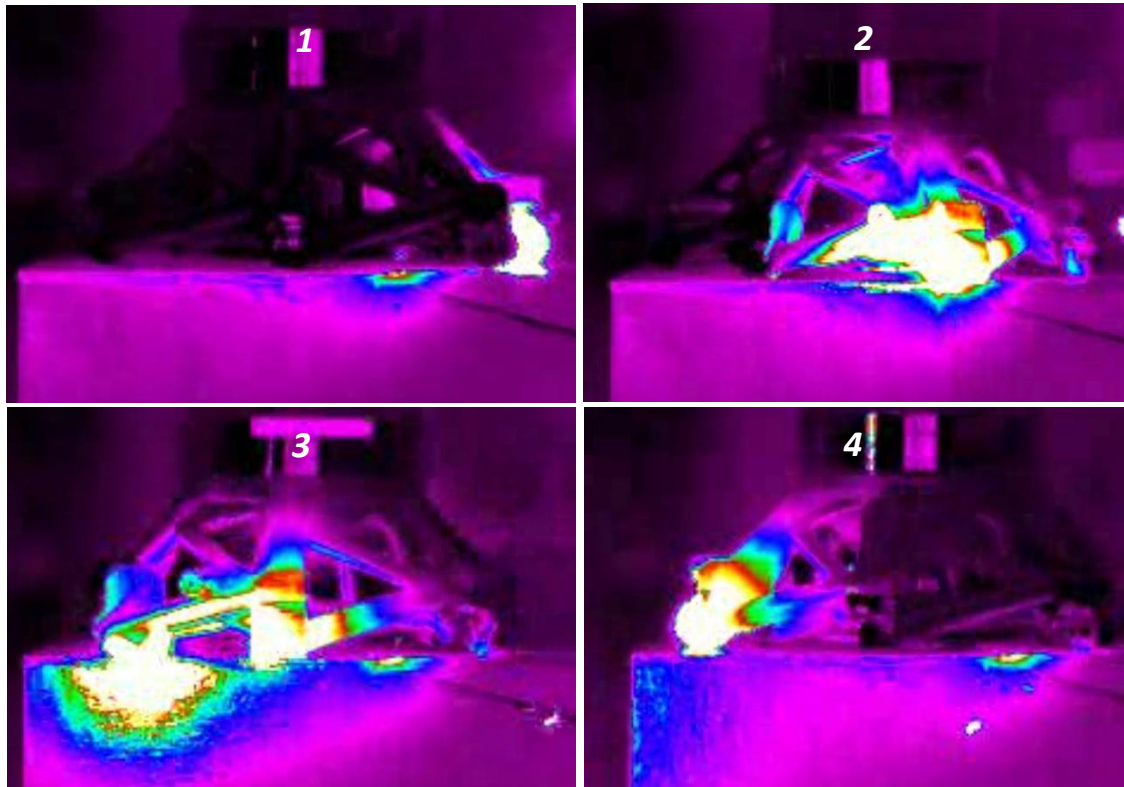
Figure 3.20 Heat generation demonstration in the end phase of milling

Maximum temperature recorded by thermal imaging camera was in increasing manner as cutting speed is increased. As cutting speed increases, forces and resistance increase which in turn mechanical energy that are used in cutting transfers into heat. During the experiment maximum temperature of 409.96°C is recorded at v_c = 350 m/min and minimum temperature of 328.81°C at v_c = 80 m/min as it is described in Graph 3.2.
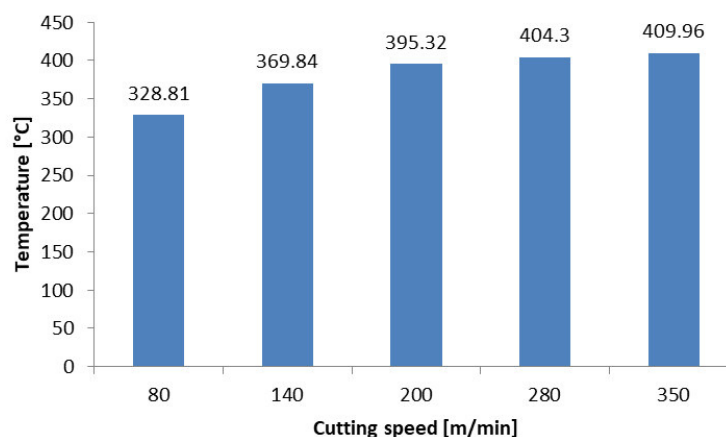
Graph 3.2 Maximum cutting temperature at different cutting speeds

In addition to temperature measurement, cutting edge condition for appropriate cutting speeds are observed. As noted above, wet and dry milling is used in the 3rd trial. In other words, 1st half (a_{e1} = 45 mm) of workpiece is milled with wet milling and cutting speed in 1st half always kept constant. 2nd half is dry milled with variable cutting speed values. Only one pass is used (or cutting length was equal to 300 mm) and cutting edges are inspected after dry milling. By observing cutting edges, BUE presence on edges is searched as BUE has higher

48

No. of passes	v_c [m/min]	f_z [mm/z]	a_p [mm]	a_e [mm]	ΔVB_{lin}
VBD-5 (another edge)					
1	80	0.3	1	45	108
VBD-6 (another edge)					
1	140	0.3	1	45	96
VBD-7 (another edge)					
1	200	0.3	1	45	117
VBD-8 (another edge)					
1	280	0.3	1	45	124
VBD-9 (another edge)					
1	350	0.3	1	45	127

Table 3.15 *TEST-3 (D_c = 125mm) cutting parameters and obtained value*

tendency to form in dry machining. Actually, during the 3rd trial, built-up edge is formed at v_c = 80 m/min and at v_c = 140 m/min with higher extent. Its extent is decreased with increasing cutting speed. Moreover, flank wear is observed on the cutting edges.

Figure 3.21 *BUE formation on the cutting edge during 3rd trial: (a) v_c = 80 m/min; (b) v_c = 140 m/min; (c) v_c = 280 m/min; (d) v_c = 350 m/min;*

In the 4th trial (TEST-4), conventional milling cutter D_c = 100 mm is tested under the same cutting conditions as 2nd trial. Only difference was feed rate in the 4th trial. It was set as

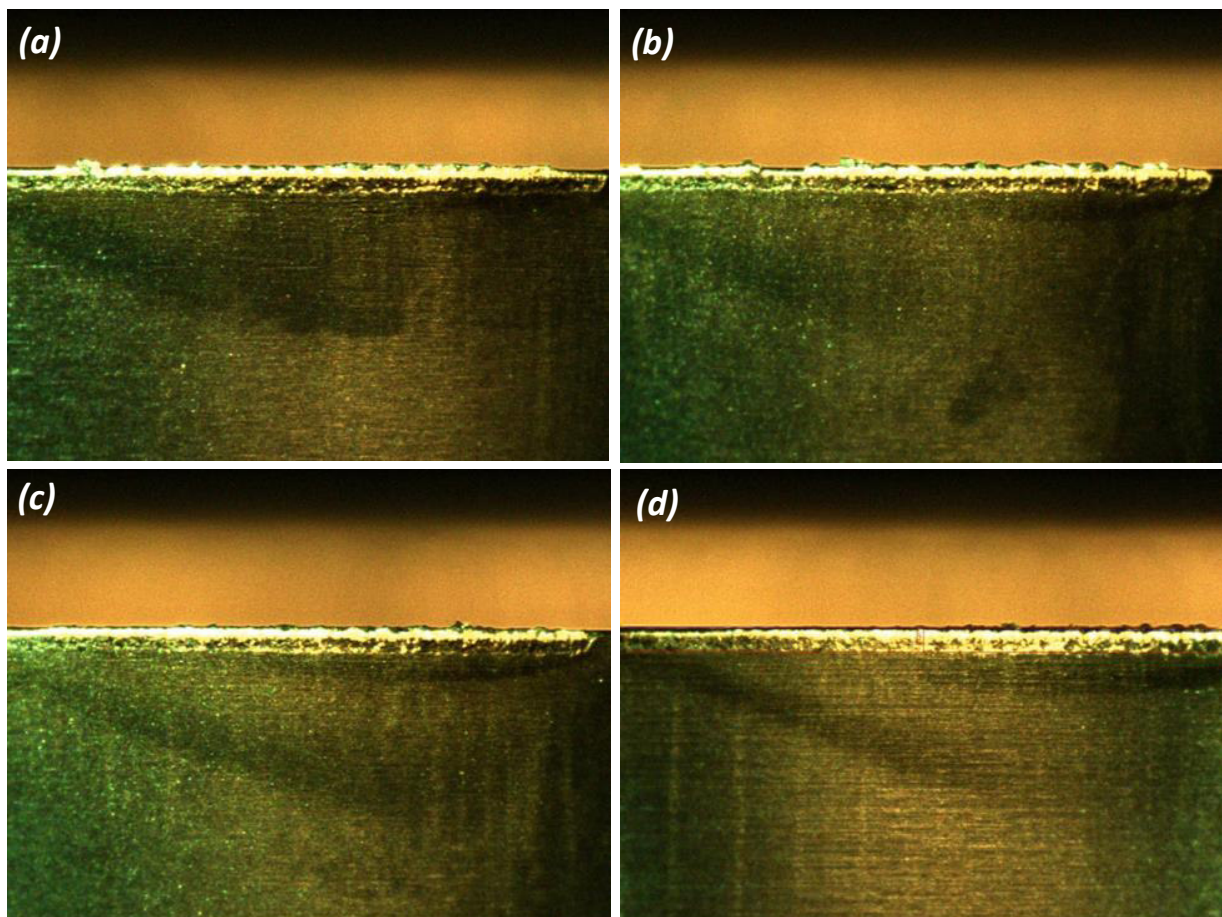0.3 mm from the beginning. Flank wear rates and cutting time obtained can be seen in Table 3.16.

No. of passes	v_c [m/min]	f_z [mm/z]	a_p [mm]	a_e [mm]	VB_{lin1} [µm]	VB_{lin2} [µm]	ΔVB_{lin}	VB_{max} [µm]	Δt [min]
VBD-10									
1	80	0.3	1	45	0	89	89	-	3.93
5	80	0.3	1	45	89	103	14	172	15.70
8	80	0.3	1	45	103	110	7	310	11.78
Max. wear has been reached									**31.41**
VBD-10 (another edge)									
1	140	0.3	1	45	0	108	108	-	2.24
3	140	0.3	1	45	108	593	485	1433	4.49
After 3rd pass, cutting edge is hardly worn, chipped									**6.73**
VBD-7 (another edge)									
1	200	0.3	1	45	0	93	93	-	1.57
2	200	0.3	1	45	93	105	12	313	1.57
Max. wear has been reached									**3.14**
VBD-8 (another edge)									
1	280	0.3	1	45	0	129	129	345	1.12
Max. wear has been reached									**1.12**
VBD-9 (another edge)									
1	350	0.3	1	45	0	91	91	308	0.90
Max. wear has been reached									**0.90**

Table 3.16 *TEST-4 (D_c = 100 mm) cutting parameters and obtained values*

Flank wear progression was increasing with increased number of paths. Average flank wear progression after 5th pass was not in fast manner as it was from 1st pass till 5th pass. During cutting edge inspection after 5th pass (1500 mm), very small notch is observed where it become large enough after last 8th pass (2400 mm) as it is clearly seen in Figure 3.22. This notch was the reason to stop the trial for v_c = 80 m/min limiting criterion for wear is achieved.
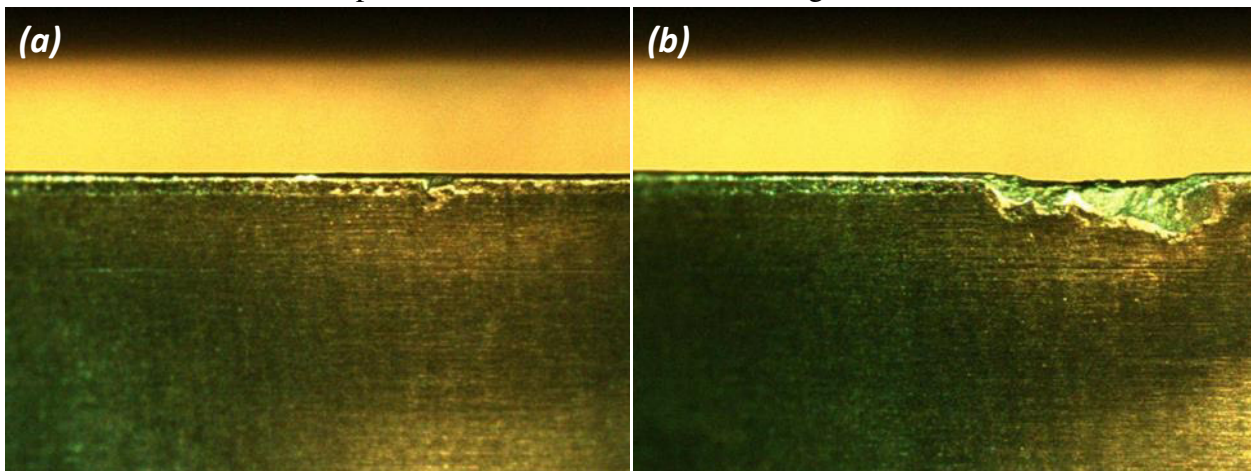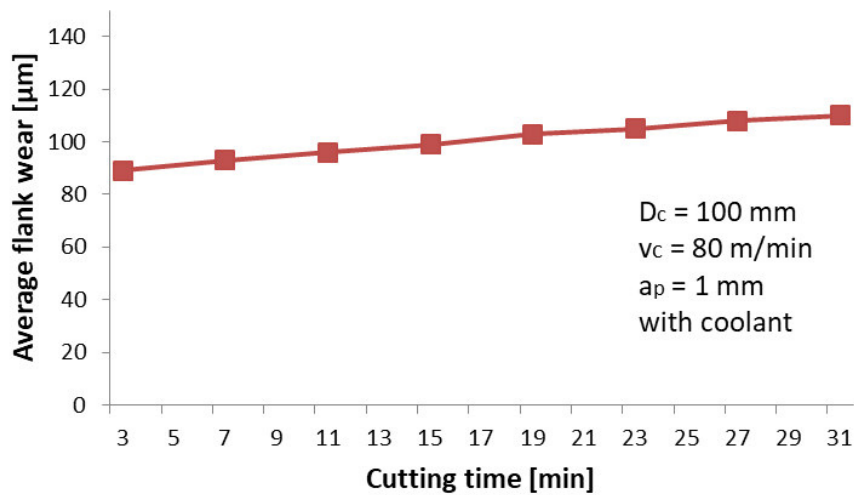

Figure 3.22 *Tool wear at vc = 80 m/min during TEST-4: (a) Flank wear and small notch formation after 1500 mm; (b) Notch wear after 2400 mm.*

Graph 3.3 *Flank wear progression at v_c = 80 m/min (D_c = 100 mm) during TEST-4*

During the 4th trial, heavily damaged insert was observed after milling 900 mm at cutting speed v_c = 140 mm as shown in Figure 3.23. When cutting edge is inspected after 1st pass (300 mm), tool wear behavior seemed to normal as in previous cases, but again some adhered shiny small fragments were observed. After 900 mm cutting, notch wear and shearing-off some tool material is recorded on the cutting edge.
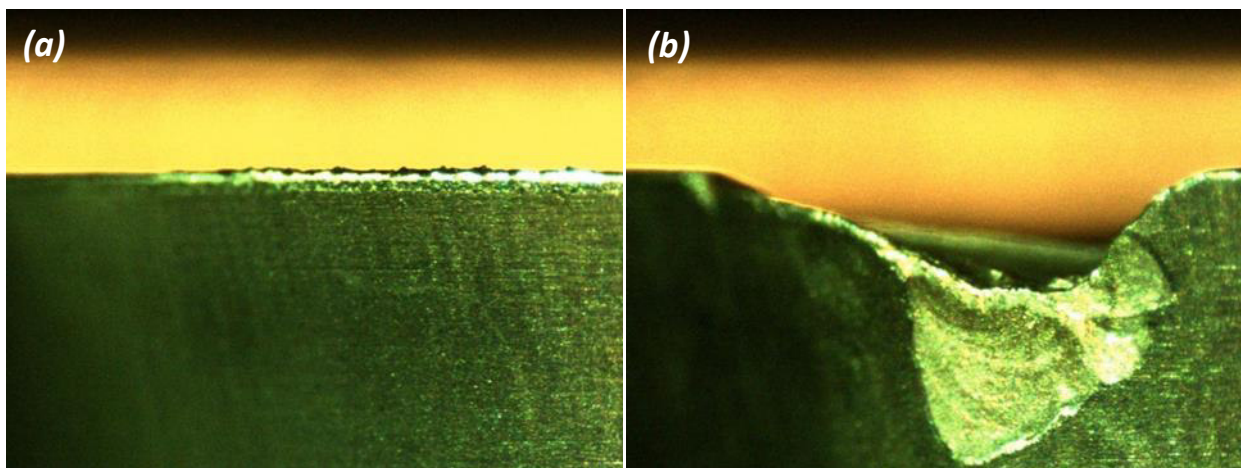
Figure 3.23 *Tool wear at v_c = 140 m/min during TEST-4: (a) after 300 mm;*
(b) Notch after 900 mm.

For shearing-off the tool material or partly loss of insert material, notch wear could be a reason as it is formed under a notch. It can be seen that in that case, wear rate was high enough till cutting 900 mm since after 1st pass, tool wear was with little adhered fragments (BUE) as in other cases. Edge frittering at relatively high cutting speeds, especially, at v_c = 280 m/min and v_c = 350 m/min after 1st pass is observed and it is described in Figure 3.24. According to some literatures, edge frittering occurs when formed BUE is ripped away by chips. But at higher speeds after 300 mm milling, chipping or edge frittering is formed. BUE at these speeds could be formed before 300 mm milling and edge frittering could be a consequence of it. But according to previous experiments by other authors, BUE usually forms at lower cutting speeds rather than higher. But if wear condition is inspected thoroughly in Figure 3.23, there is always tendency on the right side of cutting edge to form a notch. Notch depth starts to grow at this side as demonstrated with an arrow in Figure 3.24.
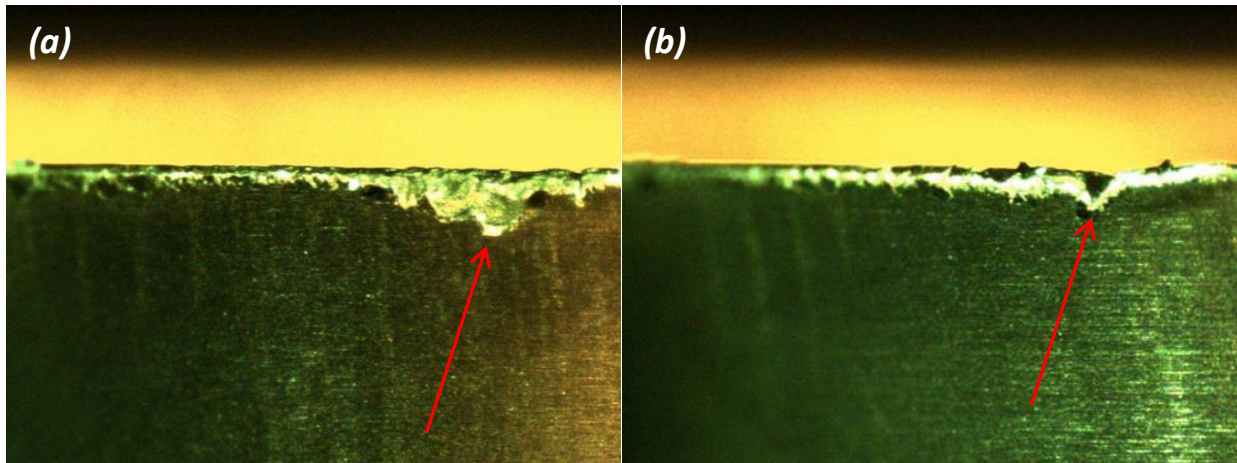
Figure 3.24 *Tool wear at high speeds during TEST-4: (a) at v_c = 280 m/min, 300 mm;*
(b) at v_c = 350 m/min, 300 mm

The 5th trial was only to check the performance of milling cutter D_c = 125 mm with fully equipped inserts. 6 inserts are inserted to the milling cutter insert pockets and only 1 insert position is marked for cutting edge inspection after milling. Cutting speed is set to the lowest, v_c = 80 m/min and feed rate was 0.2 mm/tooth. Milling included total of 10 passes (3000 mm). In the first pass, radial depth of cut was set to 90 mm to check milling cutter behavior with fully equipped inserts in full engagement milling.

VBD-2 (another edge)									
No. of passes	v_c [m/min]	f_z [mm/z]	a_p [mm]	a_e [mm]	VB_{lin1} [µm]	VB_{lin2} [µm]	ΔVB_{lin}	VB_{max} [µm]	Δt [min]
1	80	0,2	1	90	-	-	-	-	0,59
10	80	0,2	1	45	0	120	120	-	10,6
Stopped									**11,65**

Table 3.17 *TEST-5 (D_c = 125 mm, z = 6) cutting parameters and obtained values*
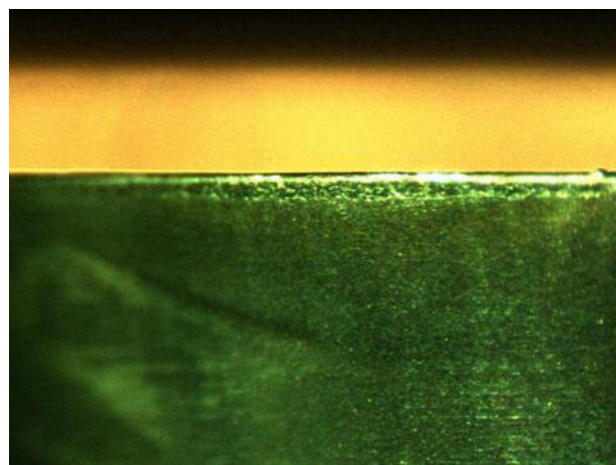
Figure 3.25 *Tool wear at v_c = 80 m/min during TEST-5: VB_B = 120 µm, 3000 mm*

Edge condition after milling 3000 mm can be seen in Figure 3.25. As in this test, all insert pockets are used, force is also distributed among inserts. In previous trials, after milling 3000 mm, usually wear was edge chipping with notch but in this case in the 5th trial only average

flank wear can be measured. In addition in this test, feed is decreased which leads to wear rate decrease, especially, there is a high tendency of notch wear formation at the high cutting feed and it is related to work-hardening effect of workpiece material.

4   Results evaluation

According to obtained values from the experiments, wear rates and machining time were compared and analysed. Machining time is measured in minutes and it is considered as tool life.

4.1   Tool life

Based on the previous experiments, cutting speed has a significant effect on tool life. Therefore, tool life was analysed in accordance with cutting speed. Table 4.1 and Graph 4.1 represents overall sum of tool life and cutting length in different cutting speeds with different milling cutters.

D_c [mm]	125		100	
v_c [m/min]	Tool life [min]	Cutting length [mm]	Tool life [min]	Cutting length [mm]
80	58,96	3000	31,41	2400
140	8,08	900	6,73	900
200	5,65	600	3,14	600
280	1,35	300	1,12	300
350	0,54	150	0,9	300

Table 4.1 *Tool life and cutting length at different vc with different milling cutters (Test-2 vs. Test-4)*
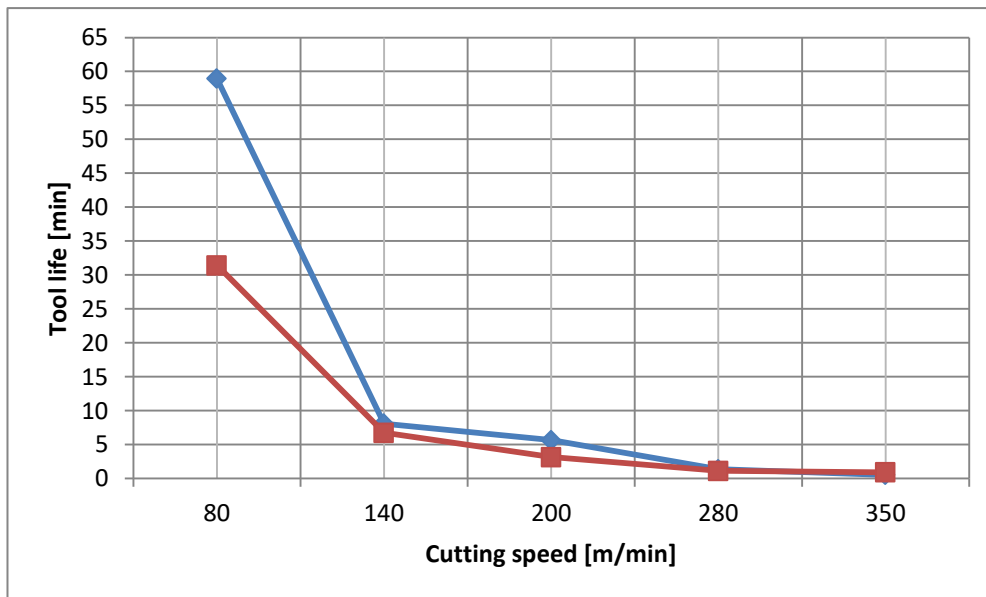
Graph 4.1 *Comparison of tool life with different milling cutters at different v_c*

From the graph it can be seen that there was a great difference on reaching tool life at lower cutting speeds. It was possible to achieve almost two times more tool life with milling cutter manufactured using additive technology. However, diameter also must be taken into account since two milling cutters have different diameters. Tool with larger diameter has a larger rotational speed. But milling cutter D_c=125 mm achieved more tool life, hence cutting length than milling cutter D_c=100 mm under the same condition with the small flank wear rate

difference. But again, their diameters are different and it also has an effect. With increasing the cutting speed, there was a decrease on tool life on both tools. Reachable tool life decreased on both tools and it was almost the same on the following cutting speeds. Milling cutter D_c=125 mm was lighter in terms of weight. As cutting speed increases, forces and resistance also increase where it leads to higher vibrations. There is a high tendency to increase the tool chattering. Tests were performed with using coolant.

According to results of temperature measurement test, temperature during cutting increased with the increasing cutting speed. A large deformation work can be a main heat source in the primary deformation zone. Moreover, tool-chip friction and friction on the flank face are other sources of heat generation. As cutting speed increases, heat generation in these zones also increases. Temperature difference during machining with varied cutting speeds was higher at low and medium cutting speeds and there was only a slight difference at high cutting speeds. If heat generation and heat transfer during milling is analysed during dry milling, there are some stages where differences in heat dissipation can be seen.

At first, heat is generated during tool-chip interaction and only insert is mostly effected by heat. As going further, the amount of heat increases and starts to dissipate. Similarly, as tool goes forward, chip thickness that milling cutter should remove increases. With chip thickness increasing, resistance also increases. As resistance of workpiece material increase, there is higher force or mechanical work required from milling cutter to remove the material. Almost all of the mechanical work during machining is converted into heat. With increase in chip removal, generated heat amount also increases.
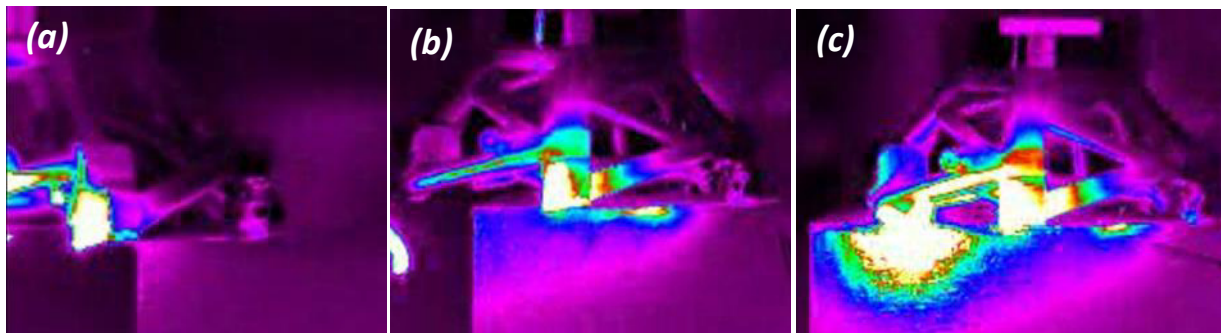
Figure 4.1 *Heat generation and dissipation at different stages of milling: (a) beginning; (b) the second intermediate; (c) end stage of experiment*

From Figure 4.1, how much milling cutter head and workpiece is effected by heat can be observed. As tool goes forward, heat effected zones on the workpiece change and more heat dissipates into milling head rib structure through insert. Therefore, not only insert and workpiece material, but tool holder material choice is also essential. During cutting, heat gathering in one place can lead to catastrophic failures of tool and workpiece. Hence, heat dissipation is crucial. If it is possible, more heat vanishing through chips are beneficial. But during machining materials with low thermal conductivity such as austenitic stainless steels, more heat transfers into tool. As stated in previous chapters, the material of tool holder is EOS MaragingSteel MS1, in other words, a low-carbon steels with martensitic structure (X3NiCoMoTi18-9-5) which has a good thermal conductivity with a low shrinkage and it is mainly used in injection moulding tools production. Therefore, this material was a good choice for milling head.

4.2   Wear analysis

During the test, flank wear, built-up edge formation, micro-chipping, edge frittering and notch wear were observed. During all tests, at lower cutting speeds, flank wear is observed as a starting wear after 1st pass (300 mm) of milling. At higher cutting speeds, edge crumbling and frittering is observed after 1st pass. As cutting speed is increased, temperature-activated wear mechanisms become dominant and edge frittering, micro-chipping and notch formation are caused by abrasion, adhesion and work-hardening effect of the workpiece material, and also by thermal fluctuations in intermittent cutting. At lower and higher cutting speeds, notch wear (groove on the rake and flank face) was the reason for tool failure or to reach critical wear limit where notch is formed after flank wear (or in combination with built-up edge) at lower cutting speeds. Notch or sometimes groove is formed after micro-chipping, edge frittering at higher speeds.

Built-up edge formation with larger extent is observed especially in dry milling with milling cutter D_c = 125 mm at lower cutting speeds such (80 m/min and 140 m/min) and partly at v_c = 200 m/min. At low cutting speeds, more contact time of tool and chip causes high friction and temperature generation. As a result, it creates more opportunity for ductile materials to adhere to the cutting tool by creation of micro-welds. Volume of built-up edge is decreased with increasing cutting speed. As cutting speed is increased, deformation rate will be accelerated where plastic flow of workpiece material is faster. When built-up edge formed in dry milling is compared to wet milling with milling cutter D_c = 125 mm at v_c = 140 m/min, distinctly difference can be seen. Adhered layer in wet milling is negligible in contrast to dry milling. Moreover, milling cutter D_c = 125 mm is equipped with a special coolant stream channel. So, direct coolant supply to tool-chip contact zone is possible. Based on Figure 4.2, coolant usage decreases BUE formation on the cutting edge. By using coolant, heat caused by tool-chip interaction can be decreased. In contrast to coolant, lubricants are more beneficial to decrease efficiently friction and micro-welds.
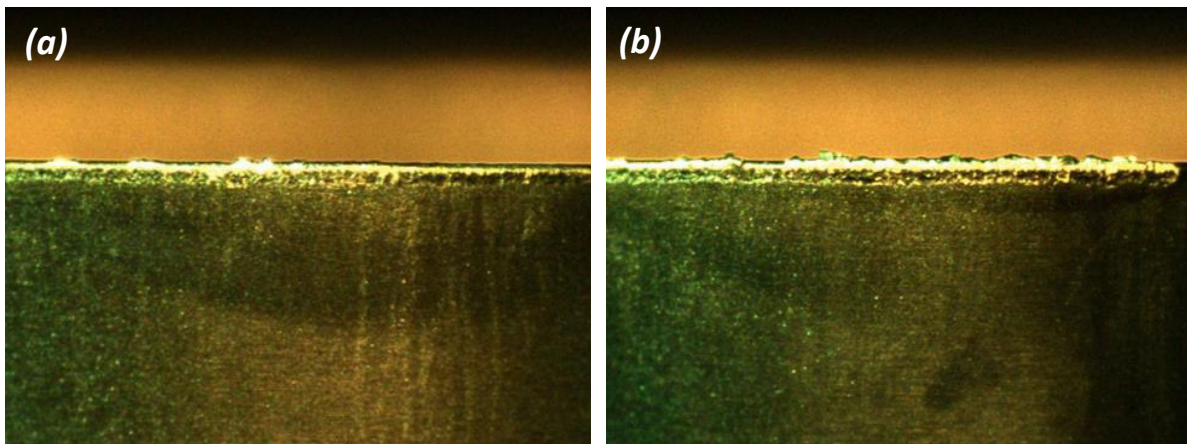
Figure 4.2 *BUE formation D_c = 125 mm at v_c = 140 m/min: (a) wet milling; (b) dry milling*

During wet milling at v_c = 200 m/min, a higher tendency to BUE formation is observed in milling cutter D_c = 100 mm. In milling cutter D_c = 125 mm, it is combined with a slight frittering as seen in Figure 4.3. Usually when BUE reaches its critical size, it tears off and it can remove some cutting tool material creating micro-chipping or edge crumbling. Edge frittering or micro-chipping after some passes can be a result of teared-off BUE. But as seen in Figure 3.22, during TEST-4 where milling cutter D_c = 100 mm is tested at v_c = 80 m/min with coolant, a slight micro-chipping after 1500 mm milling is followed by notch or slight fracture.
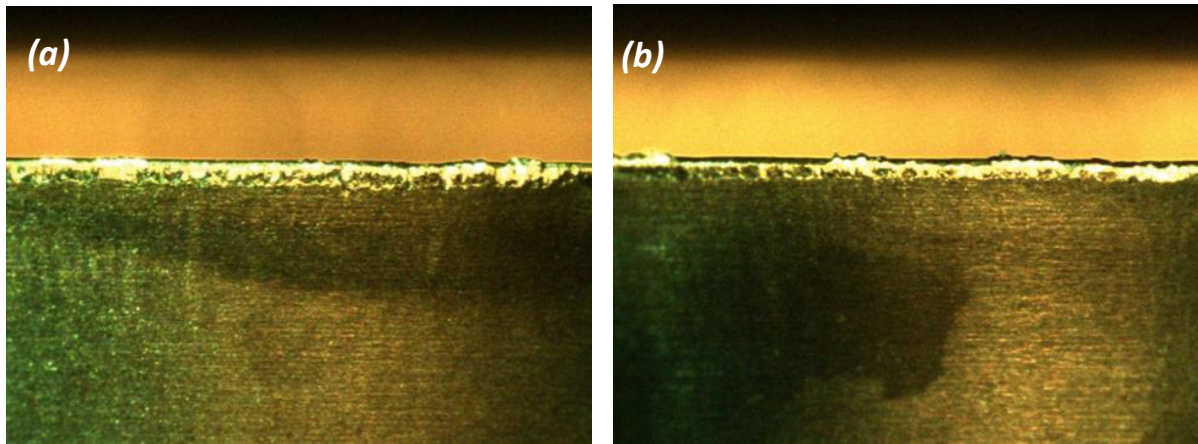
Figure 4.3 *BUE formation and cutting edge condition at vc = 200 m/min: (a) D_c = 125 mm;*
(b) D_c = 100 mm

However, when the insert is inspected after 1st pass (300 mm) or after 5th pass (1500 mm), there were no signs of adhered material on the edge, but only flank wear and slight micro-chipping as shown in Figure 3.22. So, one can assume that chipping is caused by thermal fluctuations or thermal cracking during milling, but not as a result of BUE.

The influence of cutting speed in BUE formation can be seen in Figure 4.4 where edge condition at the lowest and at the highest cutting speeds in dry milling are compared. As noted above, coolant usage can prevent BUE formation in wet milling, but in dry milling, the intensity of BUE formation can be lowered with increasing cutting speed. But as a disadvantage of it, tool life is decreased with increasing cutting speed.
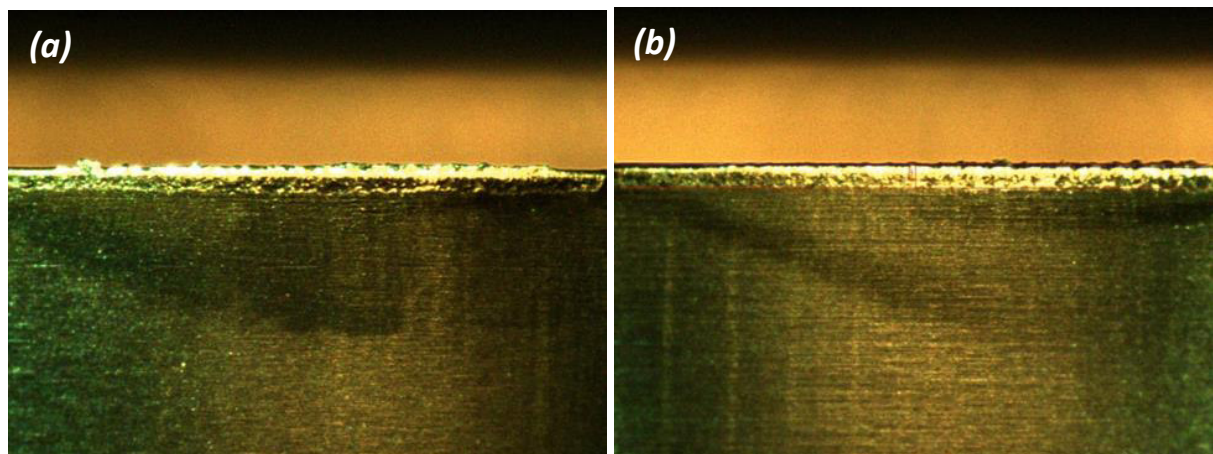

Figure 4.4 *BUE formation at different cutting speeds in dry milling Dc = 125 mm:*
(a) v_c = 80 m/min; (b) v_c = 350 m/min

As stated in previous chapters, flank wear is a typical wear that occurs during machining and it is measurable. Flank wear progression with high number of passes could be observed at the lowest cutting speed as wear rate at lower cutting speeds is not rapid. From Graph 4.2, average flank wear rate in milling cutter D_c = 125 mm was higher along entire cutting length than conventional milling cutter in wet milling. But again tool diameters are different and it has also an effect as rotational speed values are different. Flank wear usually increases rapidly after 1st pass or 1st cut, after that, its progression comes out in a slower rate. Average flank wear rate (VB_B) after 1st pass (300 mm) during 2nd trial and 4th trial are compared in order to compare cutting speed influence on flank wear progression and it is described in column

Graph 4.3. The highest values of average flank wear were achieved for both milling cutters at $v_c = 280$ m/min. If Figure 3.23 is observed, edge frittering could be seen after 1st pass. With higher cutting speeds edge crumbling or micro-chipping of edge started in both milling cutter. As a result, micro-chipping influenced on average flank wear rate value. For almost all cutting speeds, milling cutter $D_c = 125$ mm had a greater value of average flank wear after 1st pass. But its machining length in total was higher than milling cutter $D_c = 100$ mm.
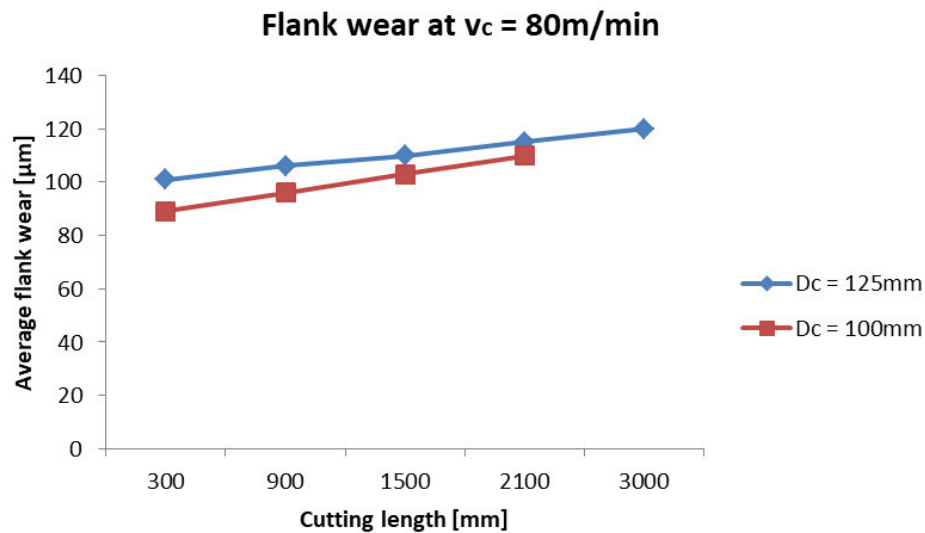
Graph 4.2 *Average flank wear progression comparison at $v_c = 80$ m/min*
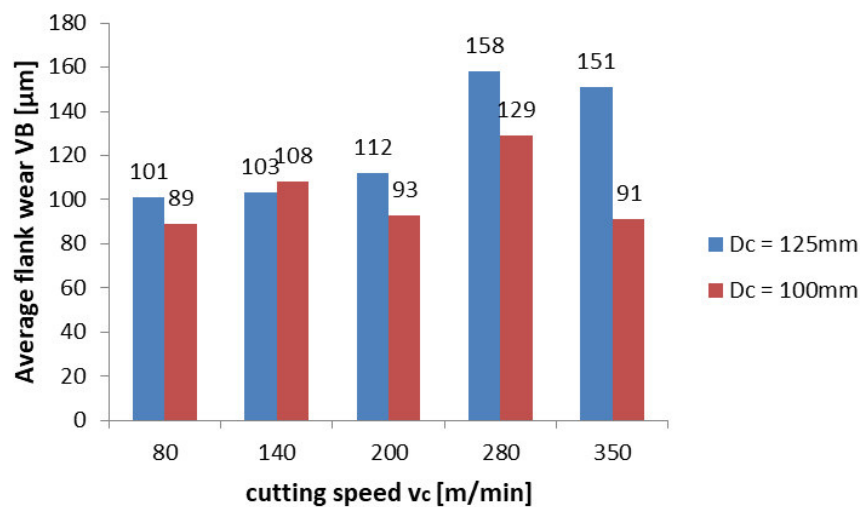
Graph 4.3 *Average flank wear progression comparison after 1st pass*

Maximum wear on flank is noted and it is also measured. Values are recorded during experiment. During experiment, in some cases, notch got wider because of cutting with initial formed notch carried on and it become in form of groove. As a reason, work-hardening of austenitic stainless steel is assumed. One of such grooves can be seen in Graph 4.4 which is formed at $v_c = 140$ m/min after milling distance of 900 mm. It can be estimated that sheared-off insert material under groove is a result of the notch wear formation. Comparing to milling cutter $D_c = 125$ mm in Figure 3.13, groove formation sequence is similar. In contrast to milling cutter $D_c = 125$ mm, insert wear in conventional milling cutter is accelerated by abrasive inclusion in workpiece material or as a result of work-hardening of austenitic stainless steel.
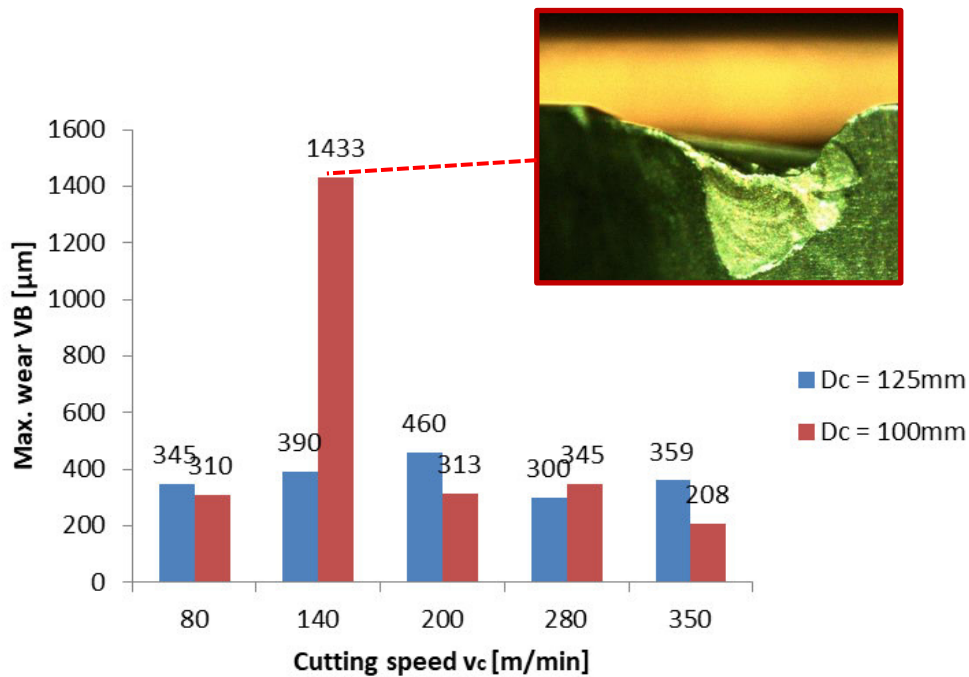
Graph 4.4 *Maximum wear values comparison*

Before notch formation, micro-chippings started to form along edge. Micro-chipping or edge crumbling intensity increased at high cutting speeds. It is assumed that their formation can be from thermal fluctuations (with increasing thermal stresses) in milling or with BUE formation. When BUE tears away, it can abrade some piece of tool material. As a result micro-chipping can occur. Consequently, BUE has an influence on tool life when it causes to edge chipping.

5 Conclusion

Experiments were carried once and based on the experiment results, formation of BUE was observed with high tendency during dry machining on TEST-3 with milling cutter D_C=125 mm. Intensity of BUE was higher at low- and medium cutting speeds than higher speeds where feed and depth of cut is kept constant. According to previous experiments and findings, BUE was formed also at low- and medium cuttings speeds during dry milling when effect of coolant methods are investigated by K.A. Abou-El-Hossein and BUE was the main tool failure mode. But cutting speed range used was different, starting from /min and ending at 260 m/min. In addition, type of milling was an end-milling in his experiment. Slightly adhered fragments are observed during TEST-2 with milling cutter D_c=125 mm and D_c=100 mm at medium cutting speeds (140 m/min, 200 m/min) with coolant as described in thesis. Basically, it can be concluded that there is a high heat temperature for BUE formation at low cutting speeds because of prolonged contact time, a low thermal conductivity of austenitic stainless steel. And tendency of BUE formation in milling without coolant is higher than milling with coolant. When BUE formation leads to micro-chipping or frittering of cutting edge. it has an influence on tool life. Consequently, countermeasures should be applied.

Flank wear was considered as typical wear type which was found at initial passes during all trials. With the increasing number of passes, intensity of flank wear is also increased and at some points maximum flank wear is achieved. In almost all cases, maximum flank wear formed as a notch wear and grooving which is also typical for austenitic stainless steel machining. According to previous experiments and findings, notch wear was found as a main cause for tool failure by K.A. Abou-El-Hossein and Z.Yahya during end-milling with coolant. And the reason could be a work-hardening effect of a material as explained above.

For both milling cutters, the highest tool life was achieved at the lowest cutting speed, v_c = 80 m/min. As cutting speed is increased, tool life amount is decreased. As stated above, feed and depth of cut is kept constant as cutting speed has a higher impact on tool life. Comparing two milling cutters where milling cutter D_c=125 mm is made using DMLS technique. Higher amount of tool life is achieved with DMLS milling cutter. It can be estimated better properties can be achieved with additive manufacturing: less weight can be achieved with rib structure of milling head, higher density as powder metallurgy used. Direct coolant supply into contact zone with high pressure. Moreover, direct metal laser sintering technique is considered as one of the most used additive technology. For further comparison of two milling cutters, quality issues of machined workpiece also should be considered. But focus of that work was a BUE formation, other types of wear and tool life.

In terms of productivity from economical point of view, milling with radially partly engagement can not be so productive in series production for example, where a high amount of parts should be produced within exact specific time. In this case, full engagement has more benefits. Time spent on milling can be decreased. But again in terms of tool life, it is not so suitable as it was observed during the experiment. As the aim of the experiment was different, but not to increase the productivity in production, these problems aren`t deeply considered during cutting parameter and methods selection.

As stated above, experiments are carried only once and there is a need for further analysis with more samples and more trials in order to get more reliable result.

6   References

[1]   P. P. ZHANG, Y. GUO, AND B. WANG, "Novel tool wear monitoring method in termín milling difficult-to-machine materials using cutting chip formation," *J. Phys. Conf. Ser.*, vol. 842, no. 1, p. 012042, 2017.

[2]   Z. WANG, V. KOVVURI, A. ARAUJO, M. BACCI, W. N. P. HUNG, AND S. T. S. BUKKAPATNAM, "Built-up-edge effects on surface deterioration in micromilling processes," *J. Manuf. Process.*, vol. 24, pp. 321–327, Oct. 2016.

[3]   "Stainless steel for machining" [Online] Available:
        https://www.nickelinstitute.org/media/1814/stainlesssteelsformachining_9011_.pdf

[4]   H. A. YOUSSEF AND H. EL-HOFY, Machining Technology: Machine Tools and Operations. CRC Press, 2008.

[5]   "Principles of Cutting", Simulation Techniques in Manufacturing Technology [Online]. Available:
        https://www.wzl.rwth-aachen.de/cms/www_content/en/f786439a4c53fb78c125709f0055702f/v1_introduction.pdf

[6]   S. KALPAKJIAN, S. R. SCHMID, AND C.-W. KOK, Manufacturing, Engineering and SI, Sixth edition. Singapore: Pearson Education, 2009.

[7]   "Dry milling or with cutting fluid." [Online]. Available:
        https://www.sandvik.coromant.com/en-gb/knowledge/milling/pages/dry-milling-or-with-cutting-fluid.aspx

[8]   S. Coromant, Metalcutting Technical Guide: Turning, Milling, Drilling, Boring, Tool-holding; Handbook from Sandvik Coromant. Sandvik Coromant, 2005.

[9]   "Machining of Products," [Online]. Available:
        http://core.materials.ac.uk/repository/eaa/talat/3100.pdf

[10]   KLOCKE, F. Manufacturing Processes 1: Cutting, Berlin Springer-Verlag, 2011 ISBN 978-3-642-11978-1

[11]   "Balancing key factors in stainless steel machining" [Online]. Available:
        https://www.secotools.com/article/21497?language=en

[12]   "Walter Turn precision cooling" [Online]. Available:
        https://www.walter-tools.com/en-/tools/standard_products/turning/overview/iso_turning/turn-precision-cooling/pages/default.aspx

[13]   **"**Walter Tools Turning Precision Cooling (-P) high pressure coolant internal coolant" [Online]. Available: *https://www.youtube.com/watch?v=9y3VtesLQGA*

[14]   BOUZAKIS, KONSTANTINOS-DIONYSIOS, NIKOLAOS MICHAILIDIS, GEORGIOS SKORDARIS, EMMANOUIL BOUZAKIS, DIRK BIERMANN, A RACHID M'SAOUBI. „Cutting with coated tools: Coating technologies, characterization methods and performance optimization". *CIRP Annals* 61, č. 2 (1. leden 2012): 703–23. [Online]. Available:
        https://www.researchgate.net/publication/256673860_Cutting_with_coated_tools_Coating_technologies_characterization_methods_and_performance_optimization

[15]   Kulkarni, Atul, G G Joshi, a Vikas Sargade. „Performance of PVD AlTiCrN coating during machining of austenitic stainless steel". *Surface Engineering* 29 (1. červen 2013): 402–7. [Online]. Available: *https://www.researchgate.net/publication/272249886_Performance_of_PVD_AlTiCrN_coating_during_machining_of_austenitic_stainless_steel*

[16]   STEPHENSON, DAVID A. *Metal Cutting Theory and Practice*. CRC Press, 1996.

[17]   J. P. DAVIM, Machining and Machine-tools: Research & Development. Elsevier, 2013

[18]   "Sandvik Metal Cutting Technology Training Handbook | Machining | Drilling." [Online]. Available: *https://ru.scribd.com/document/317281556/Sandvik-Metal-Cutting-Technology-Training-Handbook*

[19]   "Carbide". Gühring Online Academy. [Online]. Available: *https://academy.guehring.de/academies/academyLogin.do?d61bd448-d36a-485c-a656-2bada63863cf*

[20]   A. E. DINIZ, Á. R. MACHADO, AND J. G. CORRÊA, "Tool wear mechanisms in the machining of steels and stainless steels", *Int. J. Adv. Manuf. Technol.*, vol. 87, no. 9–12, pp. 3157–3168, Dec. 2016. Available: *https://www.researchgate.net/publication/301313223_Tool_wear_mechanisms_in_the_machining_of_steels_and_stainless_steels*

[21]   A. DAHLSTRÖM, "Wear mechanisms in austenitic stainless steel drilling", p. 69. Available: *https://pdfs.semanticscholar.org/3ad9/ad797f9045a5afec7ee5b18dcbe4a39bed43.pdf*

[22]   L. ČERČE, F. PUŠAVEC, AND J. KOPAC, "3D cutting tool-wear monitoring in the process" *J. Mech. Sci. Technol.*, vol. 29, pp. 3885–3895, Sep. 2015. Available: *https://www.researchgate.net/publication/283025373_3D_cutting_tool-wear_monitoring_in_the_process*

[23]   S. J. ERIC AND S. T. AB, Metal Cutting Theories and Models. Division of Production and Materials Engineering, 2012.

[24]   M. B. BILGIN, "Investigating the effects of cutting parameters on the built-up-layer and built-up-edge formation during the machining of AISI 310 austenitic stainless steels" *Mater. Tehnol.*, vol. 49, no. 5, pp. 779–784, Oct. 2015. [Online] Available: *http://mit.imt.si/Revija/izvodi/mit155/bilgin.pdf*

[25]   R. TIMINGS, Engineering Fundamentals. Routledge, 2007.

[26]   W. A. KNIGHT AND G. BOOTHROYD, Fundamentals of Metal Machining and Machine Tools, Third Edition. CRC Press, 2005.

[27]   K. A. ABOU-EL-HOSSEIN, "Cutting fluid efficiency in end milling of AISI 304 stainless steel", *Ind. Lubr. Tribol.*, vol. 60, pp. 115–120, May 2008. Available: *https://www.researchgate.net/publication/242237837_High_speed_end_milling_of_AISI_304_stainless_steel_using_new_geometrically_developed_carbide_inserts*

[28]   K. A. ABOU-EL-HOSSEIN and Z. YAHYA, "High-speed end-milling of AISI 304 stainless steels using new geometrically developed carbide inserts", *J. Mater. Process. Technol.*, vol. 162–163, pp. 596–602, May 2005. Available: *https://www.sciencedirect.com/science/article/pii/S0924013605002372*

[29]   M. NORDIN, R. SUNDSTRÖM, T.I. SELINDER, S. HOGMARK, "Wear and failure mechanisms of multilayered PVD TiN/TaN coated tools when milling austenitic stainless steel - ScienceDirect." [Online]. Available: *https://www.sciencedirect.com/science/article/pii/S0257897200009336*

[30]   Y. MUTHUSAMY, K. KADIRGAMA, Prof. Dr. Md. MUSTAFIZUR RAHMAN, R. DEVARAJAN, "Wear analysis when machining AISI 304 with ethylene glycol/TIO2 nanoparticle-based coolant," *ResearchGate*. [Online]. Available: *https://www.researchgate.net/publication/278681763_Wear_analysis_when_machining_AISI_304_with_ethylene_glycolTIO2_nanoparticle-based_coolant*

[31]   M. NALBANT, Y. YILDIZ, "Effect of cryogenic cooling in milling process of AISI 304 stainless steel - ScienceDirect." [Online]. Available: *https://www.sciencedirect.com/science/article/pii/S1003632611606808*

[32]   C. PALANISAMY and L. HONG WEE, "Surface Roughness and Tool Wear Study on Milling of AISI 304 Stainless Steel Using Different Cooling Conditions" *Int. J. Eng. Technol.*, vol. 2, Aug. 2012.

[33]   A. UYSAL, F. DEMIREN and E. ALTAN, "Investigation of Surface Roughness and Chip Forms in Milling of Stainless Steel by MQL Method," *Acta Phys. Pol. A*, vol. 129, pp. 439–441, Apr. 2016. [Online]. Available: *http://przyrbwn.icm.edu.pl/APP/PDF/129/a129z4p003.pdf*

[34]   I. KORKUT, M. KASAP, İ. ÇIFTÇI, and U. ŞEKER, "Determination of optimum cutting parameters during machining of AISI 304 austenitic stainless steel," *Mater. Des. - MATER Des.*, vol. 25, pp. 303–305, Jun. 2004.

[35]   "Main Catalogue | OSG Europe." [Online]. Available: *https://www.osgeurope.com/en/literature/main-catalogue*

[36]   "EOS Metal Materials for Additive Manufacturing." [Online]. Available: *https://www.eos.info/material-m*

[37]   KRAKEN – unikátní frézovací hlava vyrobená technologií 3D tisku kovů, Regionální technologický institut – Zaměření [Online]. Available: *https://rti.zcu.cz/laboratore/obrabeni/?fbclid=IwAR0GRHIjuvKp69B7Zv_i3XNfmLsgslJAeD1vbWnY5WNc8CVO3Rj5-jEgMDs*

[38]   "Nerezové materiály, Nerez ocel, Nerez trubky - TERAPOL s.r.o." [Online]. Available: *http://www.terapol.cz/clanek/no-tj-austeniticke*

[39]   DMU eVo Series. Available: *https://en.dmgmori.com/resource/blob/44922/3c6e9cba3551382ae5d66f744816c599/pm0uk-dmu-evo-series-pdf-data.pdf*

[40]   Multicheck PC 500 G2. Available: *http://www.polimetservice.ru/files/multicheck-pc500g2/katalog-multicheck-pc500g2-pdf.pdf*

7   Appendices

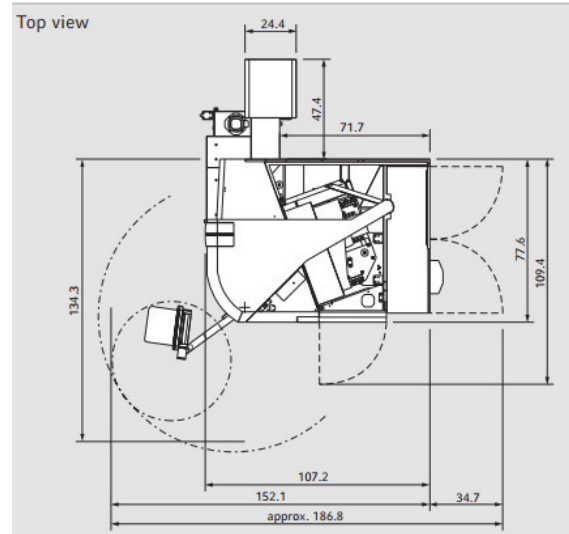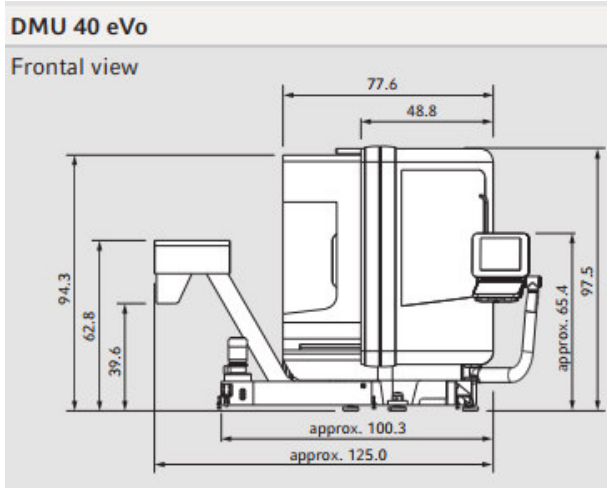Appendix no.1: DMU 40 eVo linear machining center technical data

Appendix no.2: Blickle Multicheck PC500 parameters

ATTACHMENT no. 1

DMU 40 eVo linear machining center technical data

			DMU 40 eVo
Working area			
Max. X axis	mm	400
Max. Y axis	mm	400
Max. Z axis	mm	375
Table dimensions			
Max. table load	kg	250
Table diameter	mm	480
Workpiece dimensions			
Max. workpiece height	mm	460
Spindle			
Standard speed	rpm	20000
Max. speed (Option)	rpm	40000
Drive power rating (100% DC)	kW	25
Torque (100% DC)	Nm	87
Tool magazine			
Capacity	-	30
Max. capacity	-	120
Rapid traverse			
Max. X axis	m/min	50
Max. Y axis	m/min	50
Max. Z axis	m/min	50
Controls			
DMG ERGO*line*® control panel	Siemens 840D	
with 19" monitor and 3D software	HEIDENHAIN iTNC530	
Options			
Tool magazine with 60/120 pockets			
Internal coolnt supply, 40 bar / 80 interchangeable			
Chip conveyor			
Counter support with tailstock			
Programmable coolant nozzles			
Oil emulsion mist separator			
Pallet changer			

Floor plans

DMU 40 eVo

Frontal view

77.6
48.8
94.3
62.8
39.6
approx. 65.4
97.5
approx. 100.3
approx. 125.0

Top view

24.4
47.4
71.7
134.3
77.6
109.4
107.2
152.1
34.7
approx. 186.8

Torque / performance charts

* Optional

10,000 rpm.*

Torque (ft./lbs.)
Performance (hp.)
737.6 — 67.1
590.0 — 53.6
464.7 — 40.2
147.5 — 16.8
118.0 — 13.4
92.2 — 10.7
49.4 — 6.7
8.9 — 1.5
0.7 — 0.19

61.7 hp. 40%
147.5 ft./lbs. 40%
40.2 hp. 100%
95.9 ft./lbs. 100%

Speed (rpm.): 20, 50, 160, 400, 2,200, 2,800, 4,300, 10,000, 15,000

14,000 rpm. as standard

Torque (ft./lbs.)
Perfomance (hp.)
464.7 — 53.6
232.3 — 26.8
92.2 — 13.4
24.6 — 6.7
12.7 — 2.7
7.4 — 1.3
3.7

25.3 hp. 40%
18.8 hp. 100%
73.8 ft./lbs. 40%
54.6 ft./lbs. 100%

Speed (rpm.): 20, 63, 160, 400, 1,800, 2,800, 4,000, 10,500, 14,000

18,000 rpm.*

Torque (ft./lbs.)
Performance (hp.)
737.6 — 53.6
232.3 — 26.8
92.2 — 13.4
36.9 — 6.7
18.4 — 2.7
5.9 — 1.3

46.9 hp. 40%
33.5 hp. 100%
95.9 ft./lbs. 40%
64.2 ft./lbs. 100%

Speed (rpm.): 20, 63, 160, 400, 1,000, 2,500, 6,300, 15,000, 18,000

42,000 rpm.*

Torque (ft./lbs.)
Performance (hp.)
14.8 — 26.8
7.4 — 13.4
3.7 — 6.7
1.5 — 2.7
0.7 — 1.3

17.4 hp. 40%
13.4 hp. 100%
6.1 ft./lbs. 40%
4.7 ft./lbs. 100%

Speed (rpm.): 20, 63, 160, 400, 1,000, 2,500, 6,300, 15,000, 42,000

ATTACHMENT no. 2

Blickle Multicheck PC500 parameters

Model	Multicheck PC500
Display	19" TFT-Display (1280x1024)
Measuring range	
X (horizontal)	0-150mm
Y (vertical)	0-150mm
Number of indexable lenses	4
Magnification	10x, 30x, 75x, 150x
Positioning stability	0,005mm
Tool clamping device	Rotational and non-rotational tools
Software	WMS
Options	
Radius measurement using 3 points and edge detection sensor	
Step length and angle measurement	
Wear width measurement	
Drill geometry overview using a test mask	